Spectral Measurement of Antineutrino Oscillation Amplitude and Frequency at Daya Bay

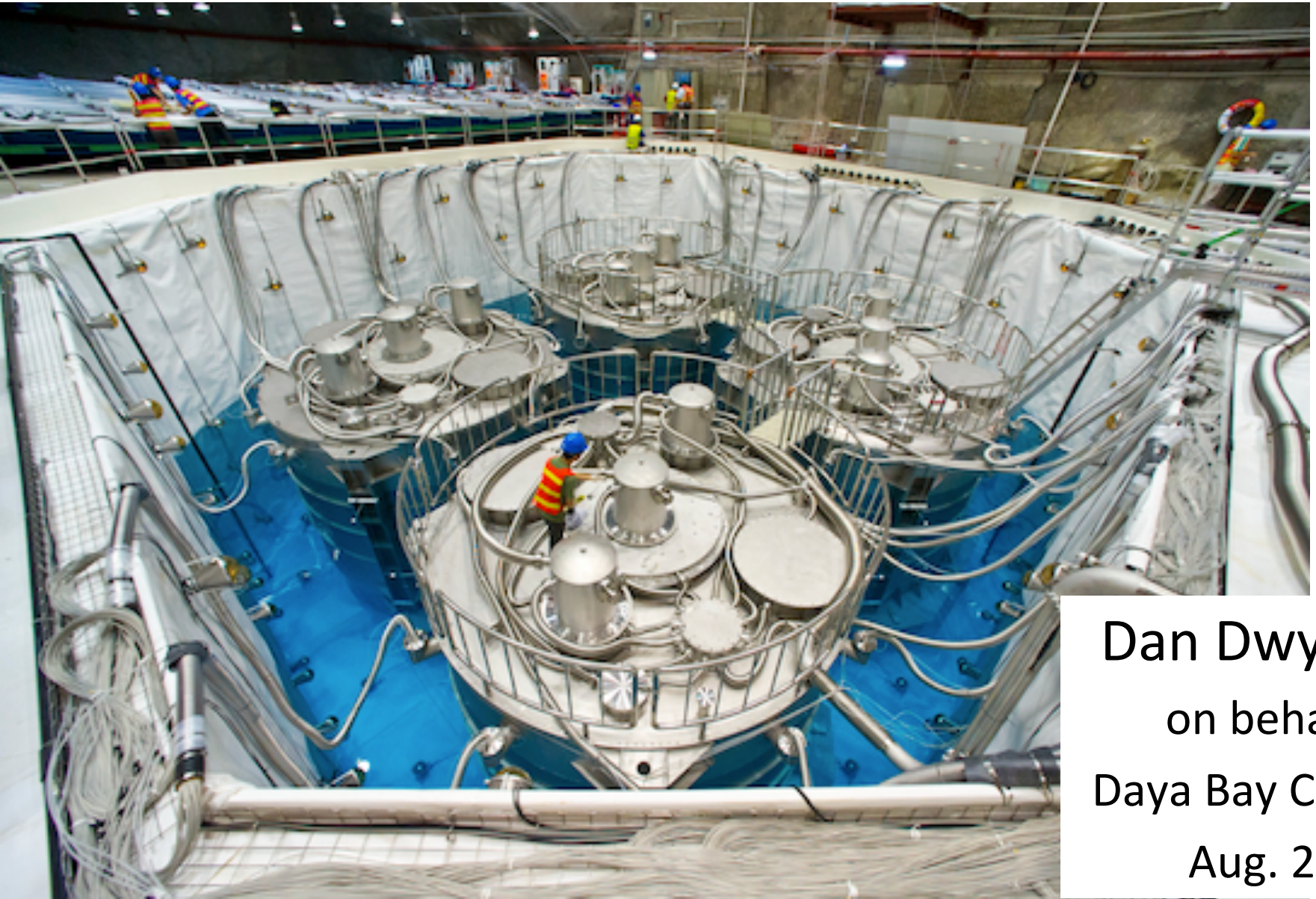

Dan Dwyer (LBNL)
on behalf of the
Daya Bay Collaboration
Aug. 22, 2013

Solar Neutrino Problem

1968: Davis detects 1/3 expected solar neutrinos

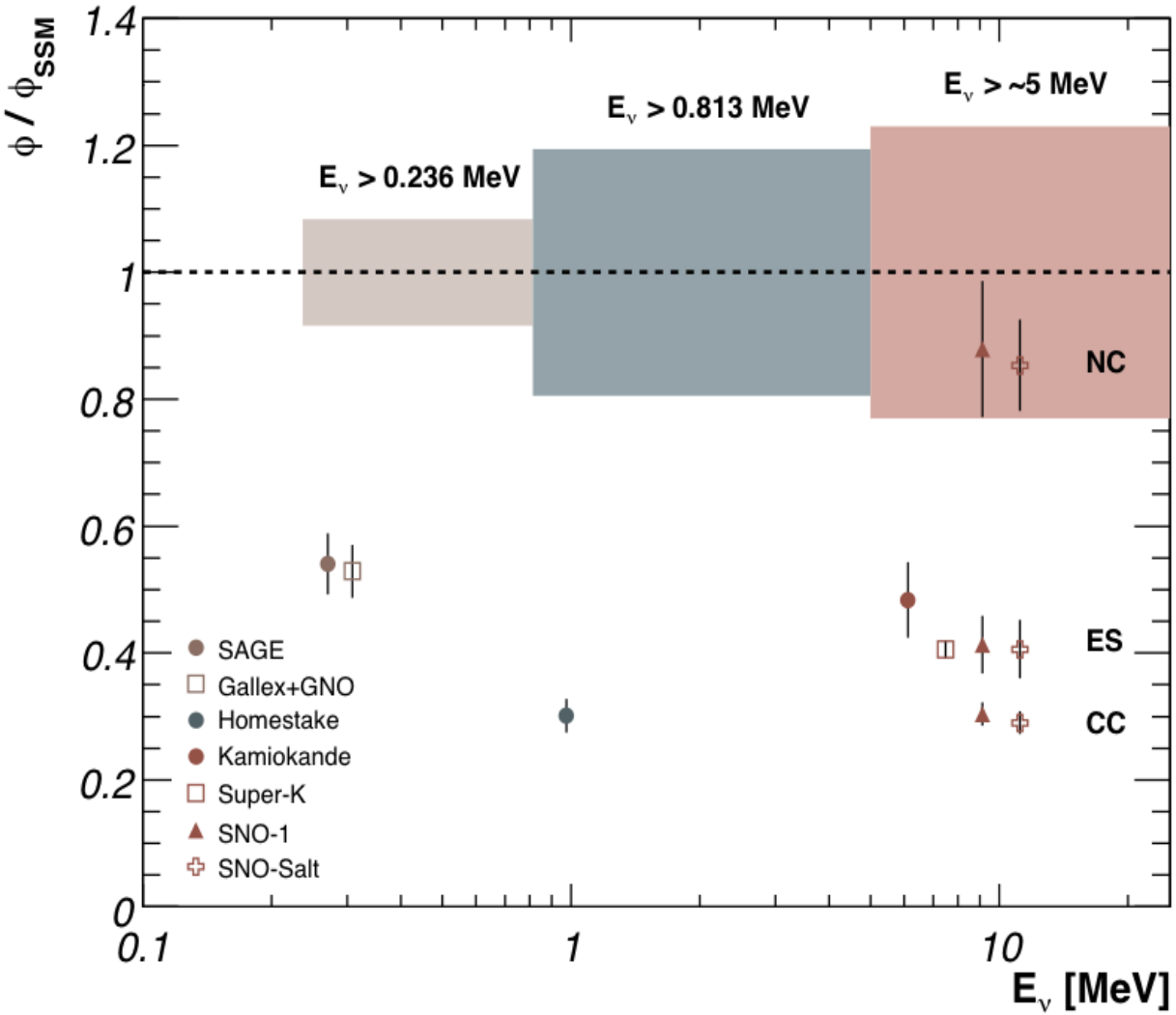

2002: SNO shows evidence for flavor-change!

Phys. Rev. Lett. 89, 011301 (2002)

Phys. Rev. Lett. 92, 181301 (2004)

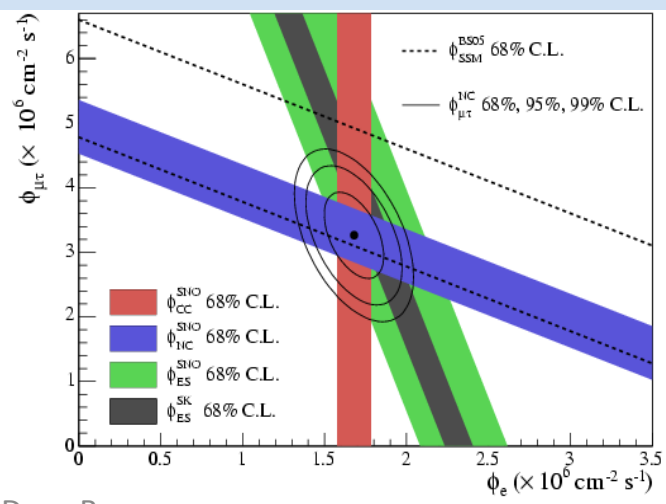

Neutrino Oscillation

Neutrinos change flavor (e,μ,τ) with time

Principle: Mass eigenstates ≠ Interaction (flavor) eigenstates

$$|\nu_\alpha\rangle = \sum_{i=1}^{3} U_{\alpha,i}\,|\nu_i\rangle$$

Physical Parameters:

θ:

3 angles between mass/flavor eigenstates set **oscillation amplitude**

Δm^2:

Differences in 3 neutrino masses determine **oscillation frequency** (distance)

We want to know θ and Δm^2

Survival Probability:

$$P_{\bar{\nu}_e \to \bar{\nu}_e} = 1 - \sin^2 2\theta_{13} \sin^2\left(\Delta m^2_{ee} \frac{L}{4E}\right) - \sin^2 2\theta_{12} \cos^4 2\theta_{13} \sin^2\left(\Delta m^2_{21} \frac{L}{4E}\right)$$

Daya Bay (~2km) KamLAND (~200km)

$$P_{\bar{\nu}_e \to \bar{\nu}_e} = 1 - \sin^2 2\theta_{13} \sin^2\left(\Delta m^2_{ee} \frac{L}{4E}\right) - \sin^2 2\theta_{12} \cos^4 2\theta_{13} \sin^2\left(\Delta m^2_{21} \frac{L}{4E}\right)$$

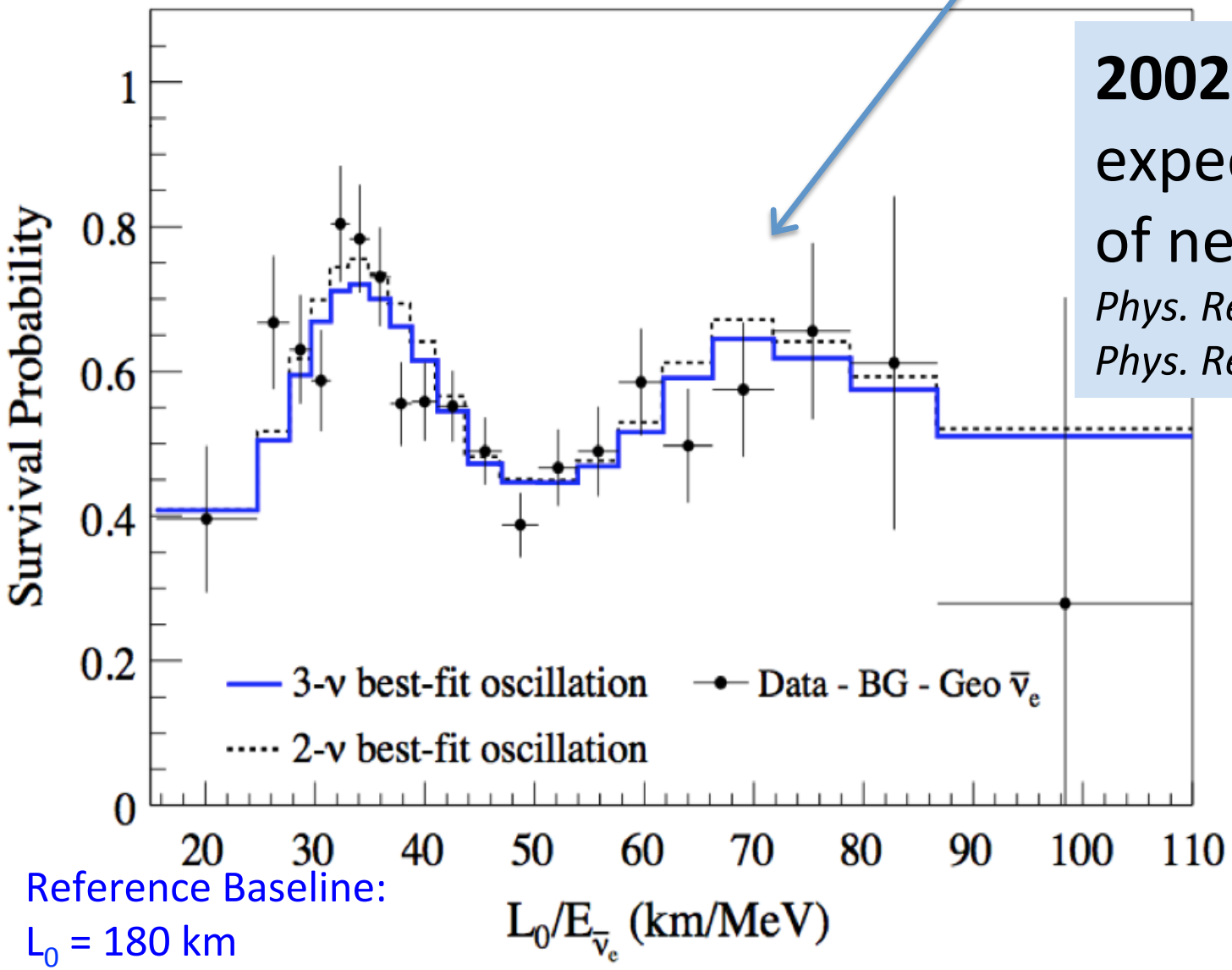

2002: KamLAND shows expected signature of neutrino oscillation.

Phys. Rev. Lett. 89, 011301 (2002)
Phys. Rev. Lett. 92, 181301 (2004)

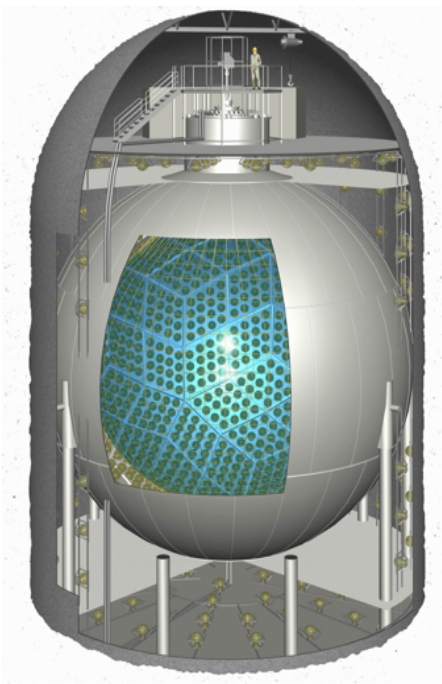

Reference Baseline:
L_0 = 180 km

A Decade of Progress

The neutrino mixing matrix only recently measured.

$$c_{ij} \equiv \cos\theta_{ij} \text{ and } s_{ij} \equiv \sin\theta_{ij}$$

$$U_{if} = \begin{pmatrix} 1 & 0 & 0 \\ 0 & c_{23} & s_{23} \\ 0 & -s_{23} & c_{23} \end{pmatrix} \times \begin{pmatrix} c_{13} & 0 & s_{13}e^{-i\delta} \\ 0 & 1 & 0 \\ -s_{13}e^{i\delta} & 0 & c_{13} \end{pmatrix} \times \begin{pmatrix} c_{12} & s_{12} & 0 \\ -s_{12} & c_{12} & 0 \\ 0 & 0 & 1 \end{pmatrix}$$

$\theta_{23} \approx 45^o$
Atmospheric ν
Accelerator ν

$\theta_{13} \approx 9^o$
Short-Baseline Reactor ν
Accelerator ν

$\theta_{12} \approx 35^o$
Solar ν
Long-Baseline Reactor ν

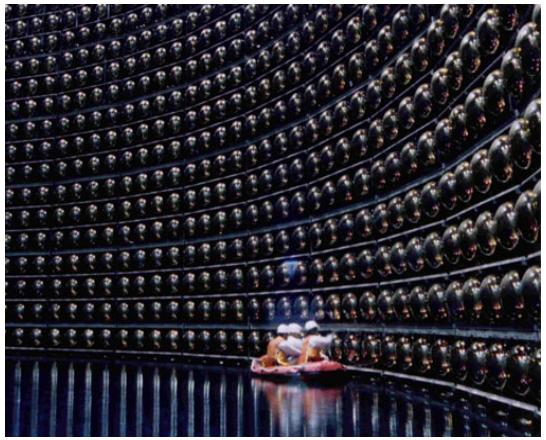

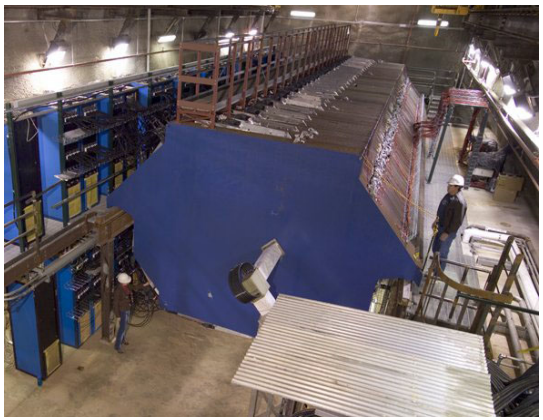

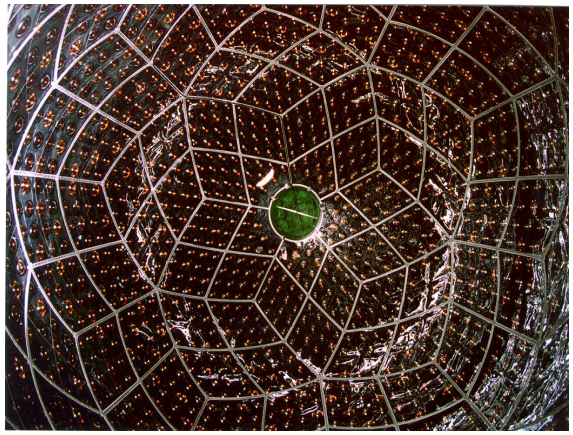

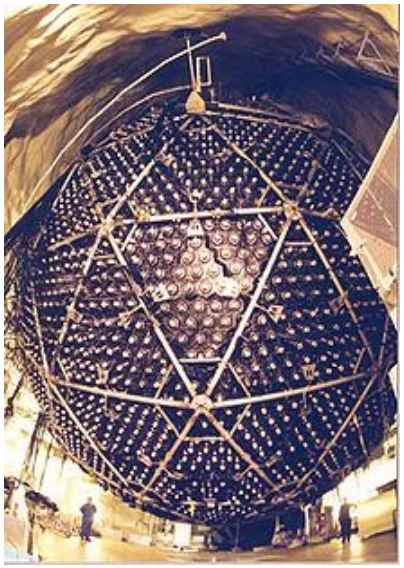

An International Effort: 230 Collaborators from 40 Institutions

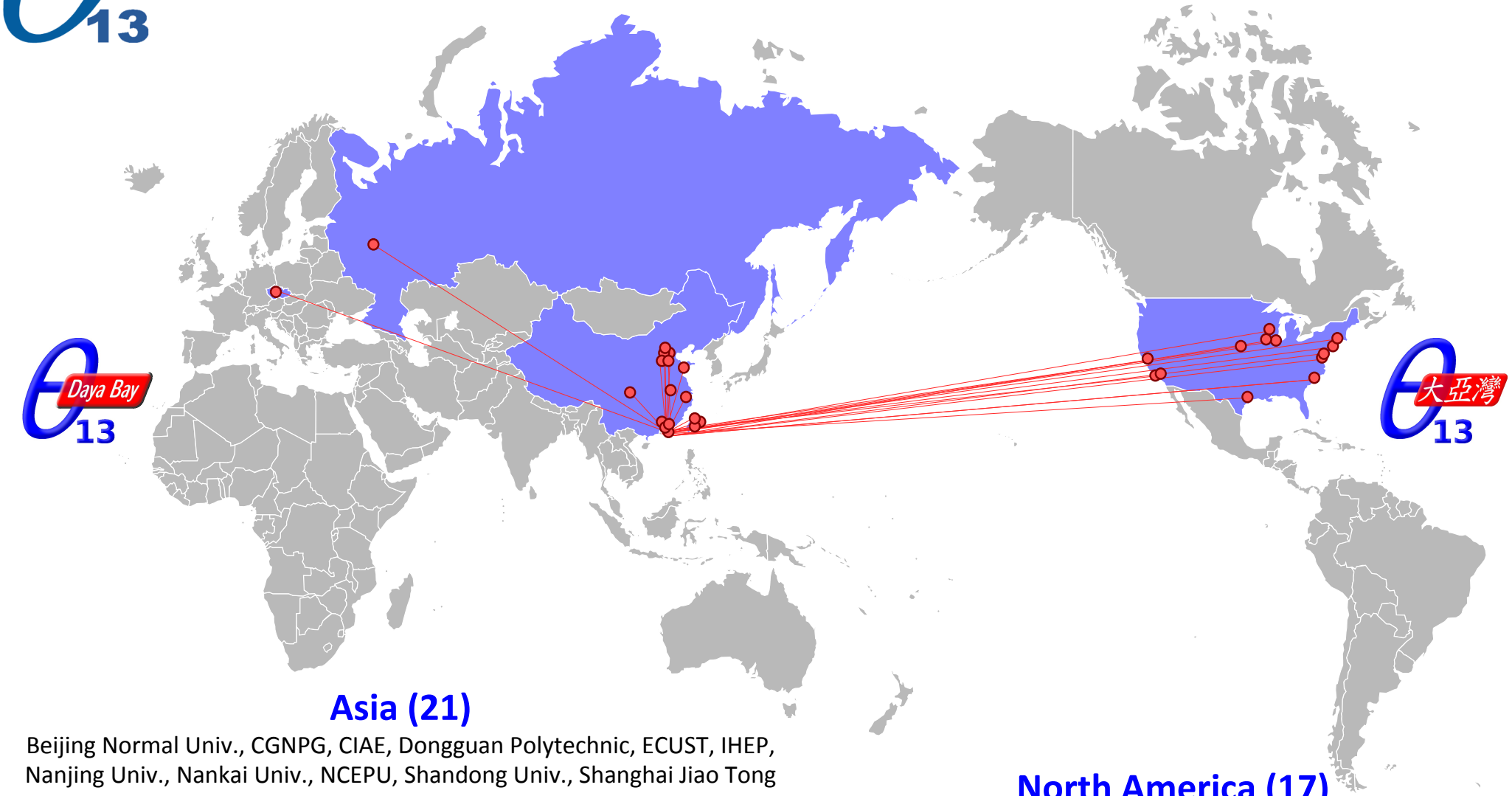

Asia (21)

Beijing Normal Univ., CGNPG, CIAE, Dongguan Polytechnic, ECUST, IHEP, Nanjing Univ., Nankai Univ., NCEPU, Shandong Univ., Shanghai Jiao Tong Univ., Shenzhen Univ., Tsinghua Univ., USTC, Xian Jiaotong Univ., Zhongshan Univ.,
Chinese Univ. of Hong Kong, Univ. of Hong Kong,
National Chiao Tung Univ., National Taiwan Univ., National United Univ.

North America (17)

Brookhaven Natl Lab, CalTech, Illinois Institute of Technology, Iowa State, Lawrence Berkeley Natl Lab, Princeton, Rensselaer Polytechnic, Siena College, UC Berkeley, UCLA, Univ. of Cincinnati, Univ. of Houston, UIUC, Univ. of Wisconsin, Virginia Tech, William & Mary, Yale

Europe (2)

Charles University, JINR Dubna

Searching for Neutrinos in China

A Powerful Neutrino Source at an Ideal Location

Among the top 5 most powerful reactor complexes in the world, 6 cores produce 17.4 GW$_{th}$ power, 35 × 10^{20} neutrinos per second

A Relative Measurement

Absolute Reactor Flux:

Largest uncertainty in previous measurements

Relative Measurement:

Multiple detectors remove absolute uncertainty

First proposed by L. A. Mikaelyan and V.V. Sinev, Phys. Atomic Nucl. 63 1002 (2000)

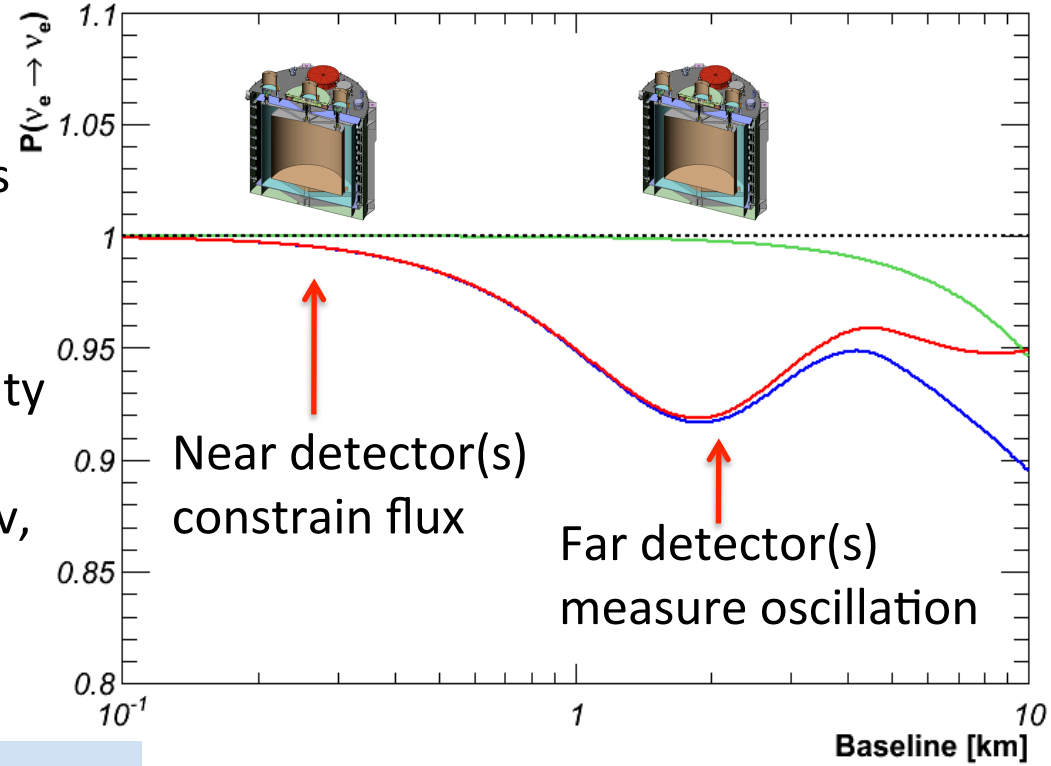

Far/Near ν_e Ratio

Distances from reactor

Oscillation deficit

$$\frac{N_f}{N_n} = \left(\frac{N_{p,f}}{N_{p,n}}\right)\left(\frac{L_n}{L_f}\right)^2\left(\frac{\epsilon_f}{\epsilon_n}\right)\left[\frac{P_{sur}(E, L_f)}{P_{sur}(E, L_n)}\right]$$

Detector Target Mass

Detector efficiency

Experiment Layout

Far hall measures oscillation

Two near halls constrain reactor flux

	Overburden	R_μ	E_μ	D1,2	L1,2	L3,4
EH1	250	1.27	57	364	857	1307
EH2	265	0.95	58	1348	480	528
EH3	860	0.056	137	1912	1540	1548

TABLE I. Overburden (m.w.e), muon rate R_μ (Hz/m^2), and average muon energy E_μ (GeV) of the three EHs, and the distances (m) to the reactor pairs.

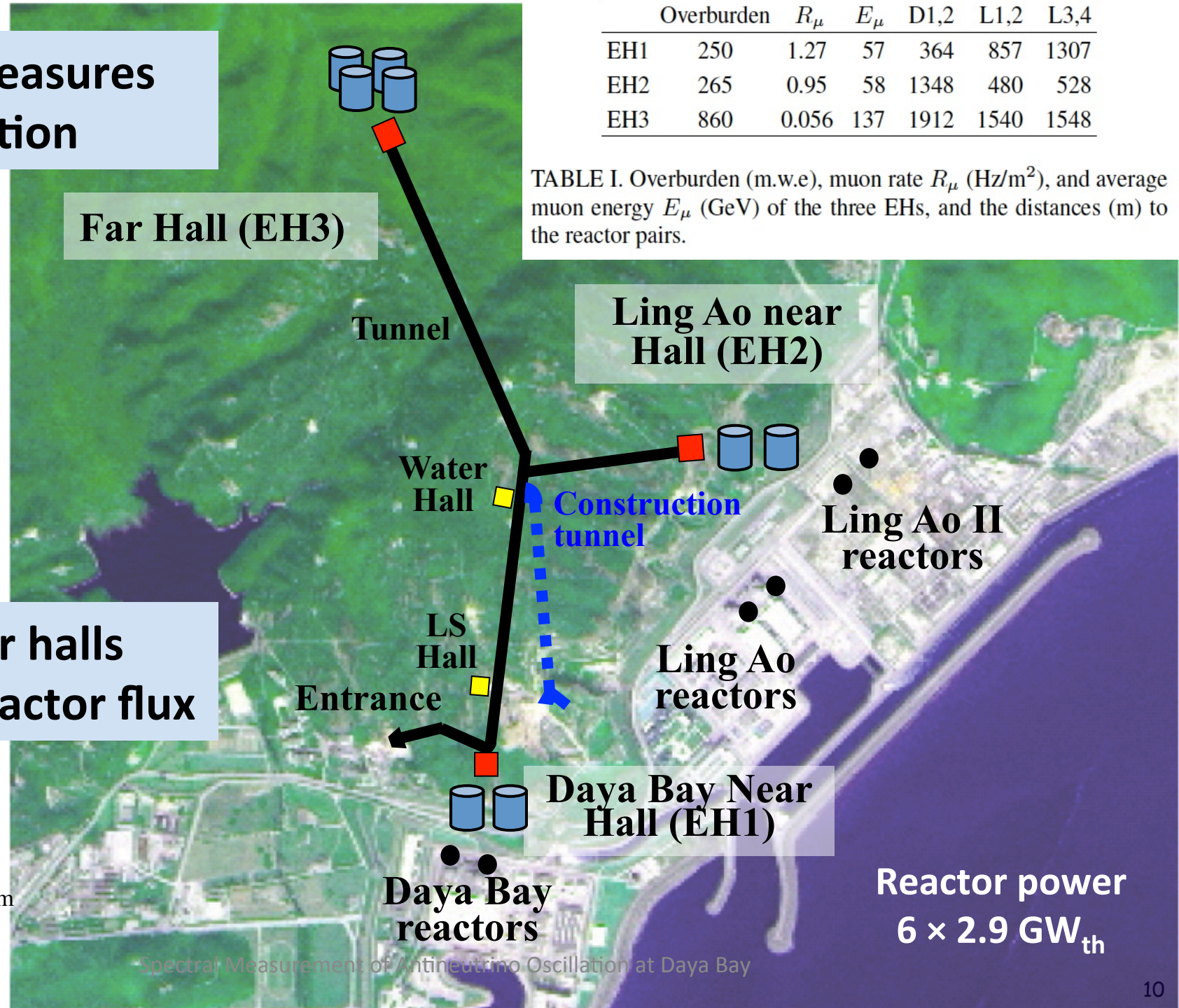

m

Reactor power
6 × 2.9 GW_{th}

Daya Bay Advantages

Baseline Optimization

- Detector locations optimized to known parameter space of $|\Delta m^2_{ee}|$
- Far site maximizes term dependent on $\sin^2 2\theta_{13}$

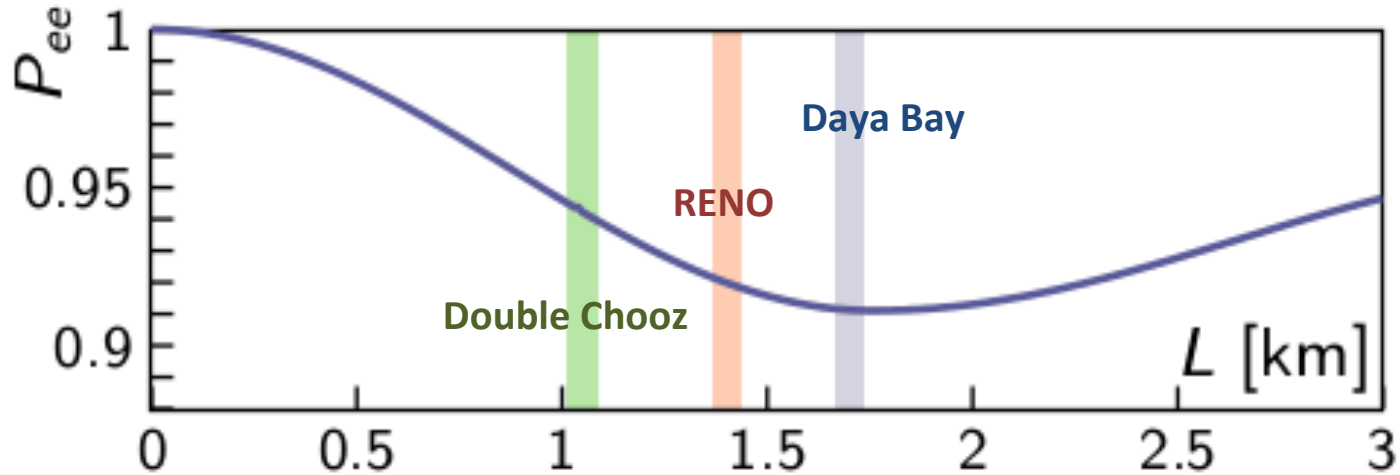

Go strong, big and deep!

	Reactor [GW_{th}]	Target [tons]	Depth [m.w.e]
Double Chooz	8.6	16 (2 × 8)	300, 120 (far, near)
RENO	16.5	32 (2 × 16)	450, 120
Daya Bay	17.4	160 (8 × 20)	860, 250
	Large Signal		Low Background

Reactor Antineutrinos

Nuclear fission releases: ~6 antineutrinos/fission

Standard electric power reactor: ~10^{20} fissions/second

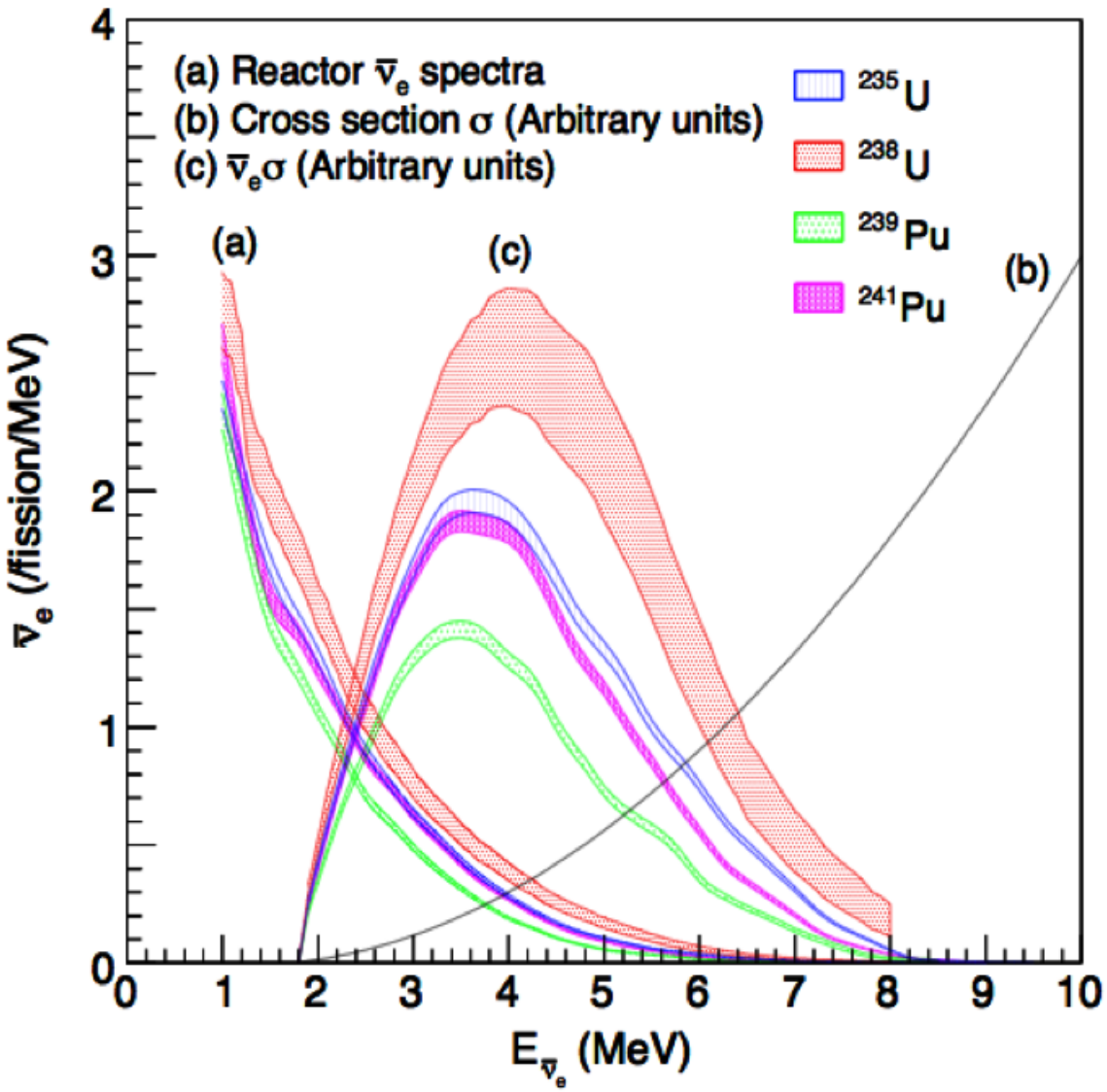

Detection Method

Inverse β-decay (IBD):

$$\bar{\nu}_e + p \rightarrow e^+ + n$$
$$\downarrow$$
$$n + {}^{x}Gd \rightarrow {}^{x+1}Gd + \gamma$$

Prompt positron:

Carries antineutrino energy

$E_{e+} \approx E_\nu - 0.8$ MeV

Delayed neutron capture:

Efficiently tags antineutrino signal

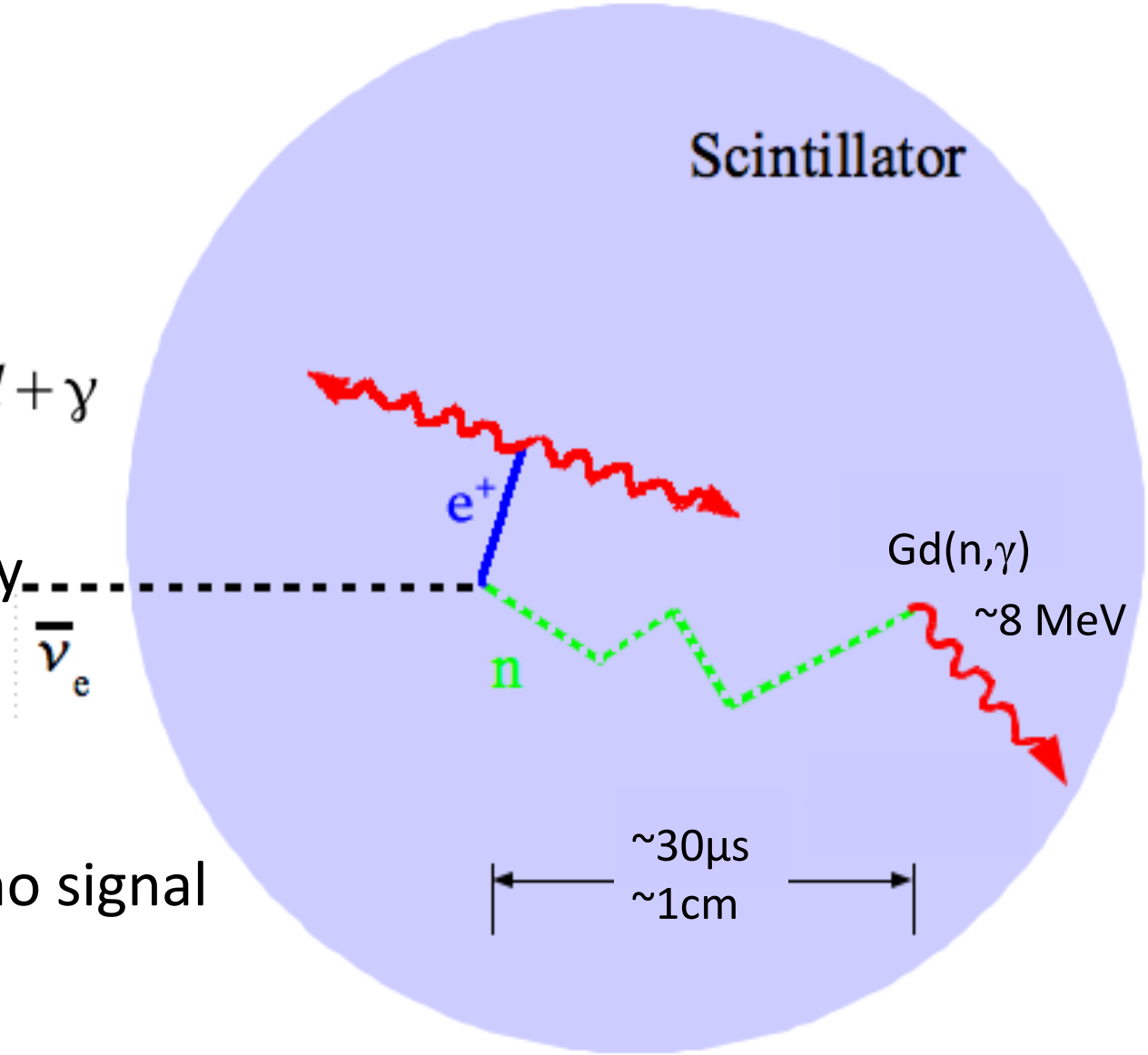

Prompt + Delayed coincidence provides distinctive signature

Antineutrino Detector (AD) Design

8 functionally identical detectors
reduce systematic uncertainties

3 zone cylindrical vessels

	Liquid	Mass	Function
Inner acrylic	Gd-doped liquid scint.	20 t	Antineutrino target
Outer acrylic	Liquid scintillator	20 t	Gamma catcher
Stainless steel	Mineral oil	40 t	Radiation shielding

192 8 inch PMTs in each detector

Top and bottom reflectors increase light yield and flatten detector response

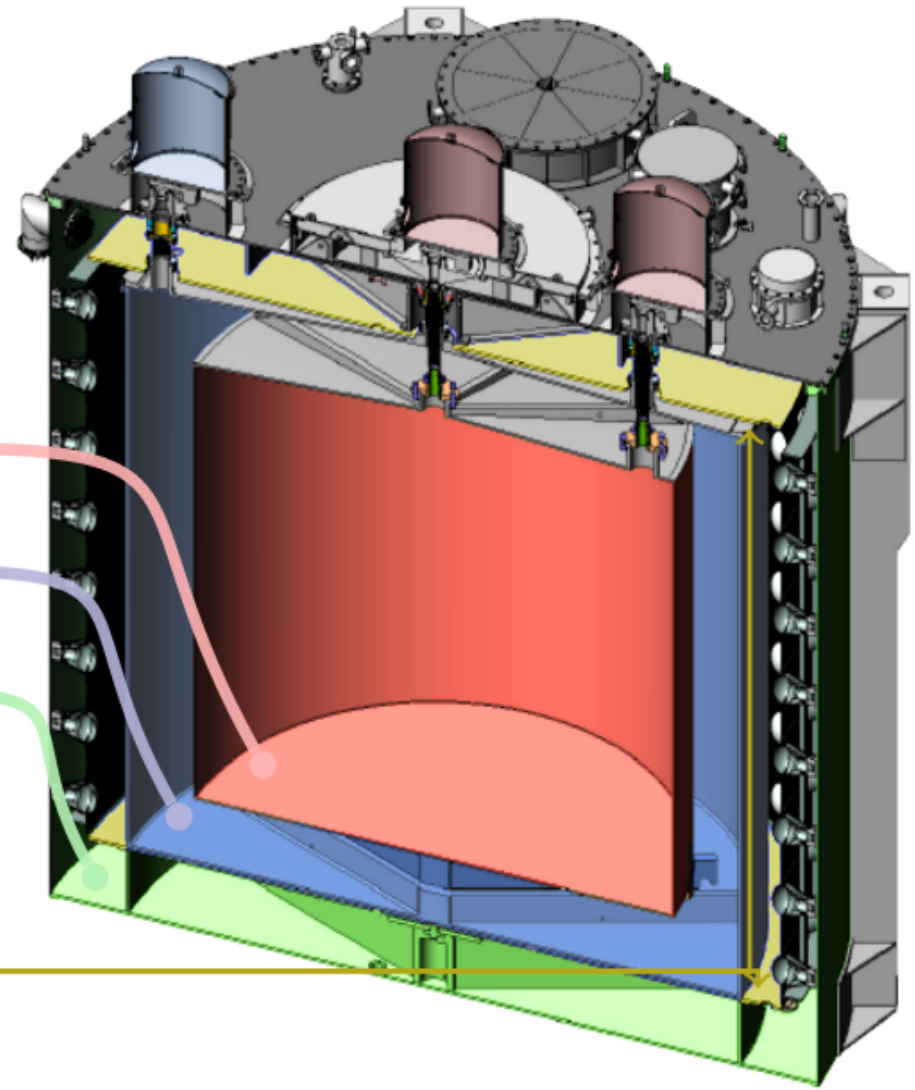

Automated Calibration System

3 Automatic calibration 'robots' (ACUs) on each detector

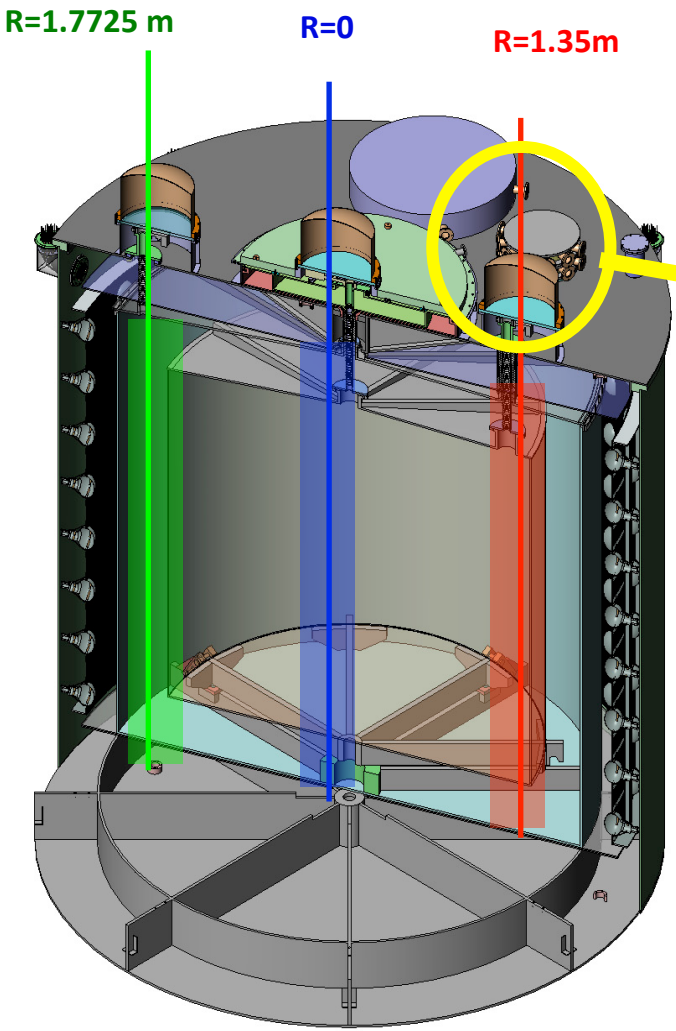

Three axes: center, edge of target, middle of gamma catcher

Top view

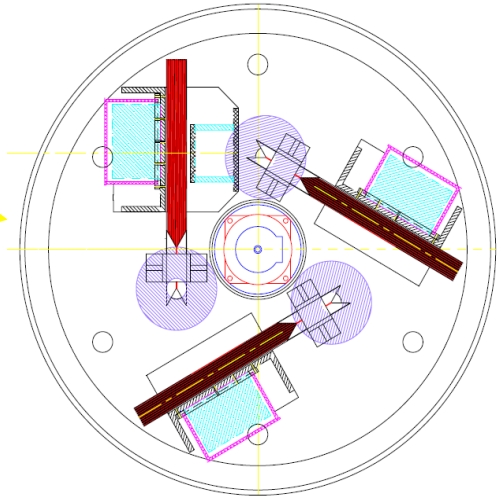

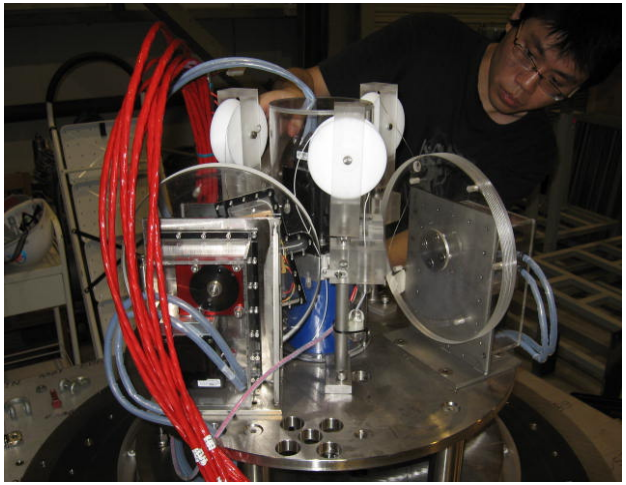

3 sources in each robot, including:

- 10 Hz ^{68}Ge (0 KE e^+ = 2×0.511 MeV γ's)
- 0.75 Hz ^{241}Am-^{13}C neutron source (3.5 MeV n without γ) + 100 Hz ^{60}Co gamma source (1.173+1.332 MeV γ)
- LED diffuser ball (500 Hz) for time calibration

Temporary special calibration sources:

γ: ^{137}Cs (0.662 MeV), ^{54}Mn (0.835 MeV), ^{40}K (1.461 MeV)

n: ^{241}Am-^{9}Be, ^{239}Pu-^{13}C

Muon Tagging System

Dual tagging systems: 2.5 meter thick two-section water shield and RPCs

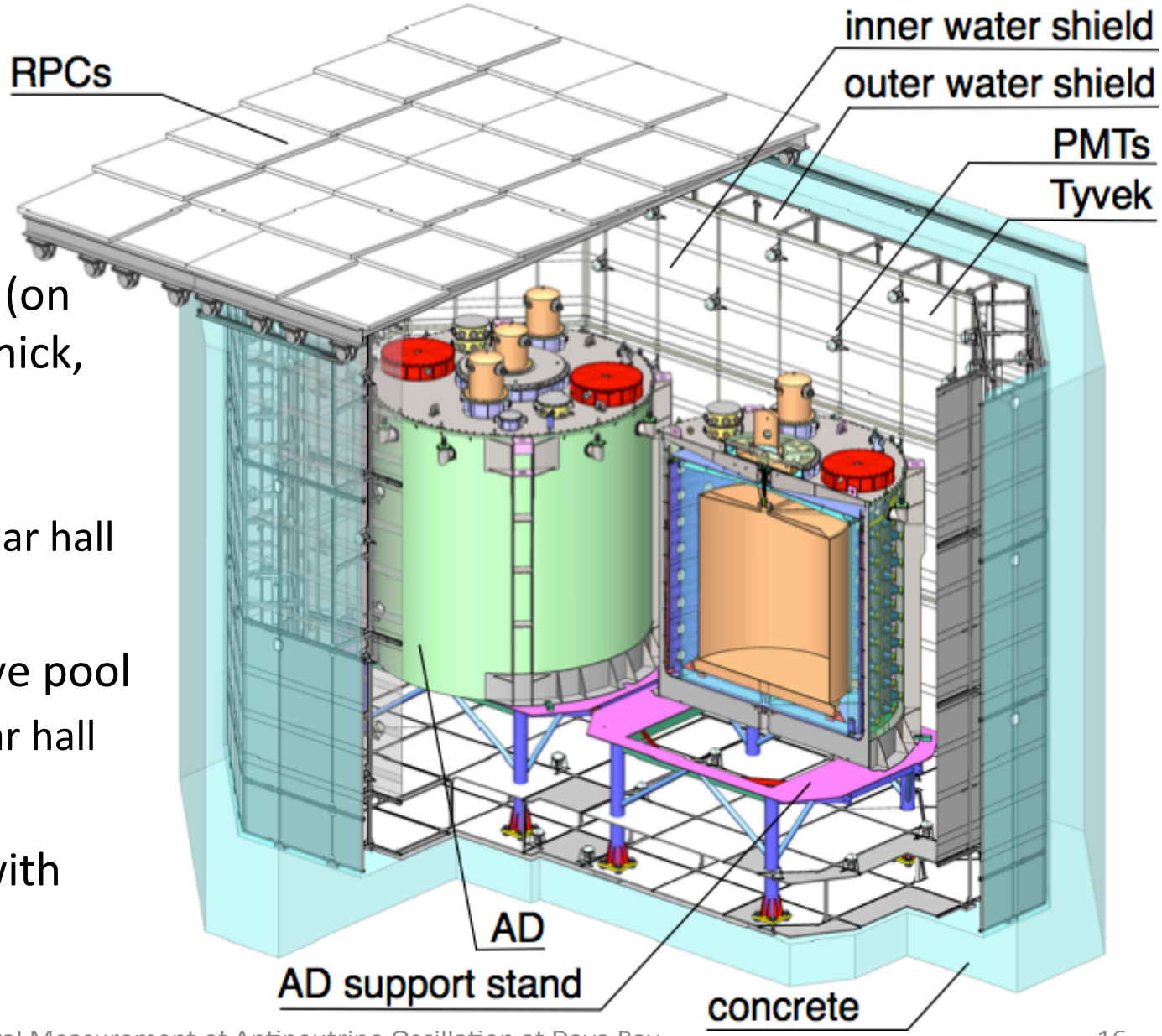

- Outer layer of water veto (on sides and bottom) is 1m thick, inner layer >1.5m. Water extends 2.5m above ADs
  - 288 8" PMTs in each near hall
  - 384 8" PMTs in Far Hall
- 4-layer RPC modules above pool
  - 54 modules in each near hall
  - 81 modules in Far Hall
- Goal efficiency: > 99.5% with uncertainty <0.25%

Underground Construction

Interior of Antineutrino Detector

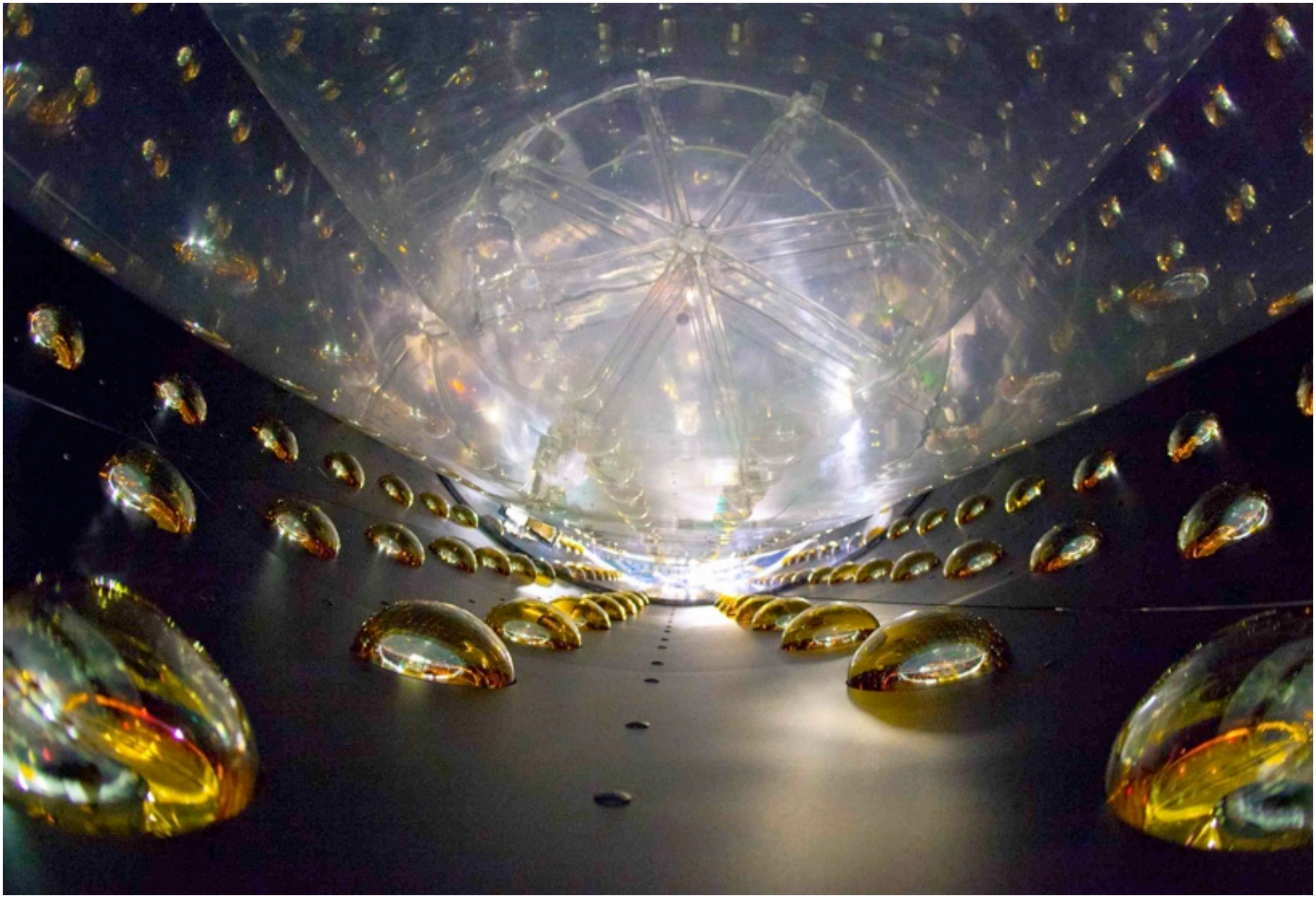

Installed Underground

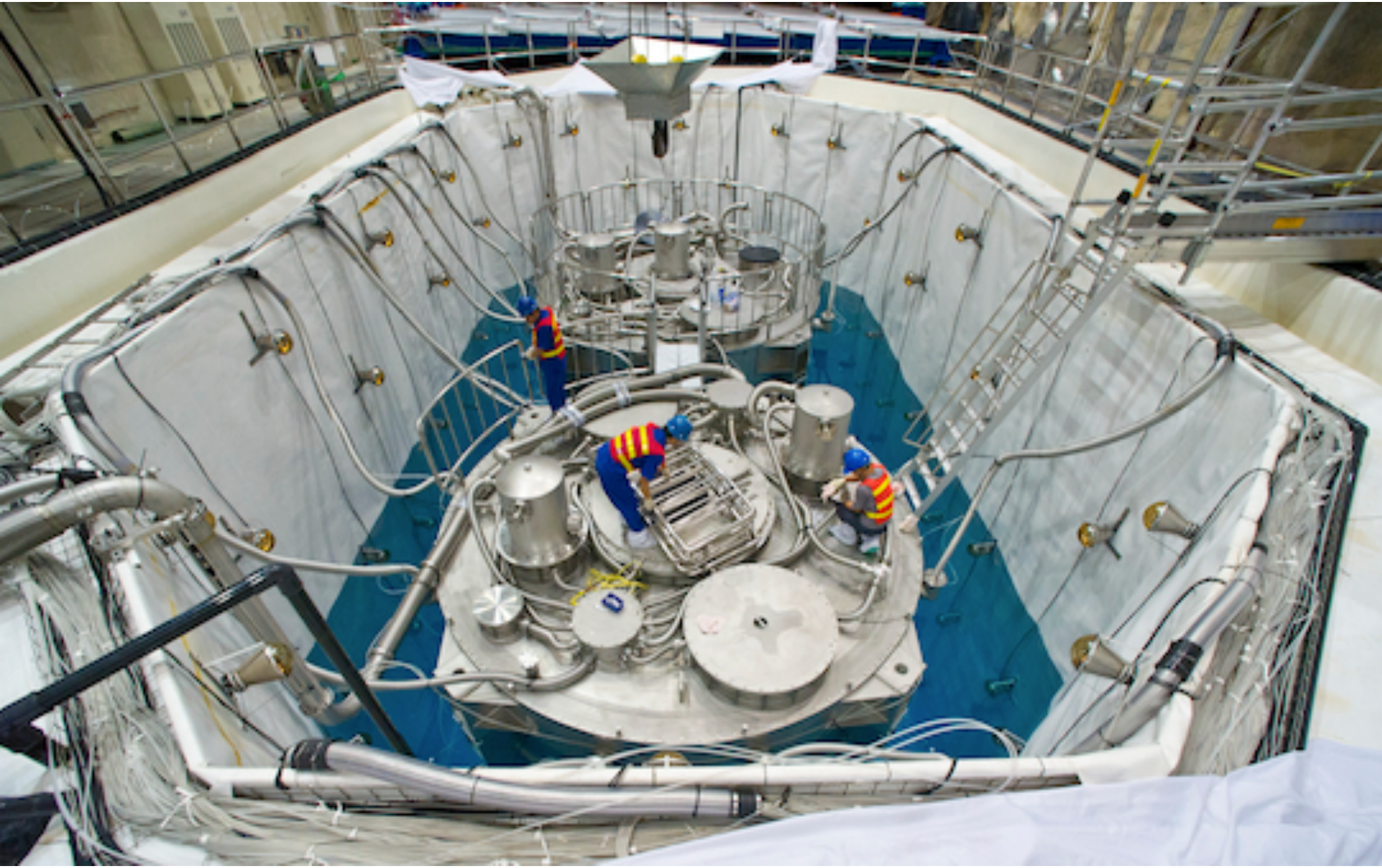

Analyzed Data Sets

Two detector comparison **[1202.6181]**

- 90 days of data, Daya Bay near only
- NIM A **685** (2012), 78-97

First oscillation analysis **[1203:1669]**

- 55 days of data, 6 ADs near+far
- PRL **108** (2012), 171803

Improved oscillation analysis **[1210.6327]**

- 139 days of data, 6 ADs near+far
- CP C **37** (2013), 011001

Spectral Analysis

- 217 days, complete 6 AD period
- 55% more statistics than CPC result

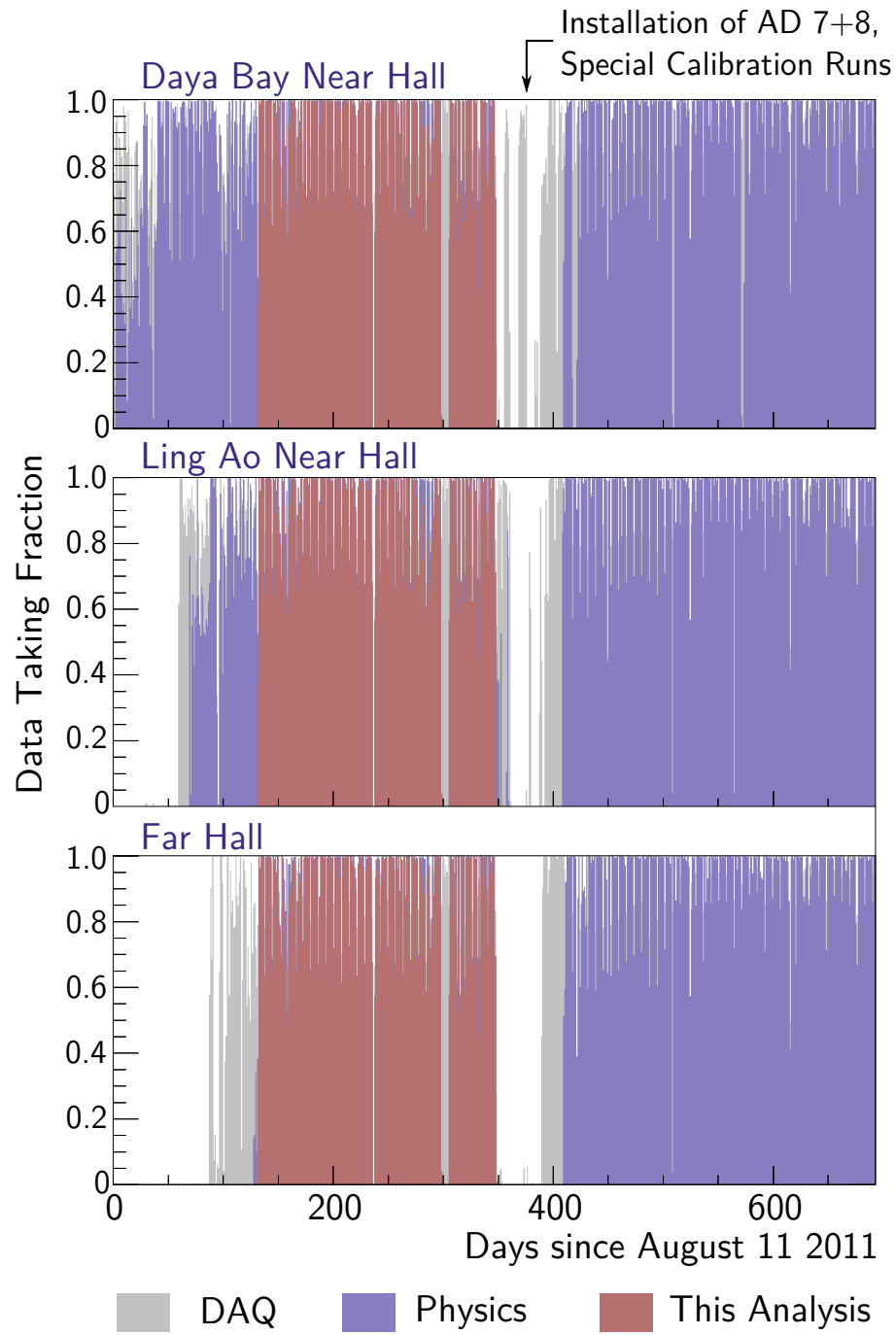

Initial Results

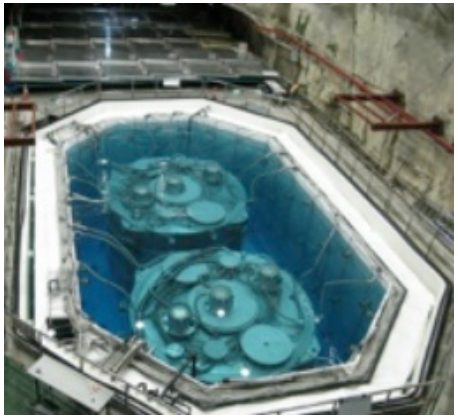
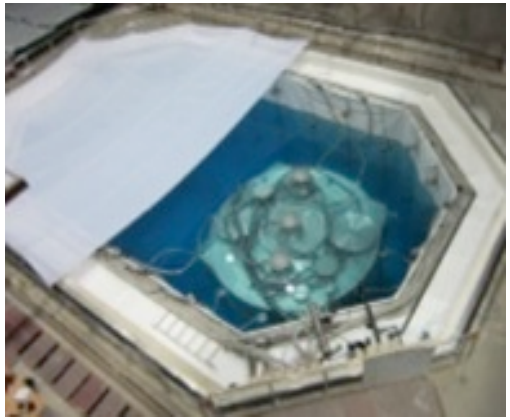
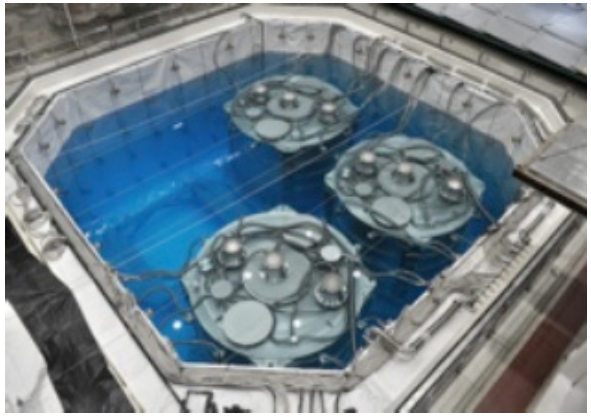

Based on 55 days of data with 6 ADs, discovered disappearance of reactor $\bar{\nu}_e$ at short baseline in March 2012. [PRL **108**, 171803]

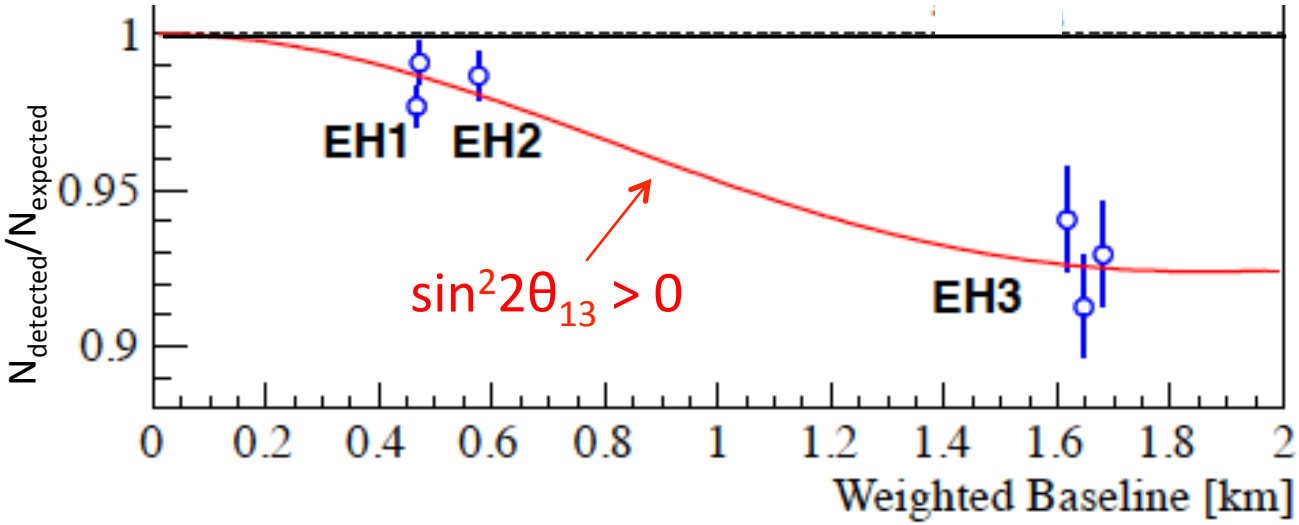

Obtained the most precise value of θ_{13} in Jun. 2012:

$$\sin^2 2\theta_{13} = 0.089 \pm 0.010 \pm 0.005$$ [CPC **37**, 011001]

A Top-10 Breakthrough of 2012

Science **338**, 1527

TALENs, and another genome-editing tool called meganucleases is that they must be reengineered for each new DNA target. These proteins have two parts: the DNA targeting section and the DNA-cutting section. The new technology substitutes RNA—which is simpler to make than a piece of a protein—for the DNA targeting section. It also makes use of a bacterial protein called Cas9, which is part of a natural bacterial defense system called CRISPR, to do the cutting.

Researchers have shown in a test-tube that they can combine these two RNAs into a single one that both matches the DNA target and holds Cas9 in place. Using this system, they were able to cut specific target DNA, demonstrating the potential of Cas9 to work like TALENs. Now, those researchers are trying this approach in organisms other than bacteria, and other genome engineers are quite excited about their prospects, suggesting that it may one day challenge zinc finger nucleases and TALENs as the core genome engineering technology.

CRASH PROJECT OPENS A DOOR IN NEUTRINO PHYSICS

Sometimes it's not the result itself so much as the promise it holds that matters most. This year, physicists measured the last parameter describing how elusive particles called neutrinos morph into one another as they zip along at near–light speed. And the result suggests that in the coming decades neutrino physics will be every bit as rich as physicists had hoped—and may even help explain how the universe evolved to contain so much matter and so little antimatter.

RUNNER-UP

Born in certain nuclear interactions, neutrinos come in three types or flavors that change into one another in so-called neutrino oscillations. The rates and extents to which the flavors mix depend on six parameters: the three differences between the neutrinos' masses, and three "mixing angles." In March, the 250 researchers with the Daya Bay Reactor Neutrino Experiment in China reported that last unknown parameter, the mixing angle known as θ_{13} (pronounced "theta one three"), equals 8.8°, give or take 0.8°.

The result itself is remarkable, as it's not every year that physicists measure a new fundamental parameter. The real excitement, however, stems from the result's broader implications. The measurement proves that all three mixing angles are greater than zero. That fact, in turn, implies that the oscillations of antineutrinos might differ from those of neutrinos, something that would not be possible had θ_{13} equaled zero.

That's a big deal. Such a difference would analogous to the effect that created the matter-antimatter imbalance in the universe.

In fact, researchers in the United States, Japan, and Europe are engaged in experiments in which they use particle accelerators to fire neutrinos hundreds of kilometers through Earth to huge particle detectors. Current efforts seek to pin down, for example, the neutrinos emanating from the reactors at the Daya Bay Nuclear Power Plant and two neighboring plants in Shenzhen. In making a definitive measurement, they beat out teams working at reactors in France and South Korea and accelerator-based experiments in Japan and the United States.

The measurement of θ_{13} wasn't the only result in particle physics this year. Researchers working with the world's largest atom smasher, the Large Hadron Collider (LHC) in Switzerland, discovered the Higgs boson, the

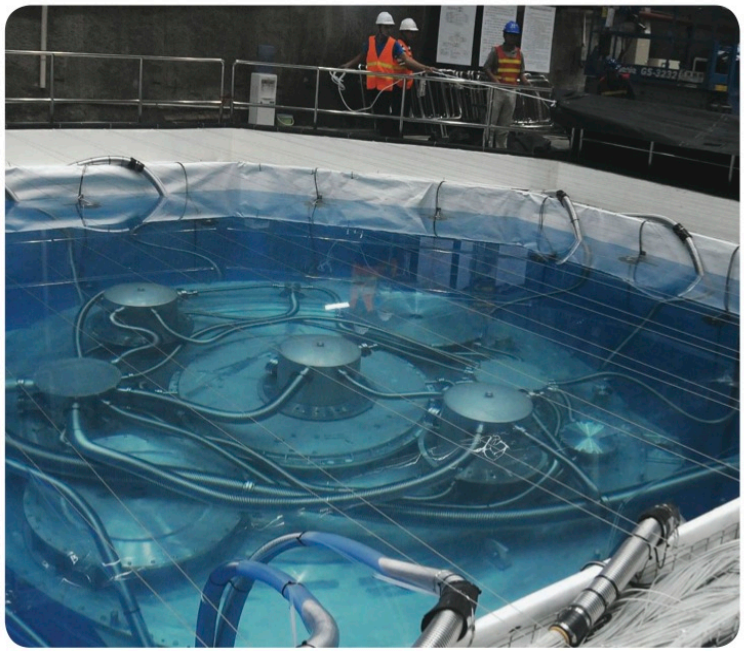

That was fast! Construction of China's Daya Bay Reactor Neutrino Experiment began in 2007. With 2 months' worth of data, it scooped competitors in Japan, France, Korea, and the United States.

D/AP IMAGES

Rate vs. Spectral Information

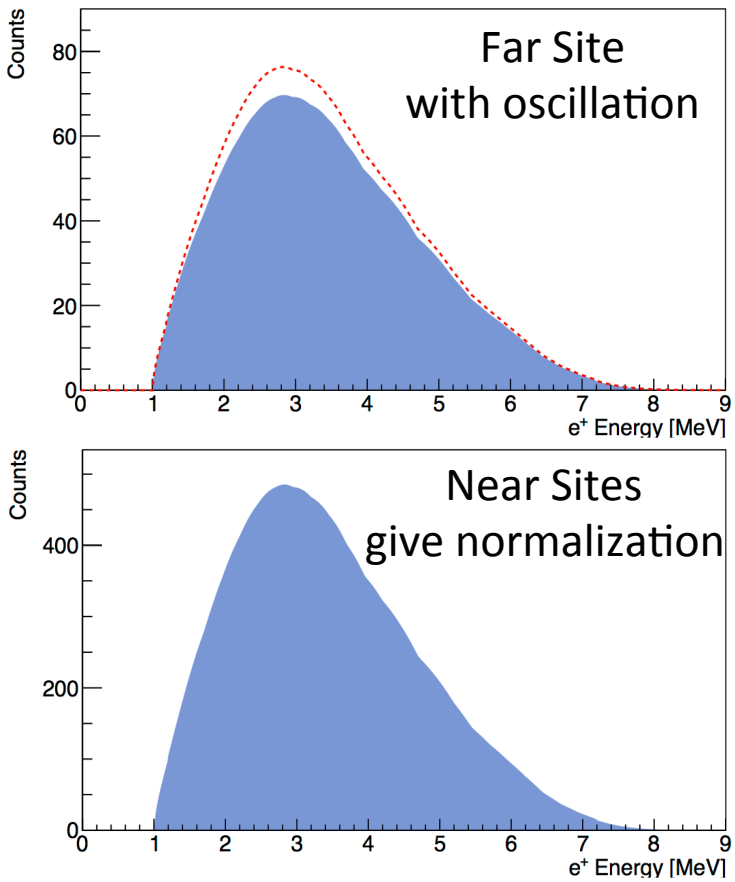

Integrate
all energies

Rate-only Analysis:

Previously reported

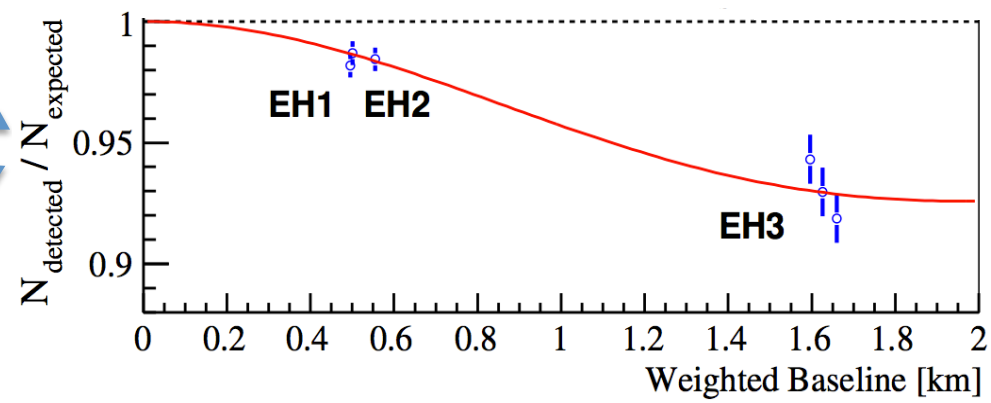

Advantages: Fewer systematic uncertainties

Disadvantages: Less sensitive, Unable to constrain Δm^2_{ee}

$$\frac{N_{far}}{N_{near}} = \frac{N_{protons,far}}{N_{protons,near}} \frac{L^2_{near}}{L^2_{far}} \frac{\epsilon_{far}}{\epsilon_{near}} \frac{\int_{E_{min}}^{E_{max}} dE\, P_{surv}(E, L_{far}; \theta_{13}, \Delta m^2_{ee})\, \sigma(E)\, \Phi(E)}{\int_{Emin}^{Emax} dE\, P_{surv}(E, L_{near}; \theta_{13}, \Delta m^2_{ee})\, \sigma(E)\, \Phi(E)}$$

Rate vs. Spectral Information

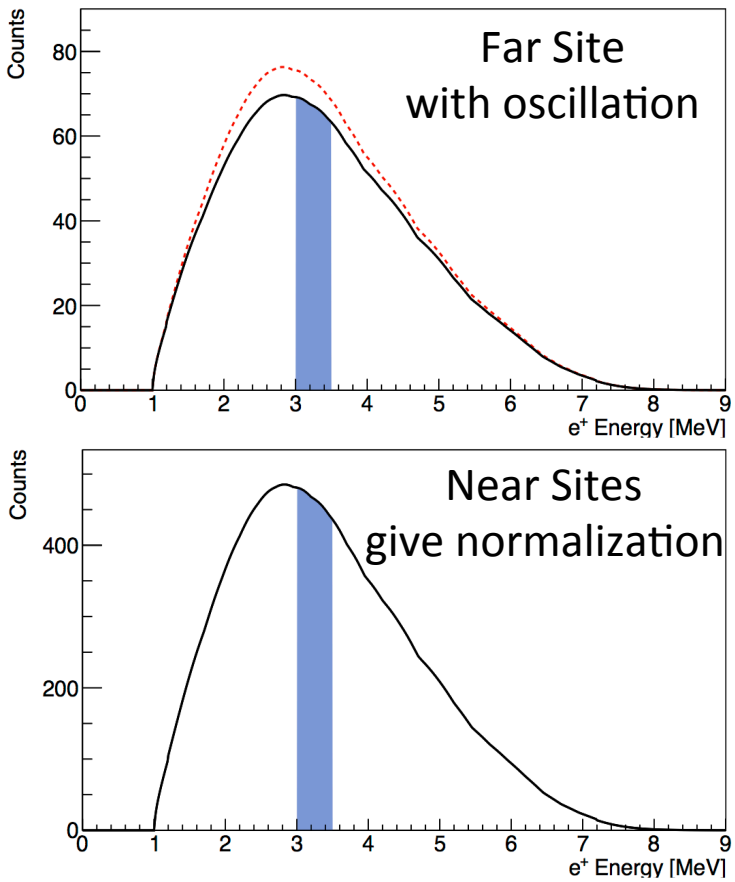

Compare each energy

Spectral Analysis:

Latest method

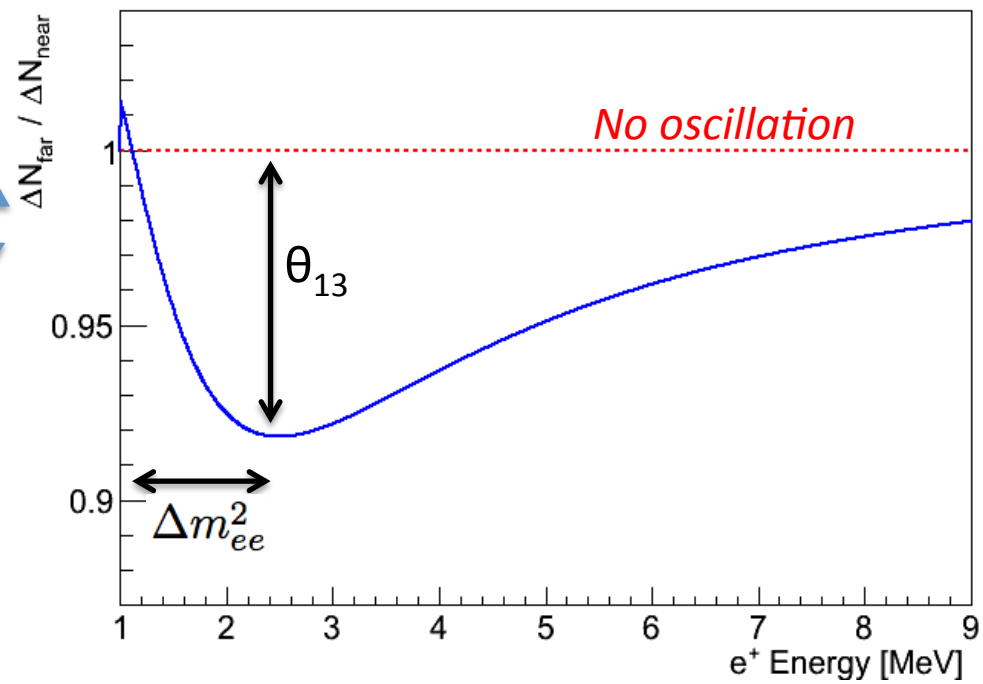

Advantages: Each energy bin is an independent oscillation measurement, Δm^2_{ee}
Disadvantages: Requires detailed understanding of detector energy response.

$$\frac{\frac{dN_{far}}{dE}}{\frac{dN_{near}}{dE}} = \frac{N_{protons,far}}{N_{protons,near}} \frac{L^2_{near}}{L^2_{far}} \frac{\epsilon_{far}}{\epsilon_{near}} \frac{P_{surv}(E, L_{far}; \theta_{13}, \Delta m^2_{ee})\, \sigma(E)\, \Phi(E)}{P_{surv}(E, L_{near}; \theta_{13}, \Delta m^2_{ee})\, \sigma(E)\, \Phi(E)}$$

Wading into the thick…

Energy Scale Systematics

Relative shift in energy between detectors can bias oscillation

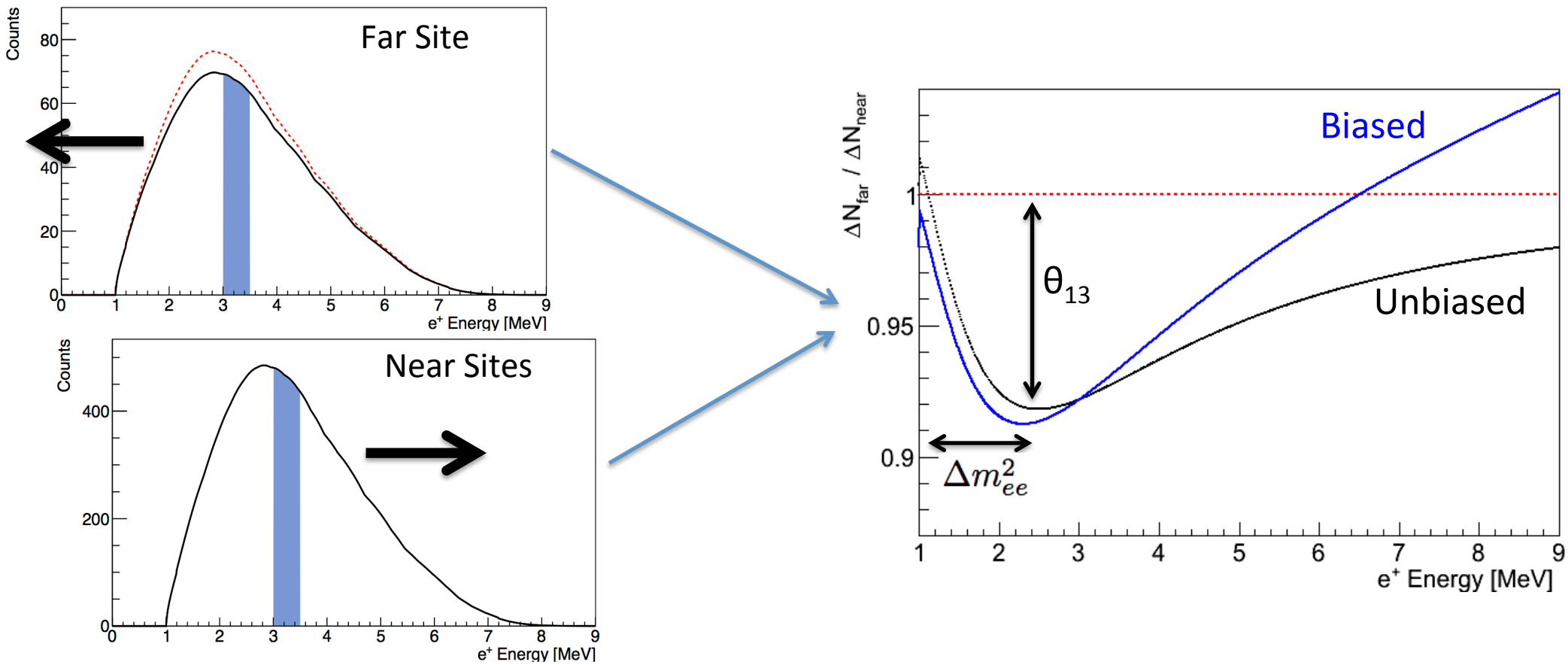

Requires careful detector calibration

Calibration: Performance

Obtain a stable and consistent Energy Response

After calibration, achieve energy response that is **stable to ~0.1%** in all detectors, with a **total relative uncertainty of 0.35%** between detectors.

Spallation *n*Gd capture peak vs. time (after all calibration)

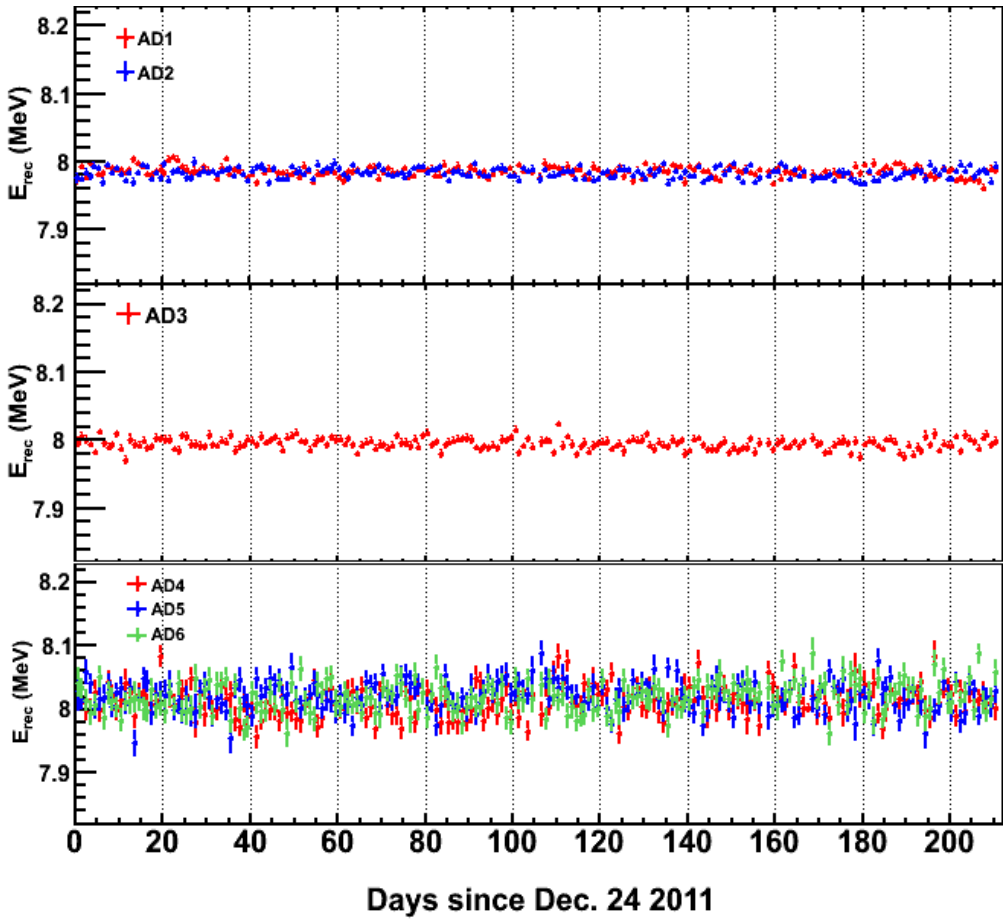

Relative energy peaks in all detectors (after calibration)

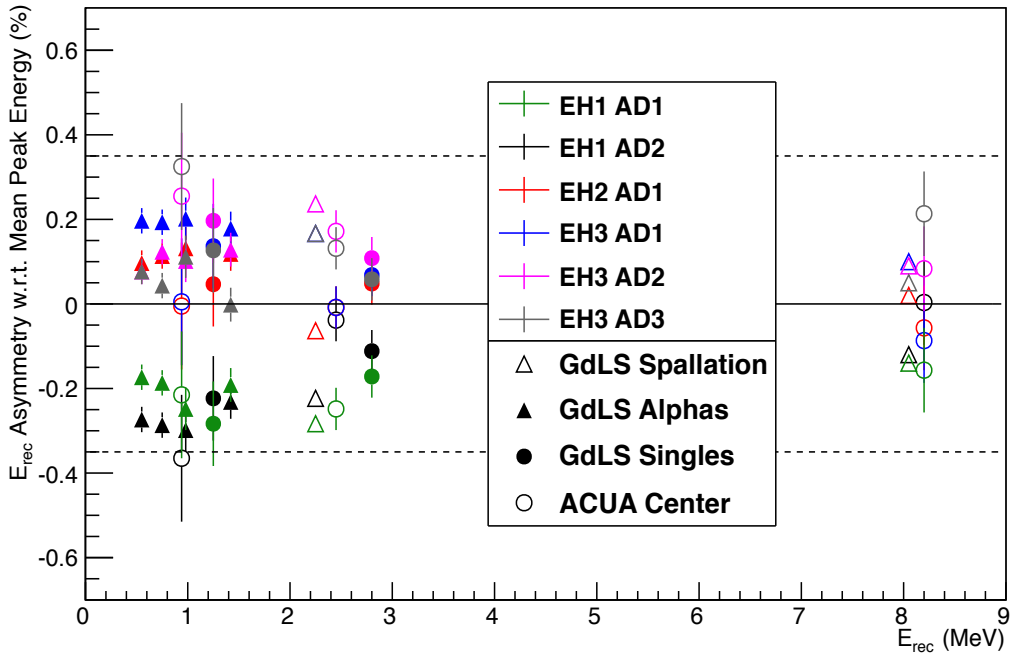

Energy Scale Systematics

Absolute shift in energy common to detectors can bias oscillation

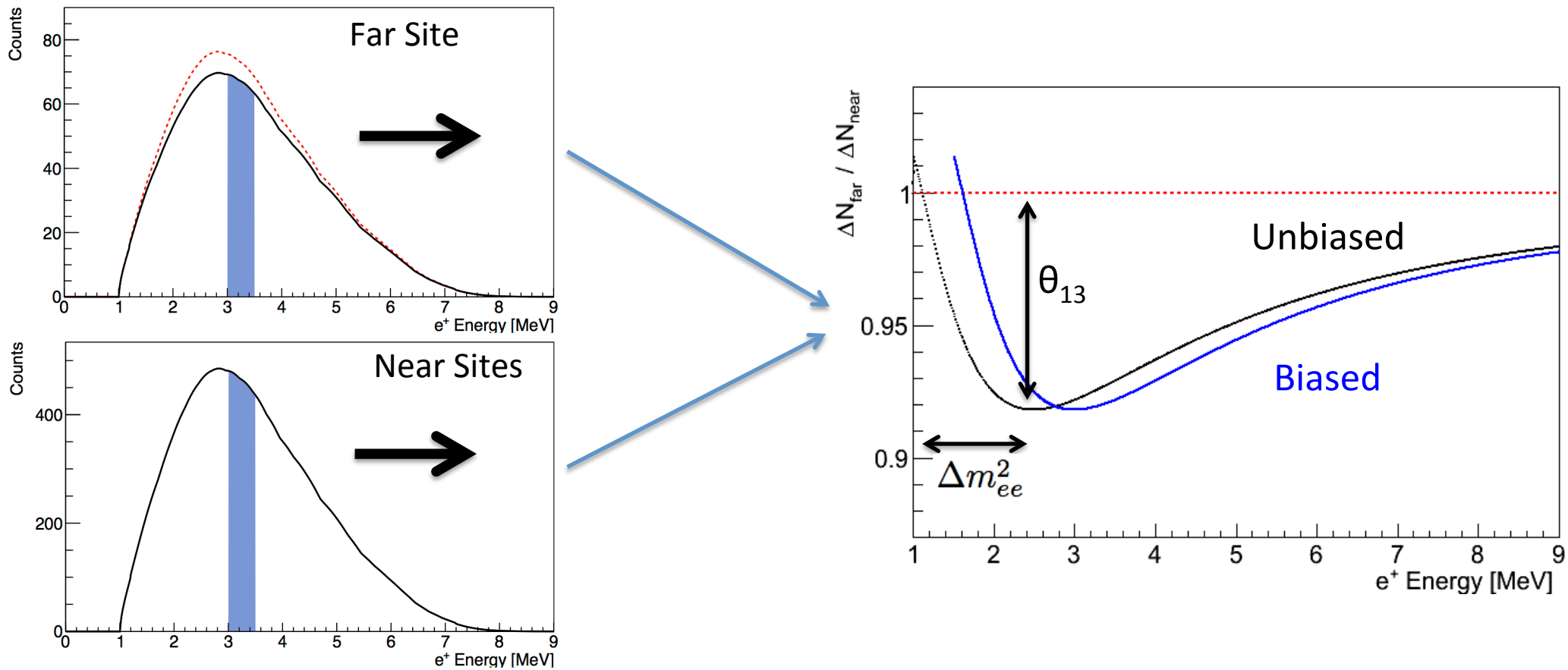

Requires detailed translation between true and detected $\overline{\nu}_e$ energy

Overview of the Energy Response Model

Particle Energy E_{true}

Energy Losses in Acrylic

Acrylic vessels non-scintillating

- Induce shape distortion
- Correction from MC

Energy Deposited in Scintillator E_{dep}

Two major sources of non-linearity. Difficult to decouple !

1: Scintillator Response

- Quenching effects
- Cherenkov radiation

Energy Converted to Visible Light E_{vis}

Energy Resolution

- Light production
- Light collection
- PMT/electronics response

2: Readout Electronics

- Charge collection efficiency decreases with visible light

Reconstructed Energy E_{rec}

Model maps true energy E_{true} to reconstructed kinetic energy E_{rec}

- Minimal impact on oscillation measurement
- Crucial for measurement of reactor spectra

Detector Response: Acrylic Vessels

Energy loss in acrylic causes small distortion of energy spectrum

If antineutrino interacts in or near acrylic vessel, a portion of the kinetic energy of inverse beta positrons will not be detected

Annihilation gammas with longer range can also deposit energy in the vessels

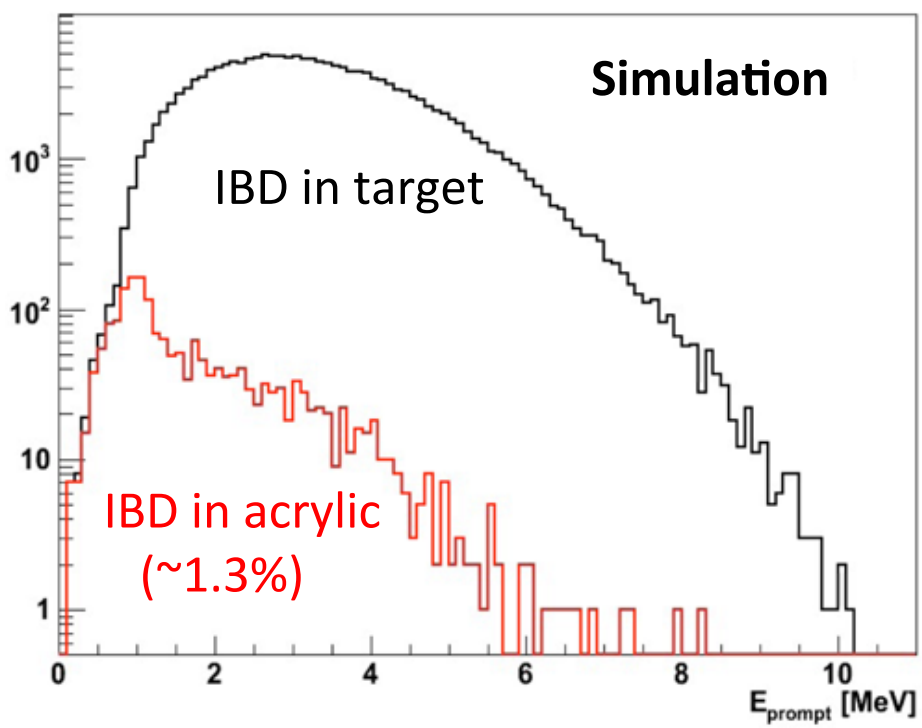

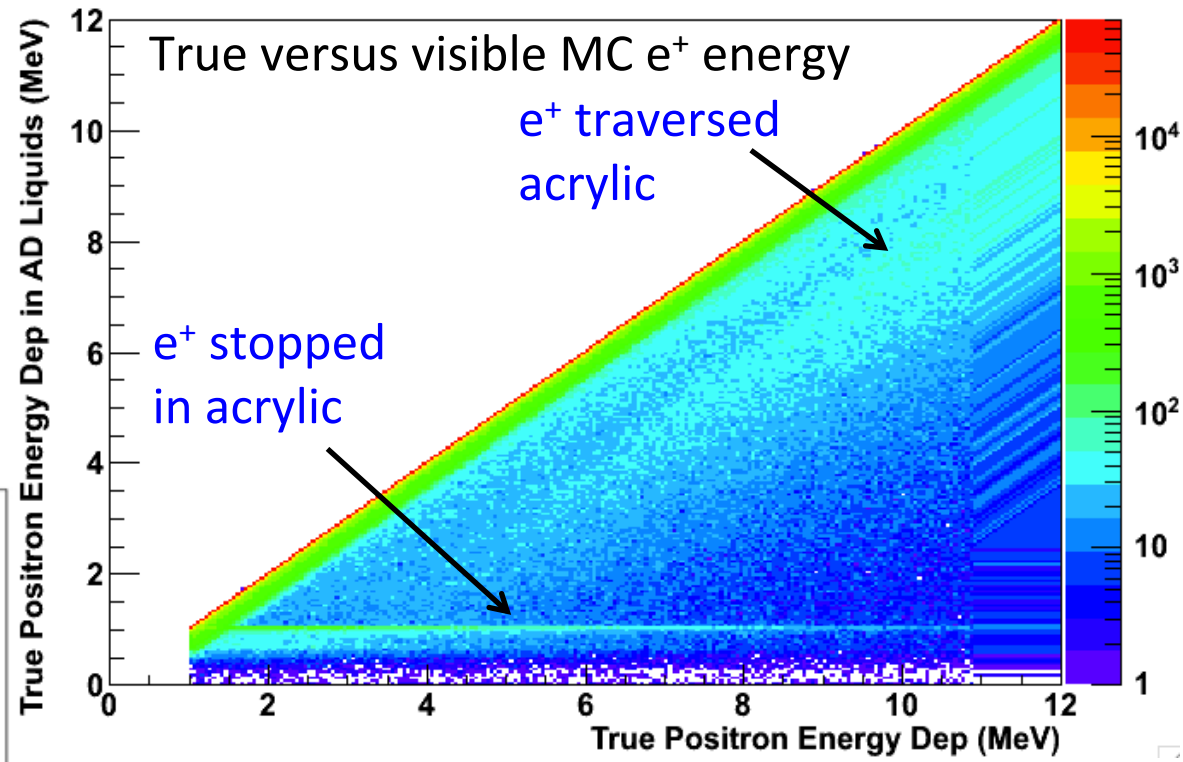

Generated 2D distortion matrix from MC to correct predicted positron energy spectrum

Uncertainties from varying acrylic vessel thicknesses and MC statistics incorporated into analysis.

Scintillator Non-linearity

Light emission is inherently non-linear relative to deposited energy

Example: Nonlinearity for γ energy deposition in KamLAND scintillator

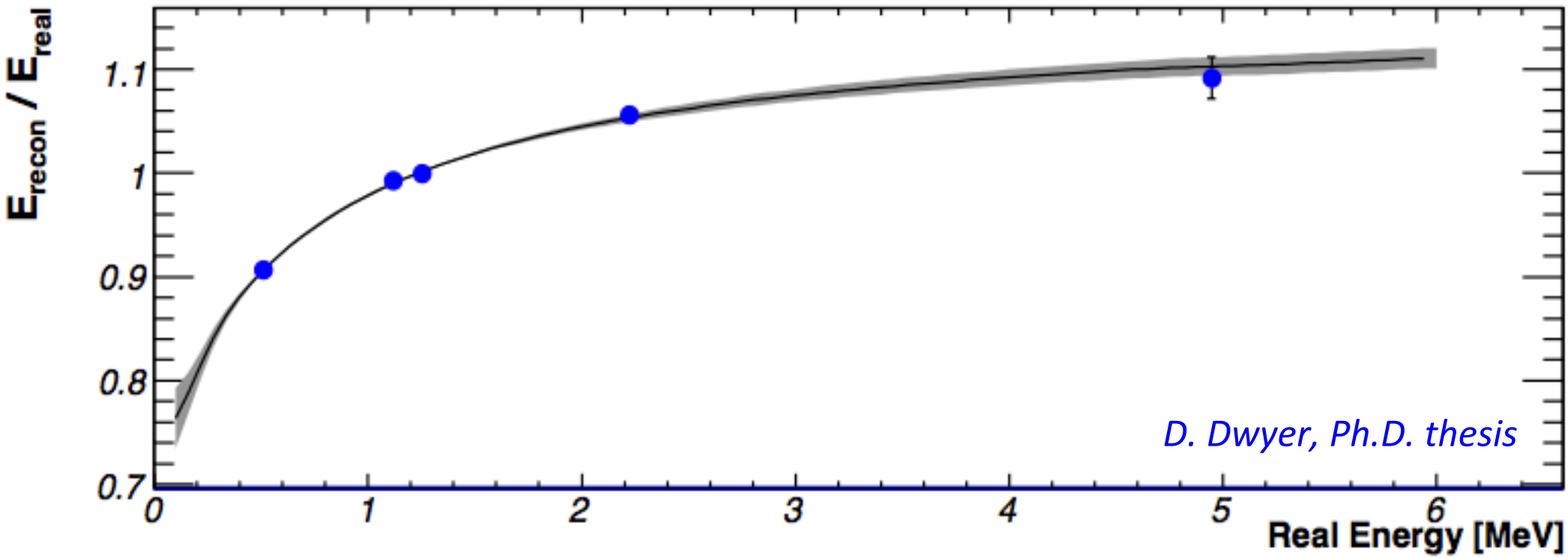

Non-linearity is also depends on particle (e^-, e^+, γ, p, α)

Scintillator Response Model

Electron response

2 parameterizations to model quenching effects and Cherenkov radiation:

1) 3-parameter purely empirical model:

$$\frac{E_{\text{vis}}}{E_{\text{true}}} = \frac{1 + p_3 \cdot E_{true}}{1 + p_1 \cdot e^{-p_2 \cdot E_{\text{true}}}}$$

2) Semi-emp. model based on Birks' law:

$$\frac{E_{\text{vis}}}{E_{\text{true}}} = f_{\text{q}}(E_{\text{true}}; k_B) + k_C \cdot f_c(E_{\text{true}})$$

k_B: Birks' constant
k_C: Cherenkov contribution

Gammas + positrons

- Gammas connected to electron model through MC:

$$E_{\text{vis}}^{\gamma} = \int E_{\text{vis}}^{e^-}\left(E_{\text{true}}^{e^-}\right) \cdot \frac{dN}{dE}\left(E_{\text{true}}^{e^-}\right) dE_{\text{true}}^{e^-}$$

- Positrons connected to electron model through MC:

$$E_{\text{vis}}^{e^+} = E_{\text{vis}}^{e^-} + 2 \cdot E_{\text{vis}}^{\gamma}(0.511\,\text{MeV})$$

Simulation of individual e^-, e^+ energies due to gamma interaction in scintillator.

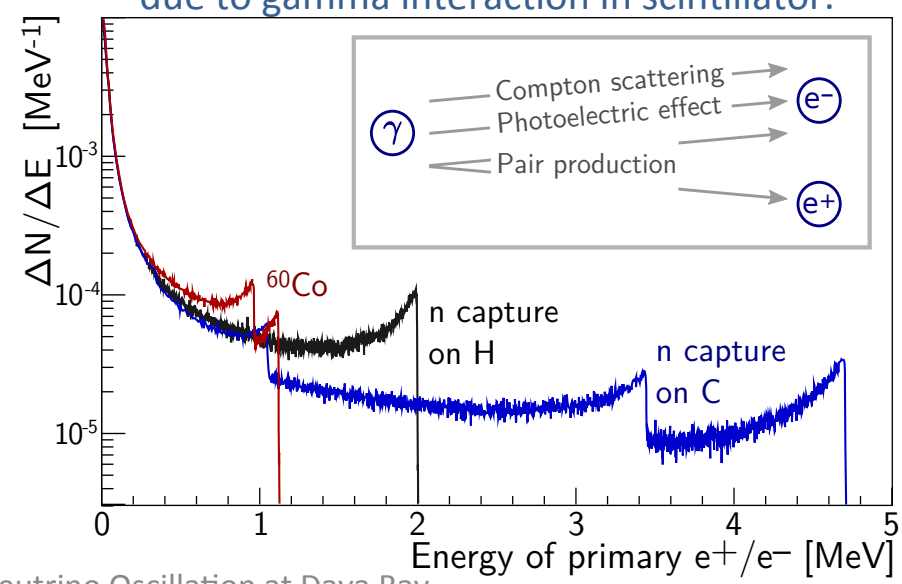

Electronics Non-Linearity Model

PMT readout electronics introduces additional biases

Electronics does not fully capture late secondary hits

- Slow scintillation component missed at high energies
- Charge collection efficiency decreases with visible light

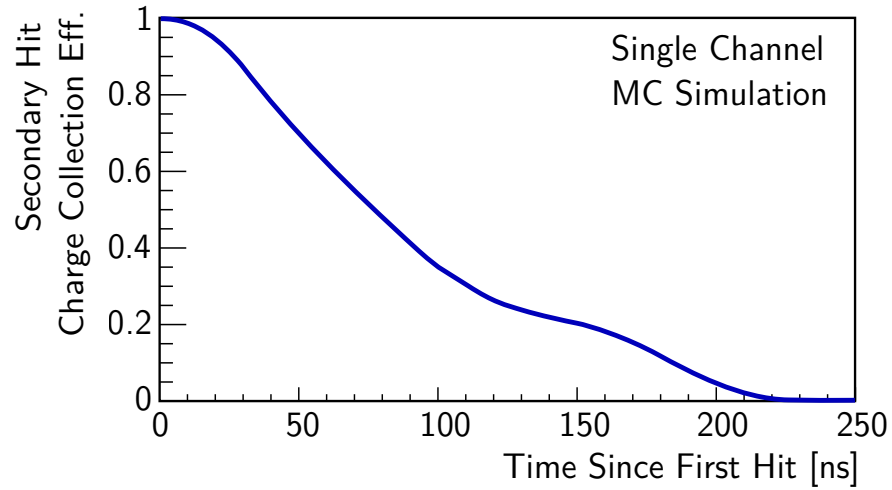

PMT readout electronics introduces additional biases

- Effective model as a function of total visible energy
- 2 empirical parameterizations: exponential and quadratic
- Total effective non-linearity f from both scintillation and electronics effects:

$$f = \frac{E_{\text{rec}}}{E_{\text{true}}} = \frac{E_{\text{rec}}}{E_{\text{vis}}} \cdot \frac{E_{\text{vis}}}{E_{\text{true}}}$$

1 Electronics non-linearity

2 Scintillator non-linearity

Energy Resolution Model

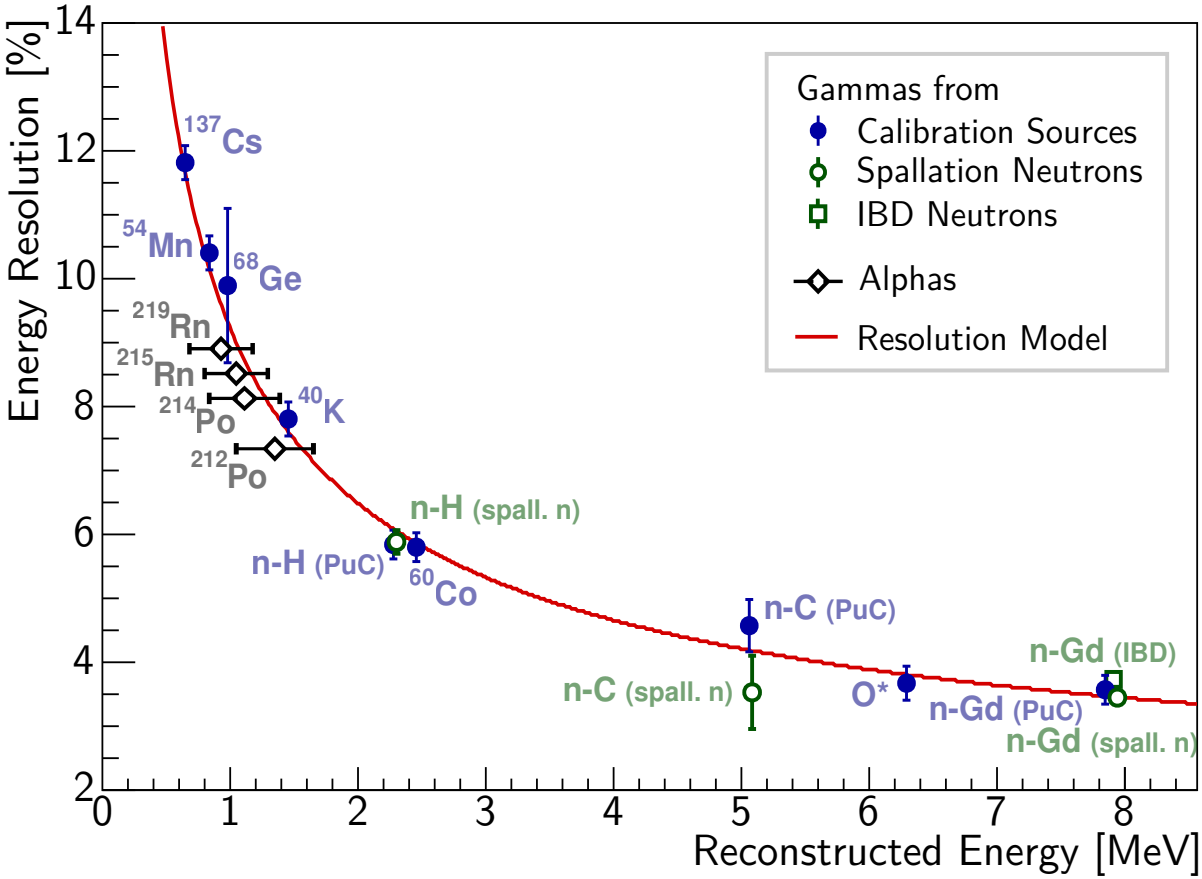

Functional form:

$$\frac{\sigma_E}{E} = \sqrt{a^2 + \frac{b^2}{E} + \frac{c^2}{E^2}}$$

Contributions from:

- a : Spacial/temp. resolution (∝E)
- b : Photon statistics (∝√E)
- c : Dark noise (const:)

Calibrated primarily using monoenergetic gamma sources

- Radioactive calibration sources placed at the detector center
- Additional data from IBD and spallation neutrons, uniformly distributed in LS
- Alpha source data used to cross-check result
  - ➢ Larger uncertainties due to different response from electronics

Constraining the Non-Linearity Parameters

Gamma Ray Energy Peaks

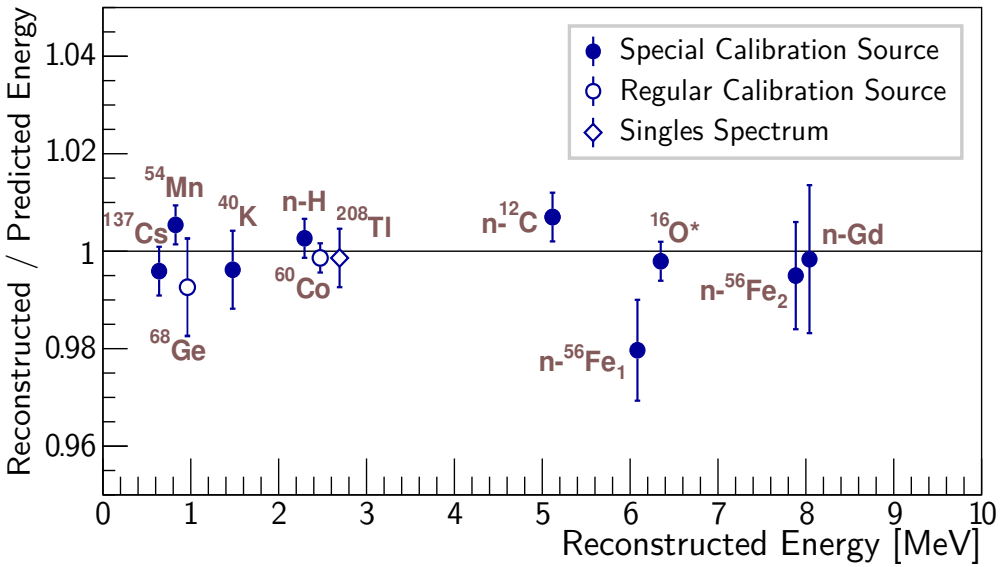

^{12}B Beta-Decay Spectrum

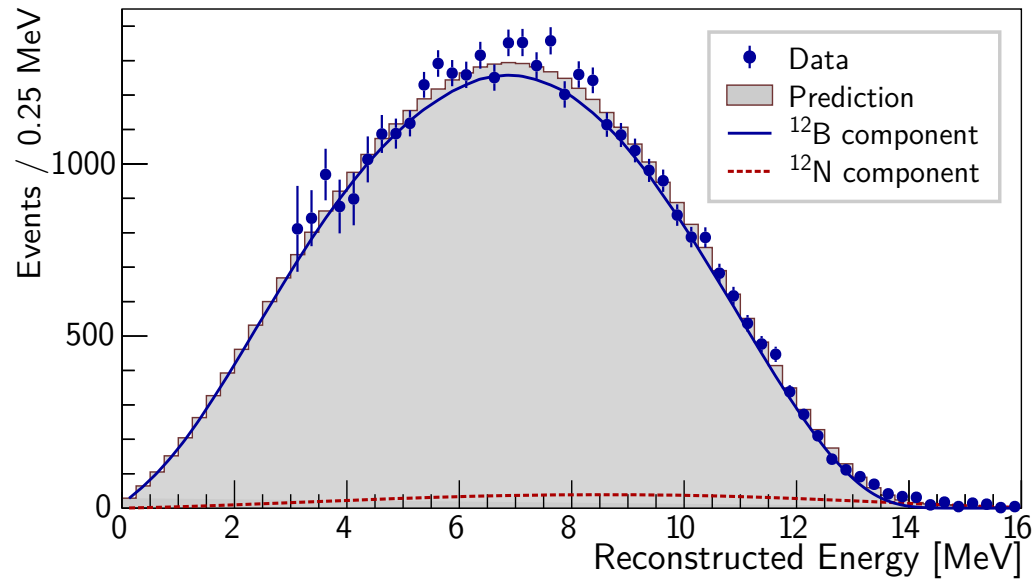

Full detector calibration data

1. Monoenergetic gamma lines from various sources
   - Radioactive calibration sources, employed regularly: ^{68}Ge, ^{60}Co, ^{241}Am-^{13}C and during special calibration periods: ^{137}Cs, ^{54}Mn, ^{40}K, ^{241}Am-^{9}Be, Pu-^{13}C
   - Singles and correlated spectra in regular physics runs (^{40}K, ^{208}Tl, n capture on H)
2. Continuous spectrum from ^{12}B produced by muon spallation inside the scintillator

Standalone measurements

- Scintillator quenching measurements using neutron beams and Compton e^-
- Calibration of readout electronics with flash ADC

Final Positron Energy Non-Linearity Response

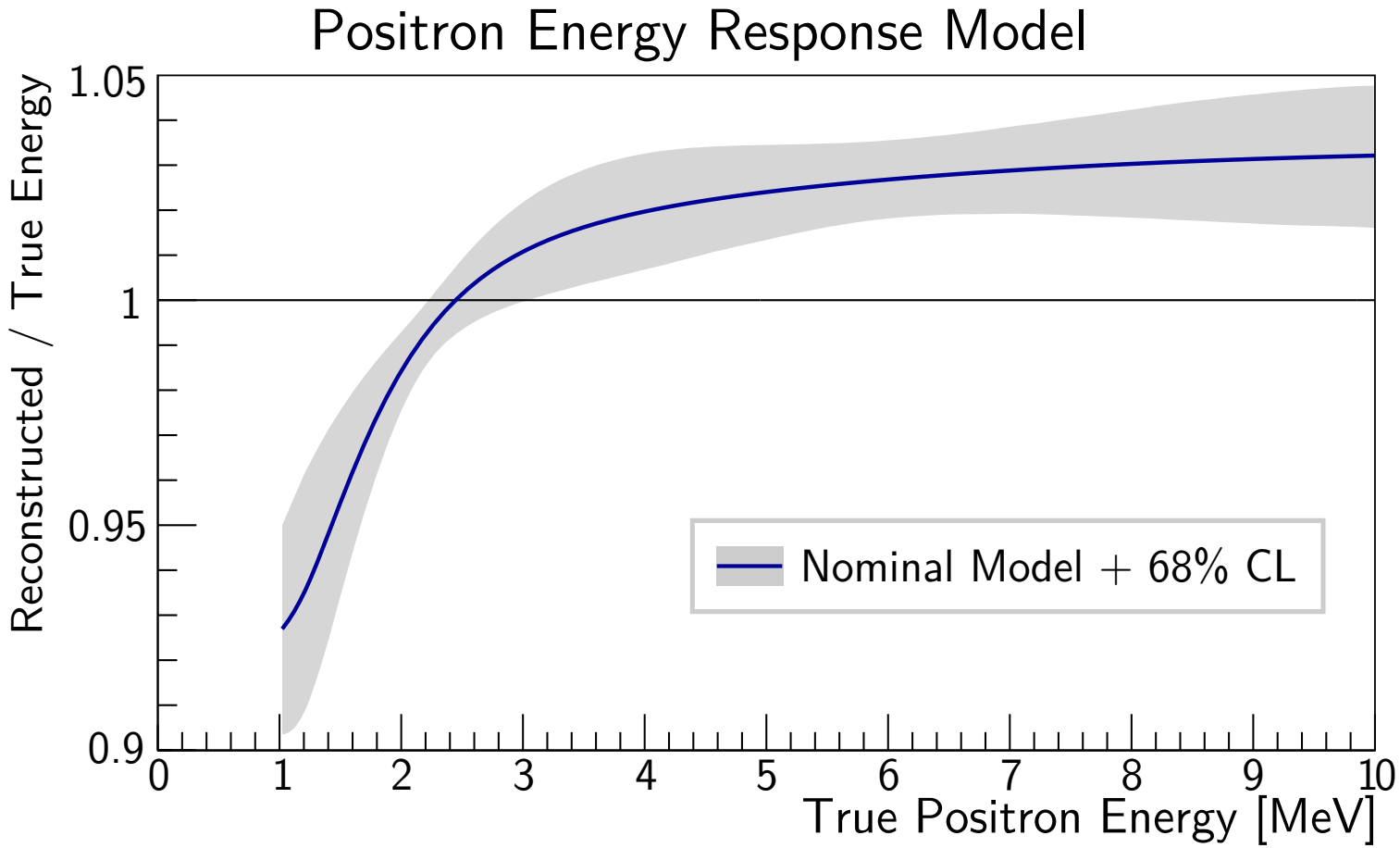

Combination of 5 models to conservatively estimate uncertainty

- Models selected so that
  1. Correlations are minimized
  2. All remaining validated curves with their uncertainties are included in resulting 68% confidence interval

Out of the Swamp…

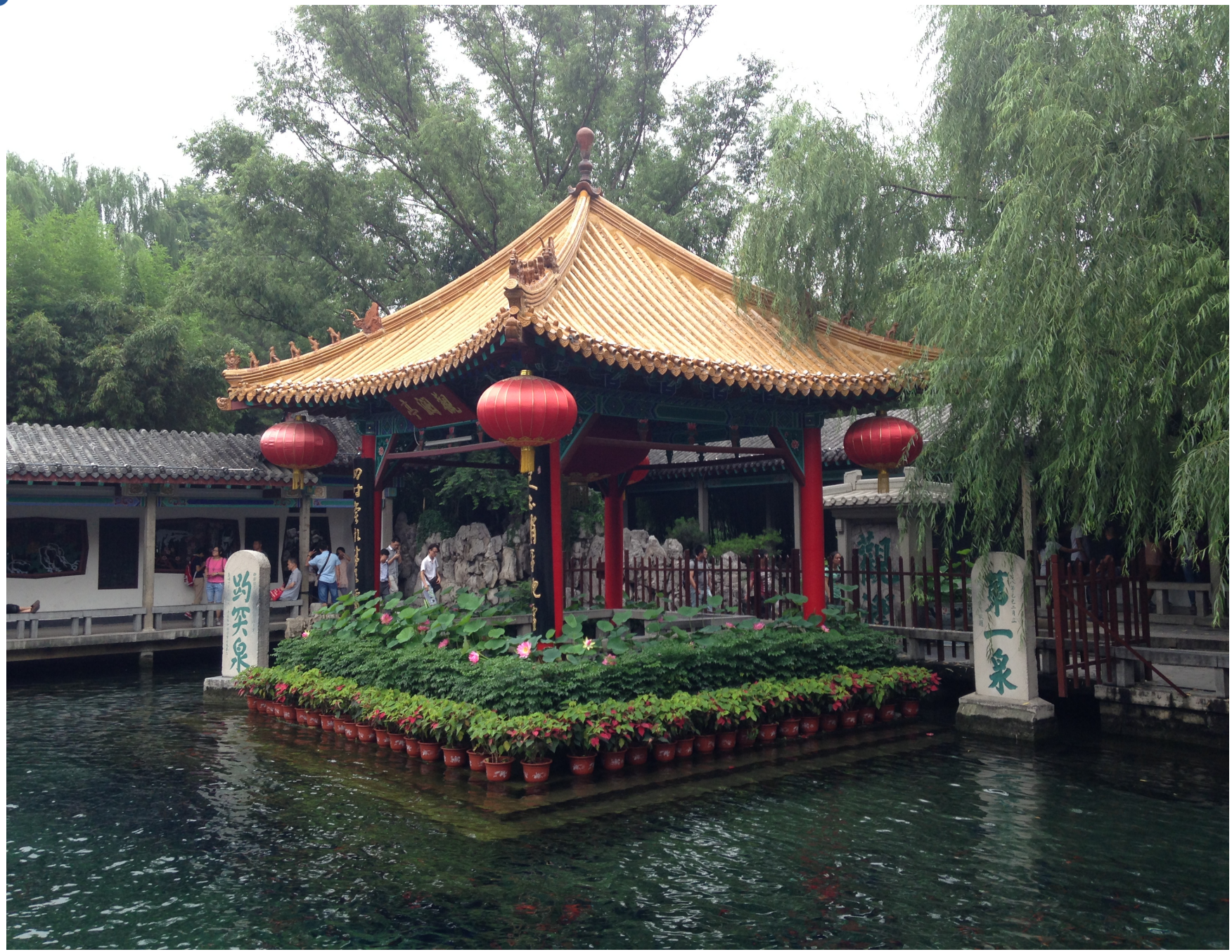

Antineutrino (IBD) Selection

Antineutrino interactions cleanly separated from backgrounds

① Reject spontaneous PMT light emission ("flashers")

② Prompt positron:
0.7 MeV < Ep < 12 MeV

③ Delayed neutron:
6.0 MeV < Ed < 12 MeV

④ Neutron capture time:
1 μs < t < 200 μs

⑤ Muon veto:

- Water pool muon (>12 hit PMTs): Reject [-2μs; 600μs]
- AD muon (>3000 photoelectrons): Reject [-2 μs; 1400μs]
- AD shower muon (>3×10^5 p.e.): Reject [-2 μs; 0.4s]

⑥ Multiplicity:

- No additional prompt-like signal
  400μs before delayed neutron
- No additional delayed-like signal
  200μs after delayed neutron

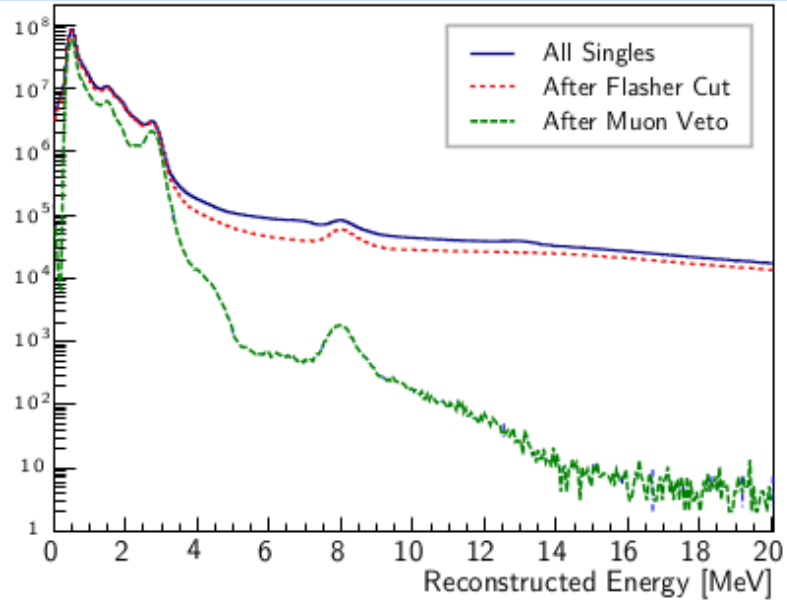

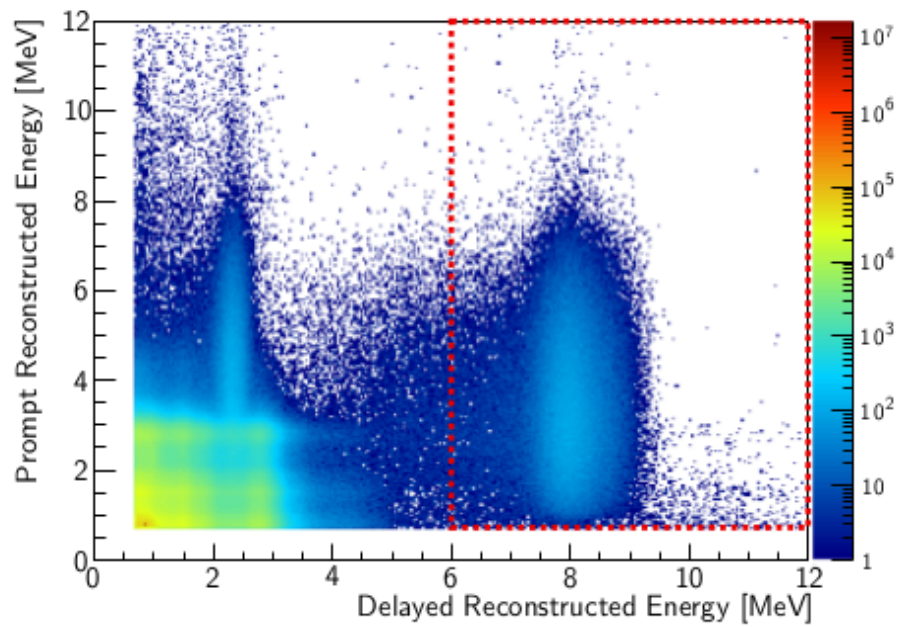

Accidental Background

Two uncorrelated signals can accidentally mimic an antineutrino signal.

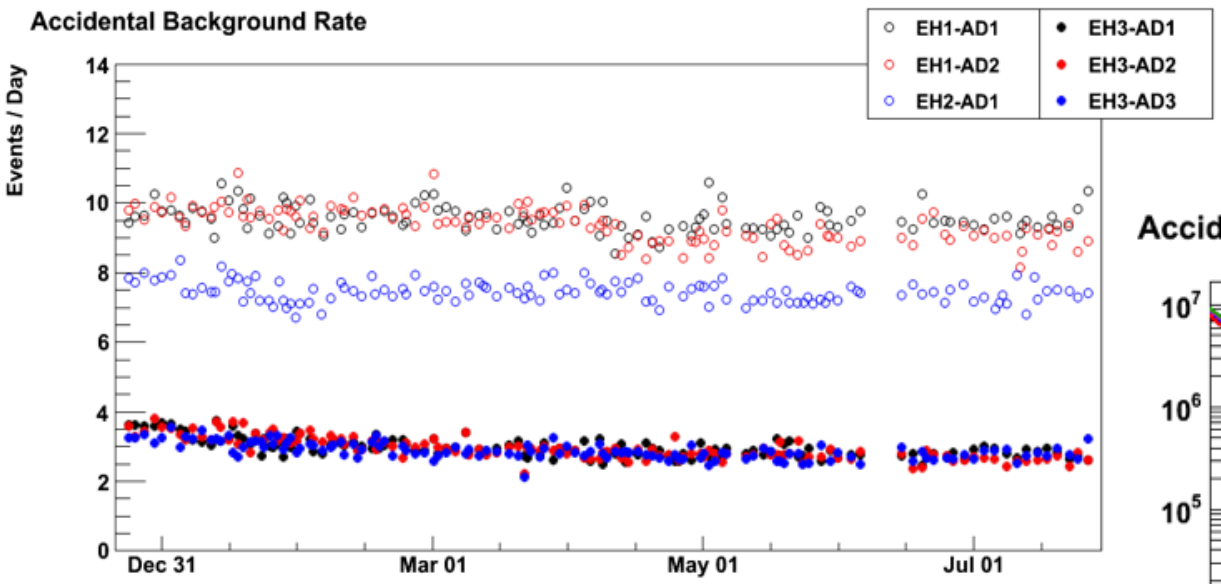

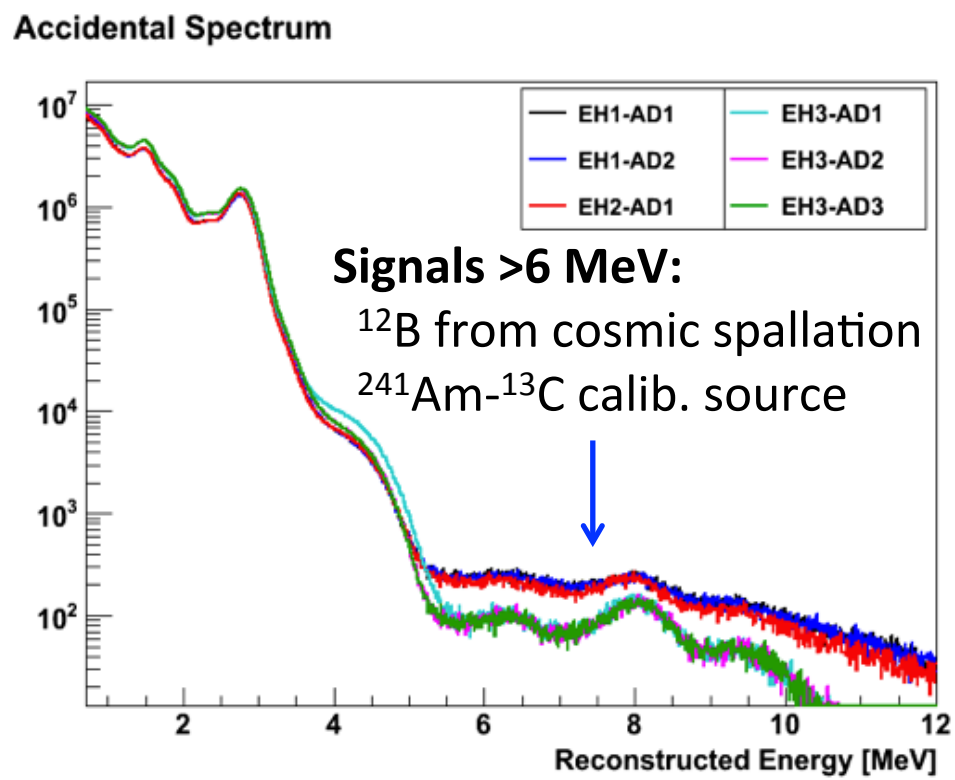

Accidental B/S is 4% (1.5%) of far (near) signal.

Accidental background be accurately modeled using uncorrelated signals in data.

➔ Negligible uncertainty in background rate or spectra.

^{241}Am-^{13}C Background

A subtle background from our calibration neutron source

- ^{241}Am-^{13}C source produces ~0.75 Hz neutrons via ^{13}C(α,n)^{16}O.
- Neutrons interact with steel to produce fake (prompt,delayed) pair

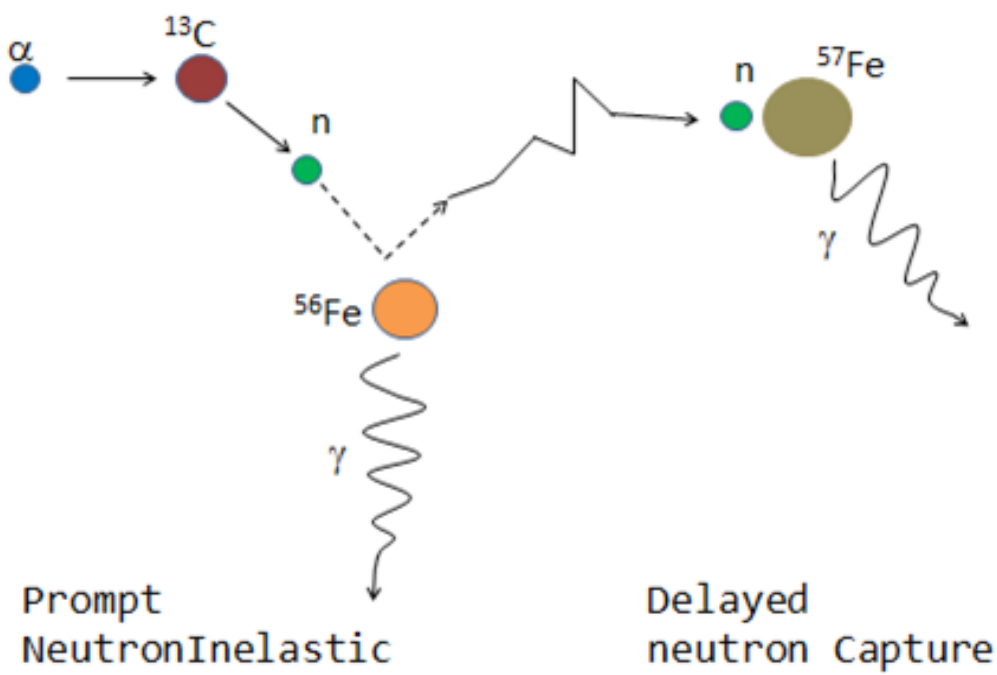

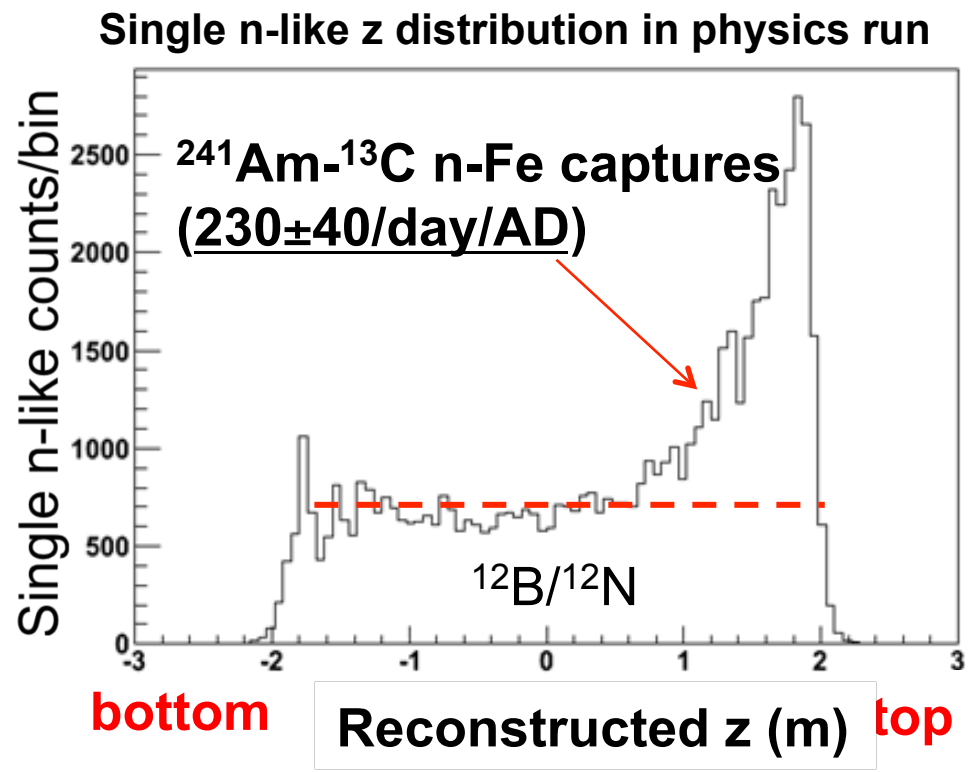

- Correlated background expected small — 0.2~0.3/day/module (MC)
- Constrained with data, special calibration

^{241}Am-^{13}C Background

Background rate and shape constrained using intense source

A special x80 stronger ^{241}Am-^{13}C source placed on the AD

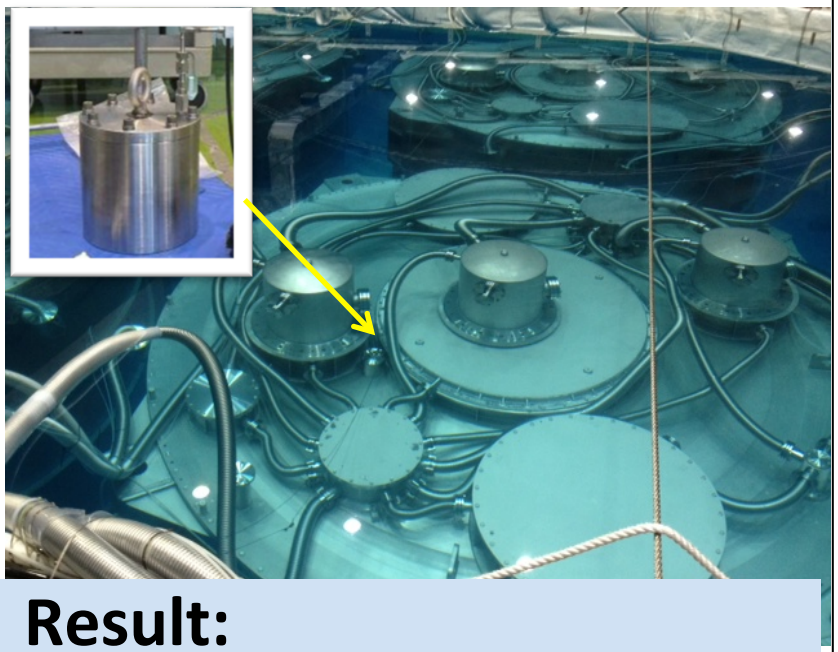

Result:
Reduced background uncertainty by a factor of 2.

Removed 2 of 3 sources in far detectors to reduce future bkgd.

Single n-like

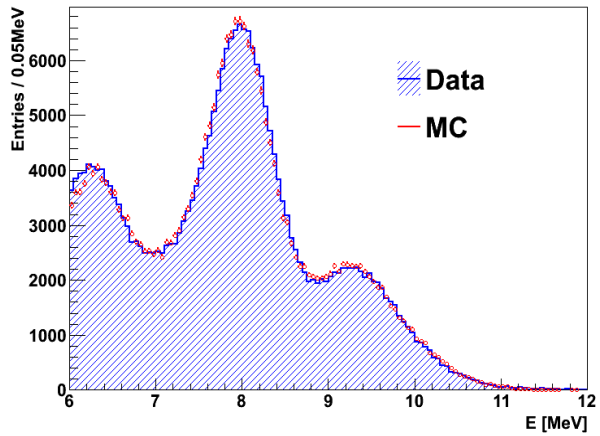

Correlated prompt spectrum

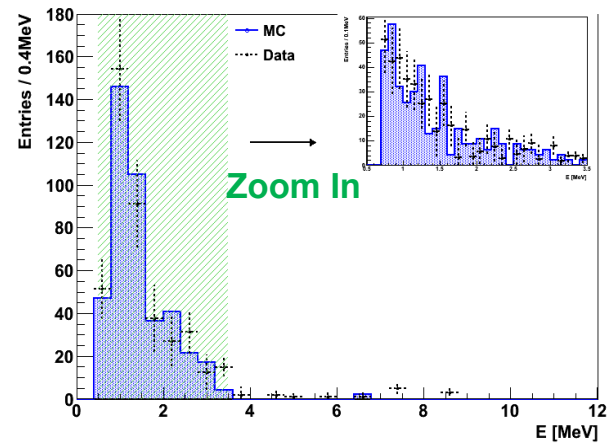

Correlated background in physics run = measured single n-like due to AmC (normalization) x correlated/single ratio (MC benchmarked and corrected by strong AmC, spectrum)

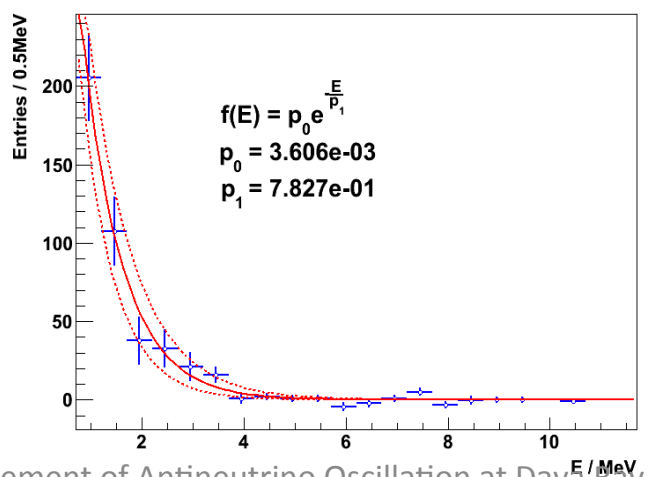

- Rate: 0.26/day/module (global uncert. 45%)
- Spectrum: exponential (global uncert 15%)

Background: β-n decay

β-n decay:
- Prompt: β-decay
- Delayed: neutron capture

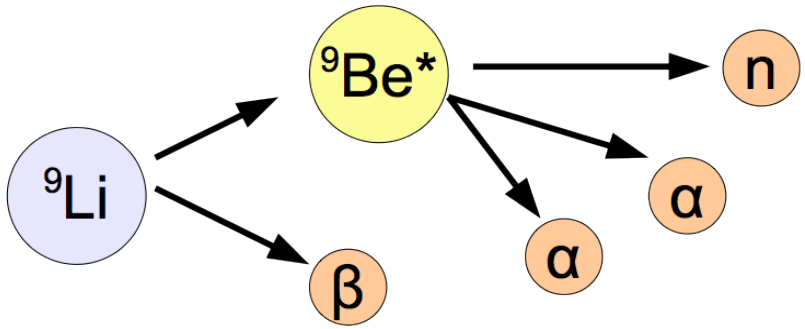

^{9}Li: $\tau_{1/2}$ = 178 ms, Q = 13. 6 MeV
^{8}He: $\tau_{1/2}$ = 119 ms, Q = 10.6 MeV

- Generated by cosmic rays
- Long-lived
- Mimic antineutrino signal

This background is directly measured by fitting the distribution of IBD candidates vs. time since last muon.

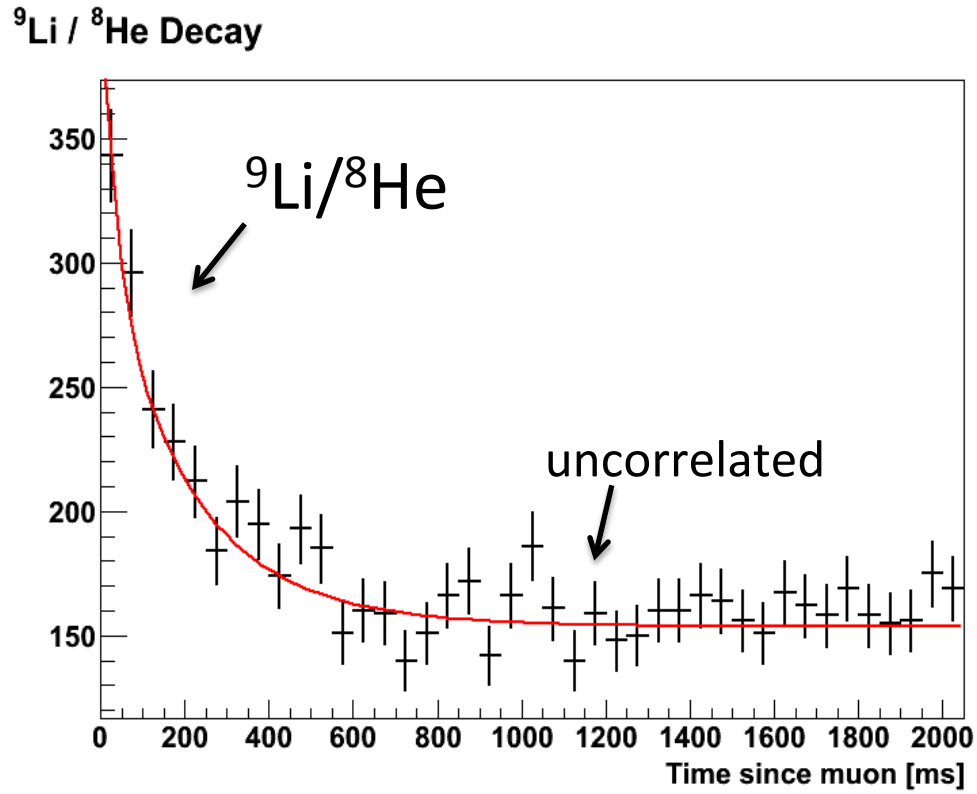

Analysis muon veto cuts control B/S to ~0.3±0.1%.

Background: β-n decay (shape)

Shape for ^{9}Li and ^{8}He is predicted from a simulation benchmarked with external data and which accounts for all daughter particles.

Uncertainty in shape is conservatively accounted for by varying the ^{9}Li/(^{9}Li+^{8}He) ratio, as well as the parameters of the detector response model.

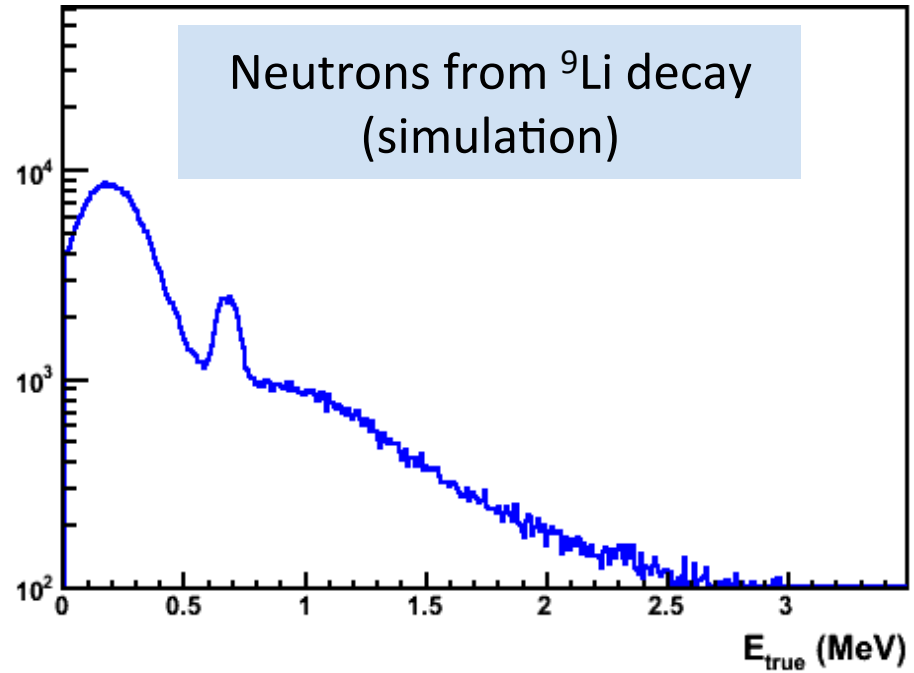

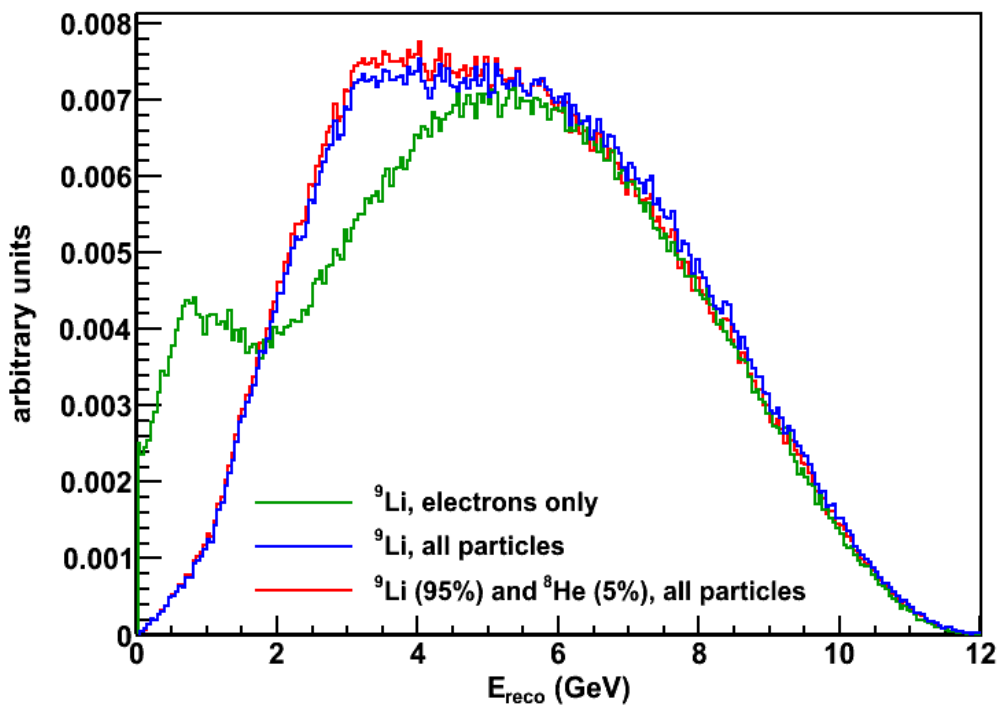

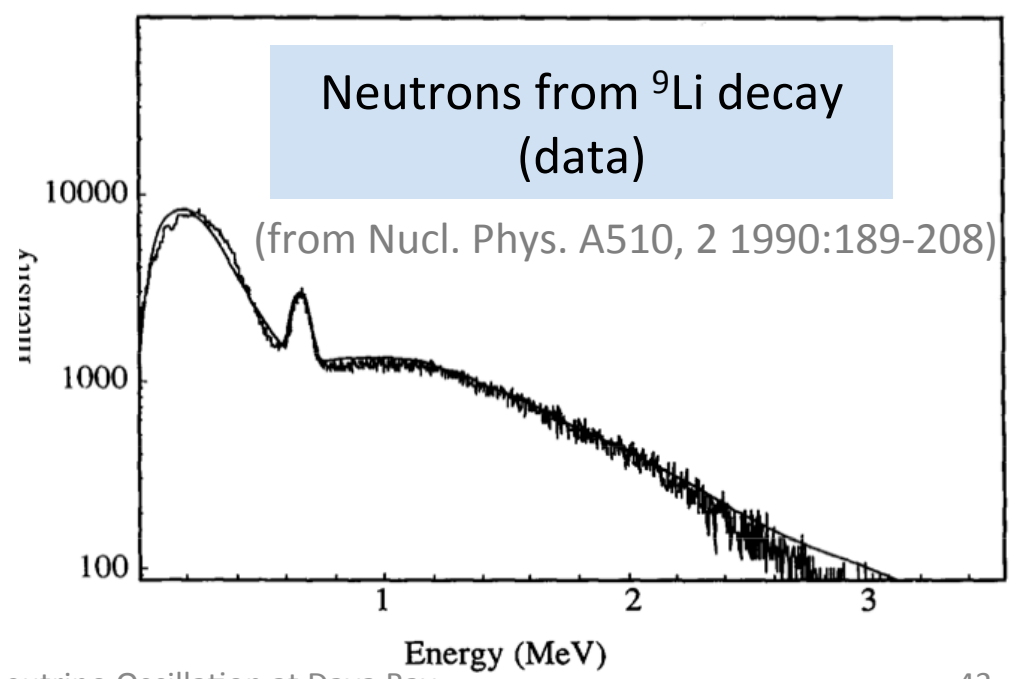

Signal and Background Summary

	Near Halls			Far Hall		
	AD 1	AD 2	AD 3	AD 4	AD 5	AD 6
IBD candidates	101290	102519	92912	13964	13894	13731
DAQ live time (days)	191.001		189.645		189.779	
Efficiency $\epsilon_\mu \cdot \epsilon_m$	0.7957	0.7927	0.8282	0.9577	0.9568	0.9566
Accidentals (per day)*	9.54±0.03	9.36±0.03	7.44±0.02	2.96±0.01	2.92±0.01	2.87±0.01
Fast-neutron (per day)*	0.92±0.46		0.62±0.31		0.04±0.02	
$^{9}Li/^{8}He$ (per day)*	2.40±0.86		1.2±0.63		0.22±0.06	
Am-C corr. (per day)*	0.26±0.12					
$^{13}C^{16}O$ backgr. (per day)*	0.08±0.04	0.07±0.04	0.05±0.03	0.04±0.02	0.04±0.02	0.04±0.02
IBD rate (per day)*	653.30±2.31	664.15±2.33	581.97±2.07	73.31±0.66	73.03±0.66	72.20± 0.66

* Background and IBD rates were corrected for the efficiency of the muon veto and multiplicity cuts $\epsilon_\mu \cdot \epsilon_m$

Collected more than 300k antineutrino interactions

- Consistent rates for side-by-side detectors
- Uncertainties still dominated by statistics

Uncertainty Summary

Detector			
	Efficiency	Correlated	Uncorrelated
Target Protons		0.47%	0.03%
Flasher cut	99.98%	0.01%	0.01%
Delayed energy cut	90.9%	0.6%	0.12%
Prompt energy cut	99.88%	0.10%	0.01%
Multiplicity cut		0.02%	<0.01%
Capture time cut	98.6%	0.12%	0.01%
Gd capture ratio	83.8%	0.8%	<0.1%
Spill-in	105.0%	1.5%	0.02%
Livetime	100.0%	0.002%	<0.01%
Combined	78.8%	1.9%	0.2%

For near/far oscillation, only uncorrelated uncertainties are used.

Largest systematics are smaller than far site statistics (~1%)

Reactor			
Correlated		Uncorrelated	
Energy/fission	0.2%	Power	0.5%
$\overline{\nu}_e$/fission	3%	Fission fraction	0.6%
		Spent fuel	0.3%
Combined	3%	Combined	0.8%

Influence of uncorrelated reactor systematics reduced by far vs. near measurement.

Antineutrino Rate vs. Time

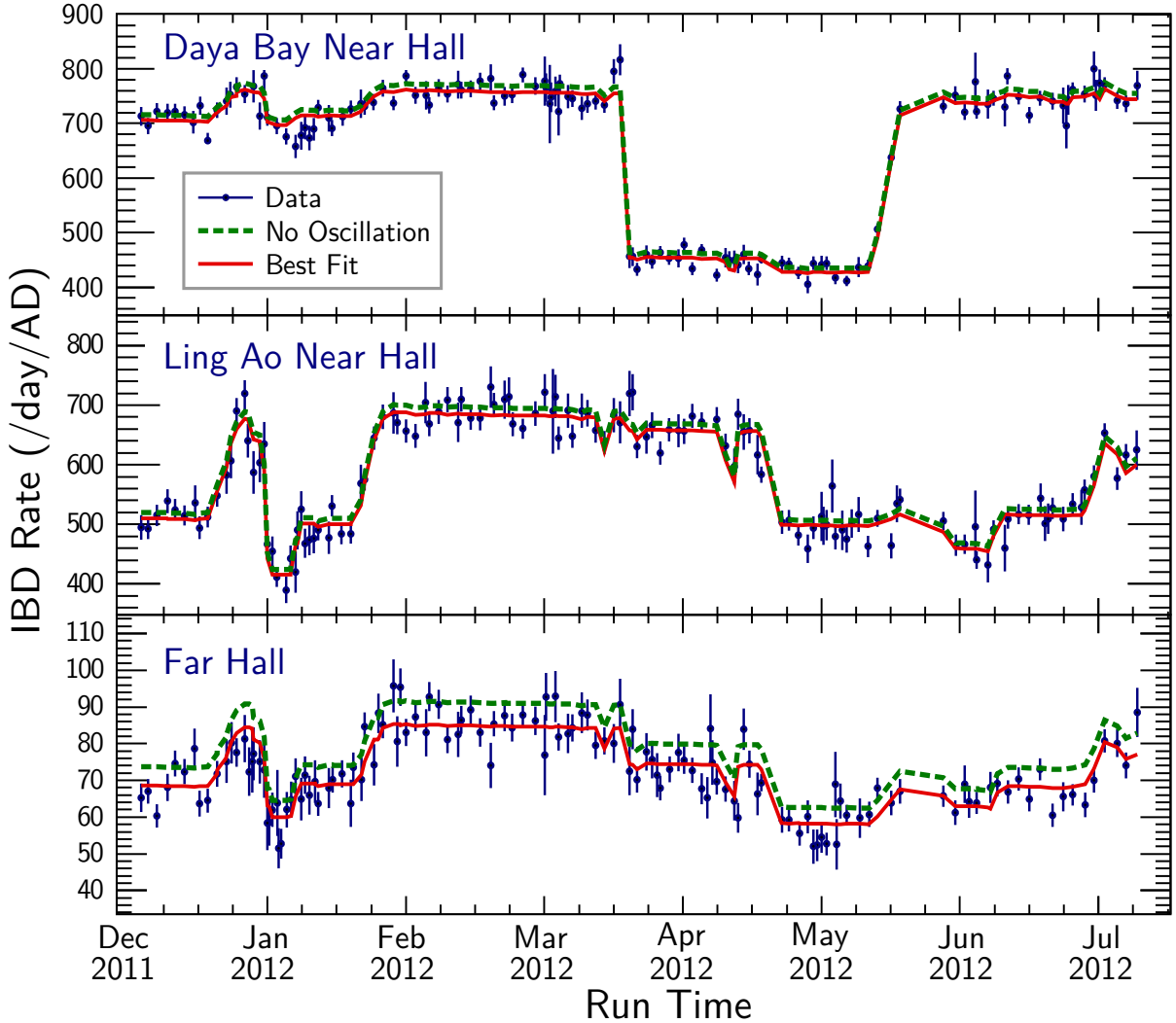

Detected rate strongly correlated with reactor flux expectations

- Predicted Rate assumes no oscillation
- Absolute normalization determined by fit to data
- Normalization within a few percent of expectations

Rate-Only Oscillation Results

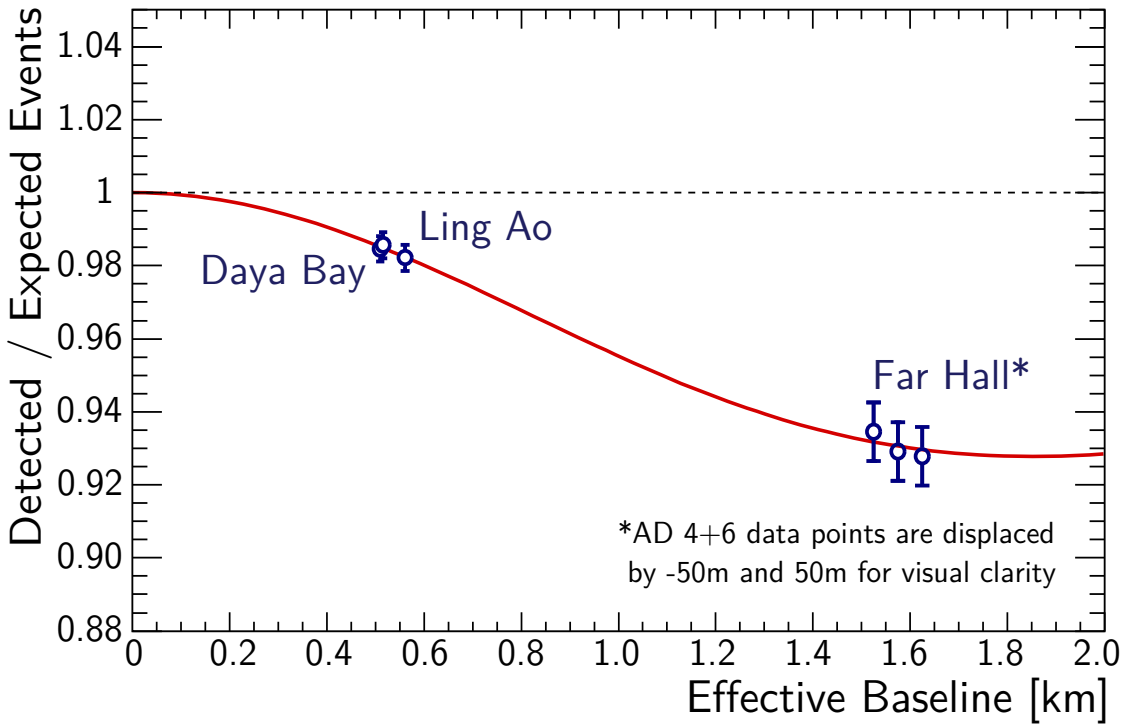

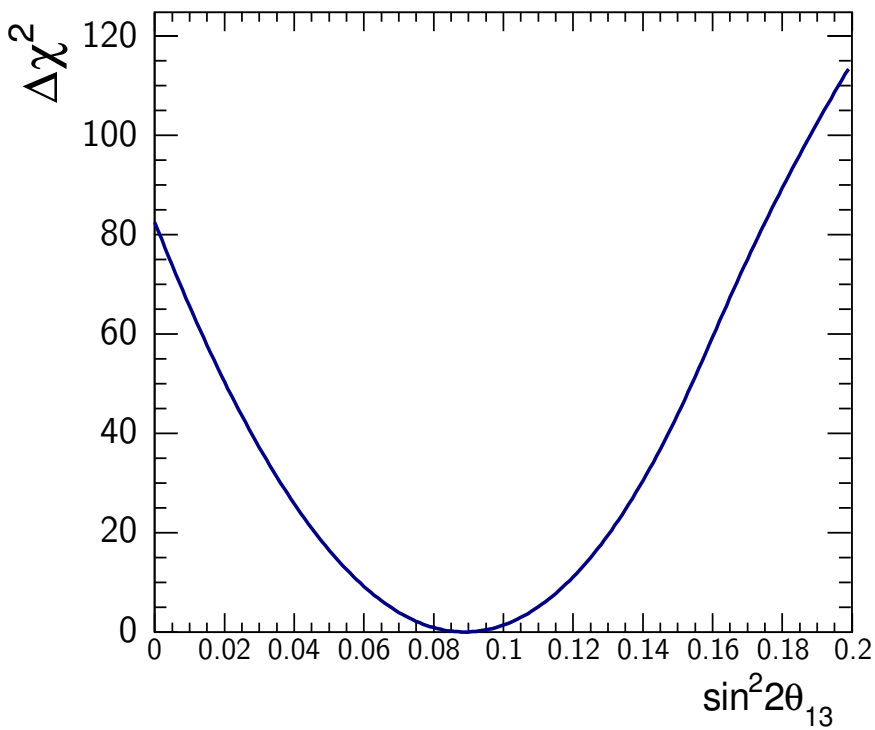

$$\sin^2 2\theta_{13} = 0.089 \pm 0.009$$

- Uncertainty reduced by statistics of complete 6 AD data period
- Standard approach: $\chi^2/N_{DoF} = 0.48/4$
- $|\Delta m^2_{ee}|$ constrained by MINOS result for $|\Delta m^2_{\mu\mu}|$
- Far vs. near relative measurement: absolute rate not constrained
- Consistent results from independent analyses, different reactor flux models

Prompt IBD Spectra

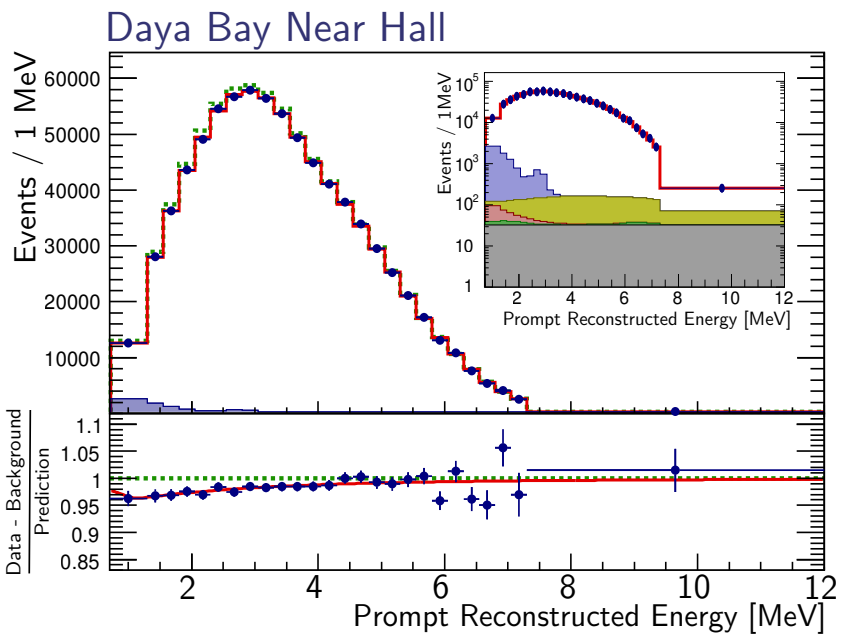

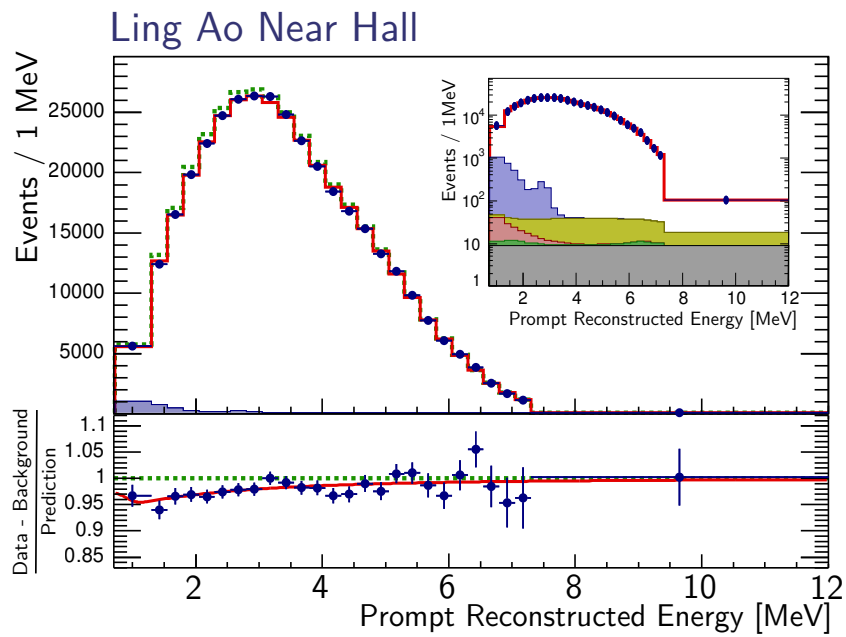

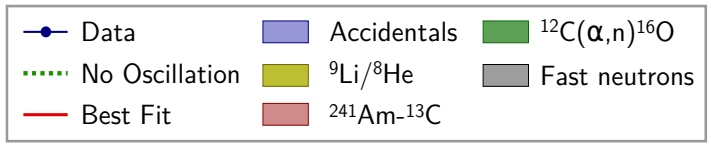

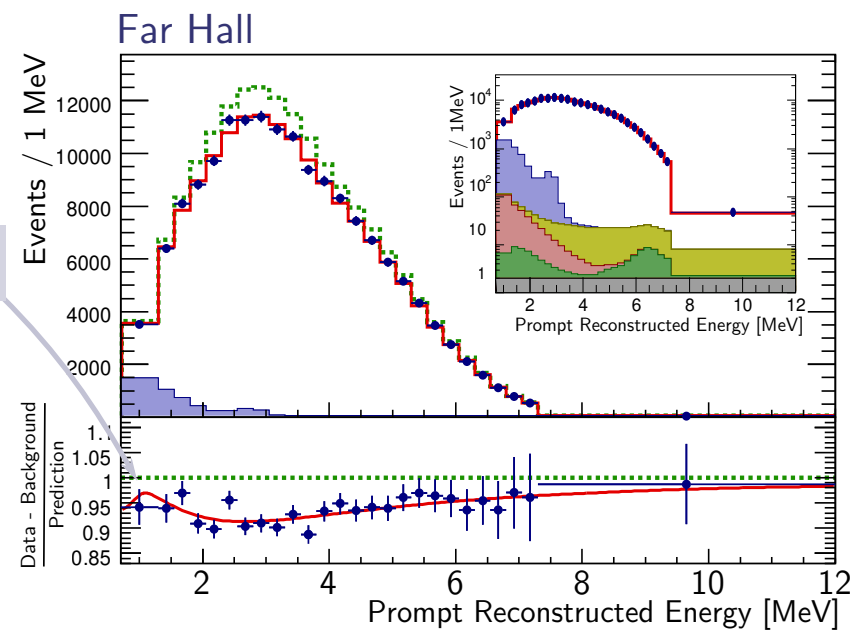

Shape distortion from energy losses in acrylic

Spectral distortion consistent with oscillation

- Both background and predicted no oscillation spectrum determined by best fit
- Errors statistical only

A Comment on Δm^2

Short-baseline reactor experiments insensitive to neutrino mass hierarchy.

Cannot discriminate two frequencies contributing to oscillation Δm^2_{31} , Δm^2_{32}

One effective oscillation frequency is measured:

$$P_{\bar{\nu}_e \to \bar{\nu}_e} = 1 - \sin^2 2\theta_{13} \sin^2\left(\Delta m^2_{ee} \frac{L}{4E}\right) - \sin^2 2\theta_{12} \cos^4 2\theta_{13} \sin^2\left(\Delta m^2_{21} \frac{L}{4E}\right)$$

$$\sin^2(\Delta m^2_{ee} \tfrac{L}{4E}) \equiv \cos^2\theta_{12} \sin^2(\Delta m^2_{31} \tfrac{L}{4E}) + \sin^2\theta_{12} \sin^2(\Delta m^2_{32} \tfrac{L}{4E})$$

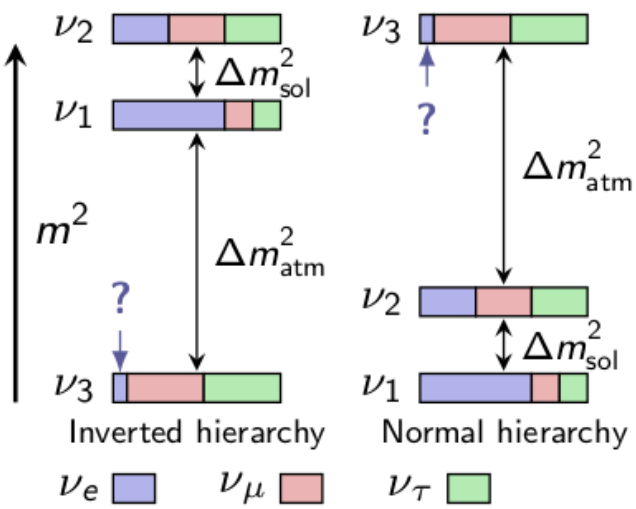

Result can be easily related to actual mass splitting, based on true hierarchy:

$$\left|\Delta m^2_{ee}\right| \simeq \left|\Delta m^2_{32}\right| \pm 5.21 \times 10^{-5}\mathrm{eV}^2$$

+: Normal Hierarchy
–: Inverted Hierarchy

Hierarchy discrimination requires ~1% precision on both Δm^2_{ee} and $\Delta m^2_{\mu\mu}$

Rate+Spectra Oscillation Results

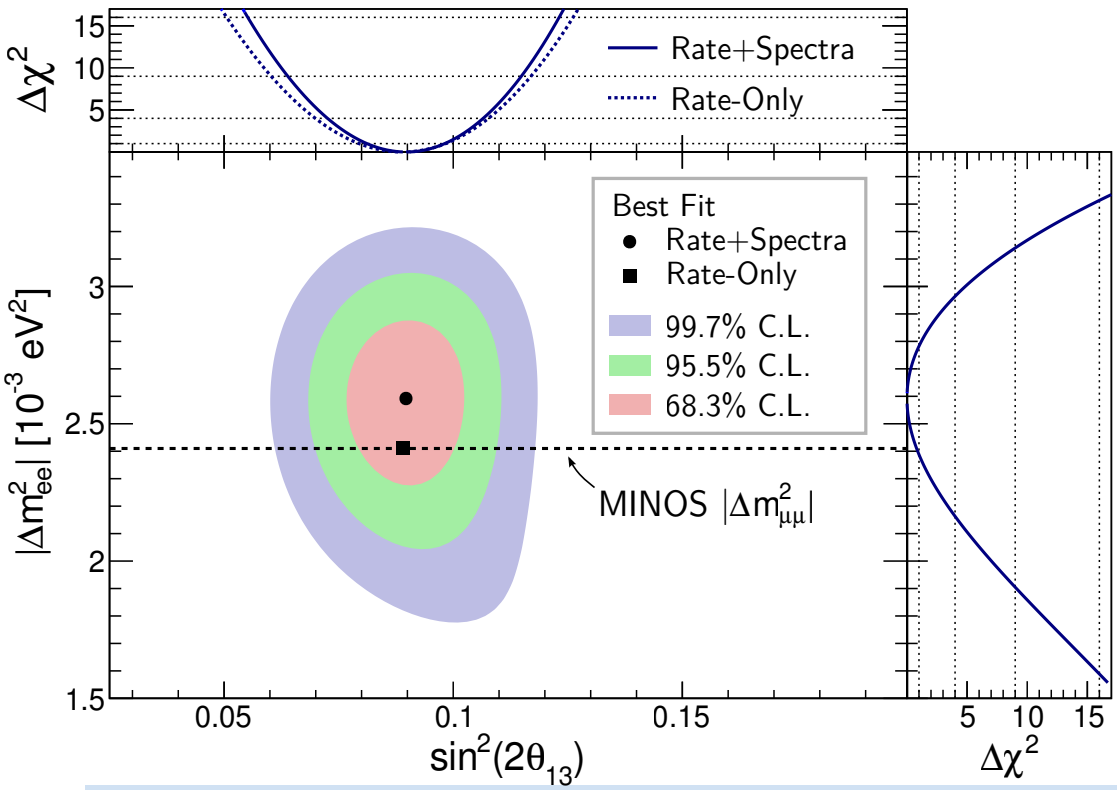

$$\sin^2 2\theta_{13} = 0.090^{+0.008}_{-0.009}$$

$$|\Delta m^2_{ee}| = 2.59^{+0.19}_{-0.20} \cdot 10^{-3}\,\mathrm{eV}^2$$

$$\chi^2/N_{\mathrm{DoF}} = 162.7/153$$

Strong confirmation of oscillation-interpretation of observed $\bar{\nu}_e$ deficit

	Normal MH Δm^2_{32} [10^{-3}eV^2]	Inverted MH Δm^2_{32} [10^{-3}eV^2]
From Daya Bay Δm^2_{ee}	$2.54^{+0.19}_{-0.20}$	$-2.64^{+0.19}_{-0.20}$
From MINOS $\Delta m^2_{\mu\mu}$	$2.37^{+0.09}_{-0.09}$	$-2.41^{+0.11}_{-0.09}$

A. Radovic, DPF2013

Near vs. Far Spectral Study

Independent crosscheck with minimal reactor assumptions

Predict far spectra directly from measured near site spectra

→ Minimizes impact of absolute flux and spectra prediction.

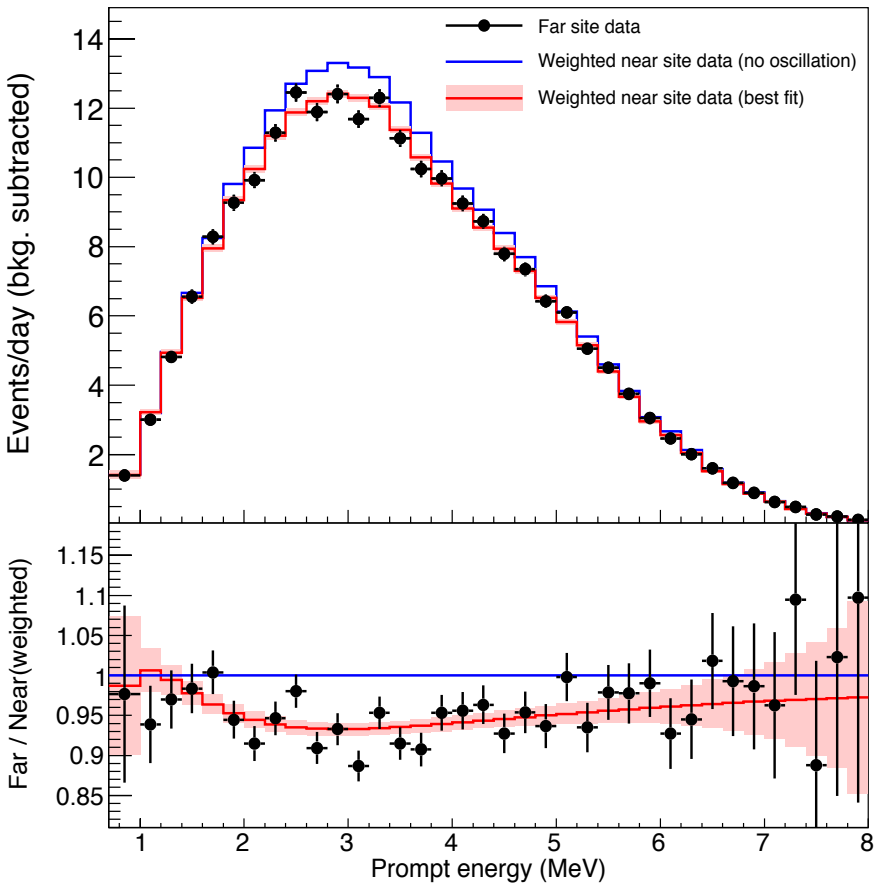

Use covariance matrices to account for systematic errors

→ Alternate method finds consistent uncertainties for neutrino parameters.

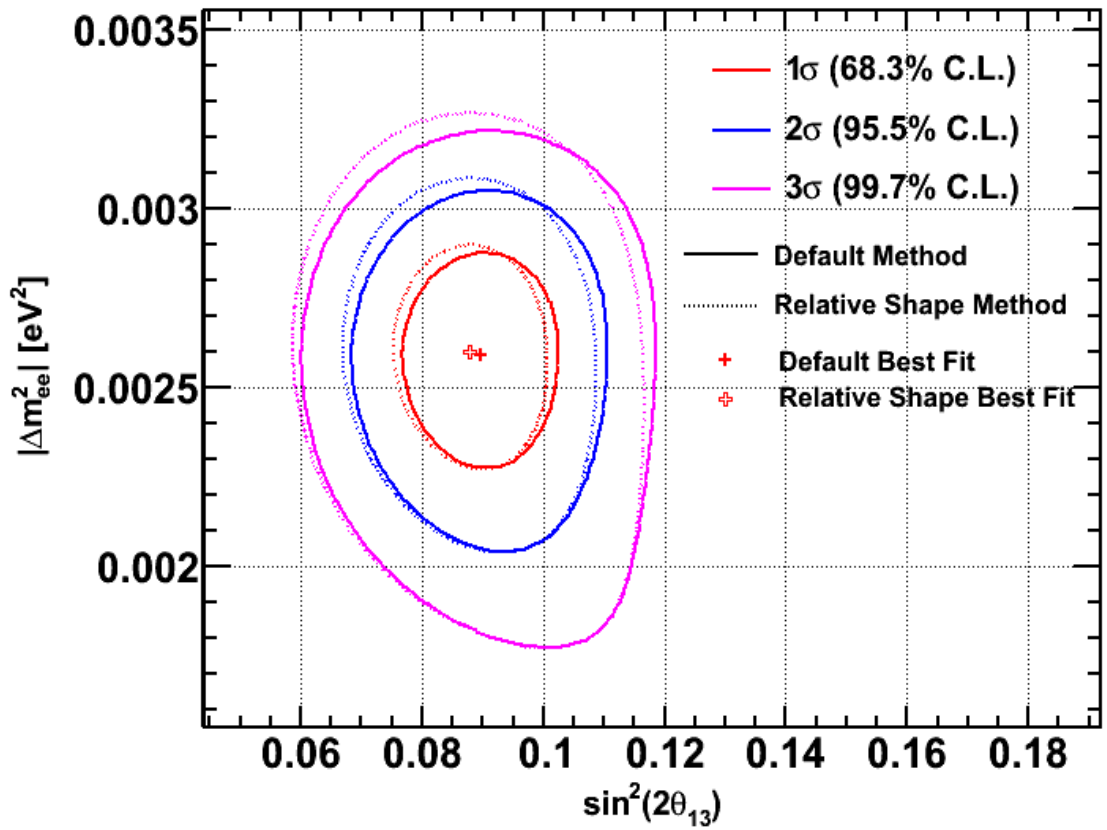

Antineutrino Oscillation

Consider each energy bin an independent measurement

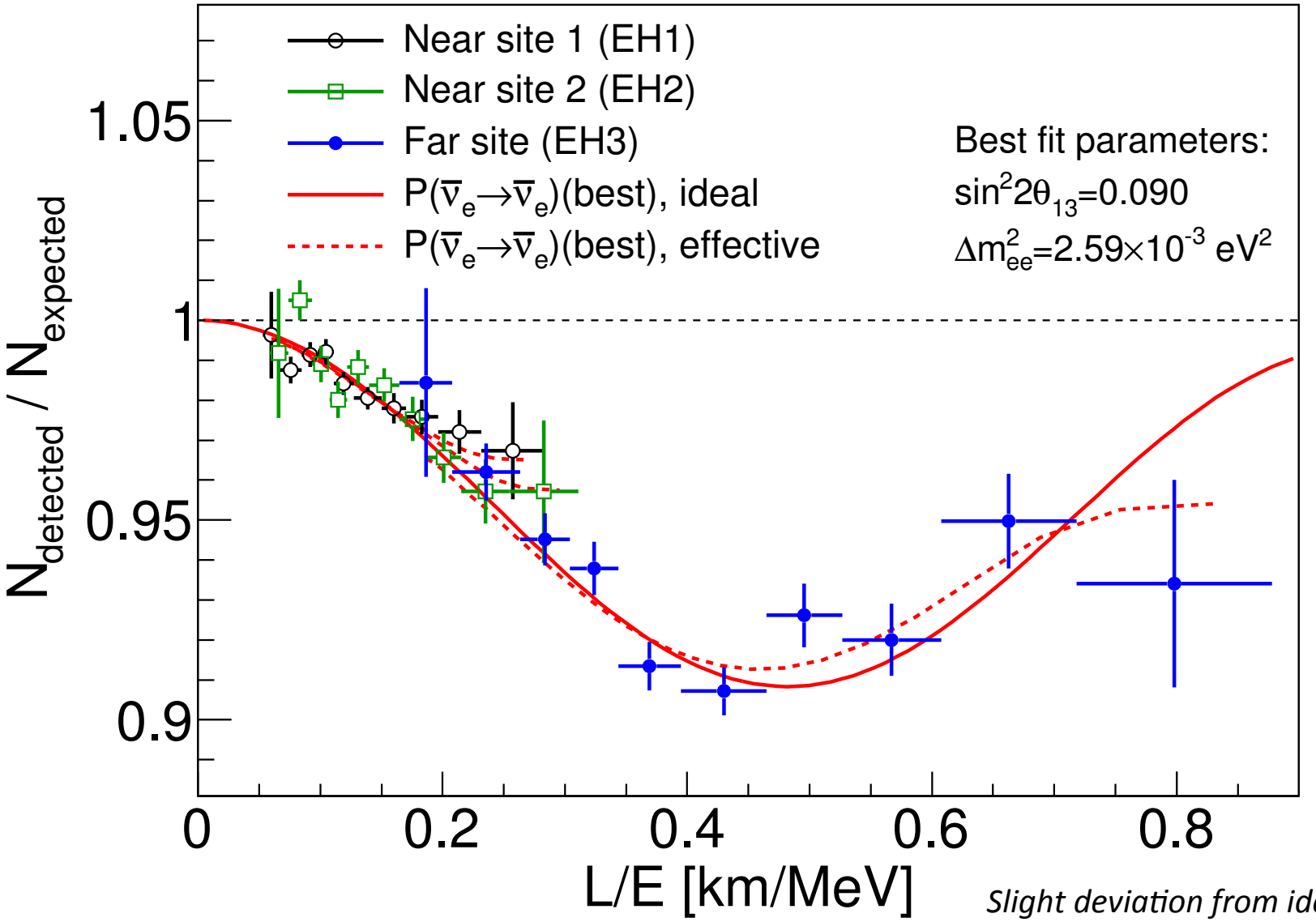

Slight deviation from ideal due to multiple reactors and detector resolution.

Global Comparison of θ_{13} Measurements

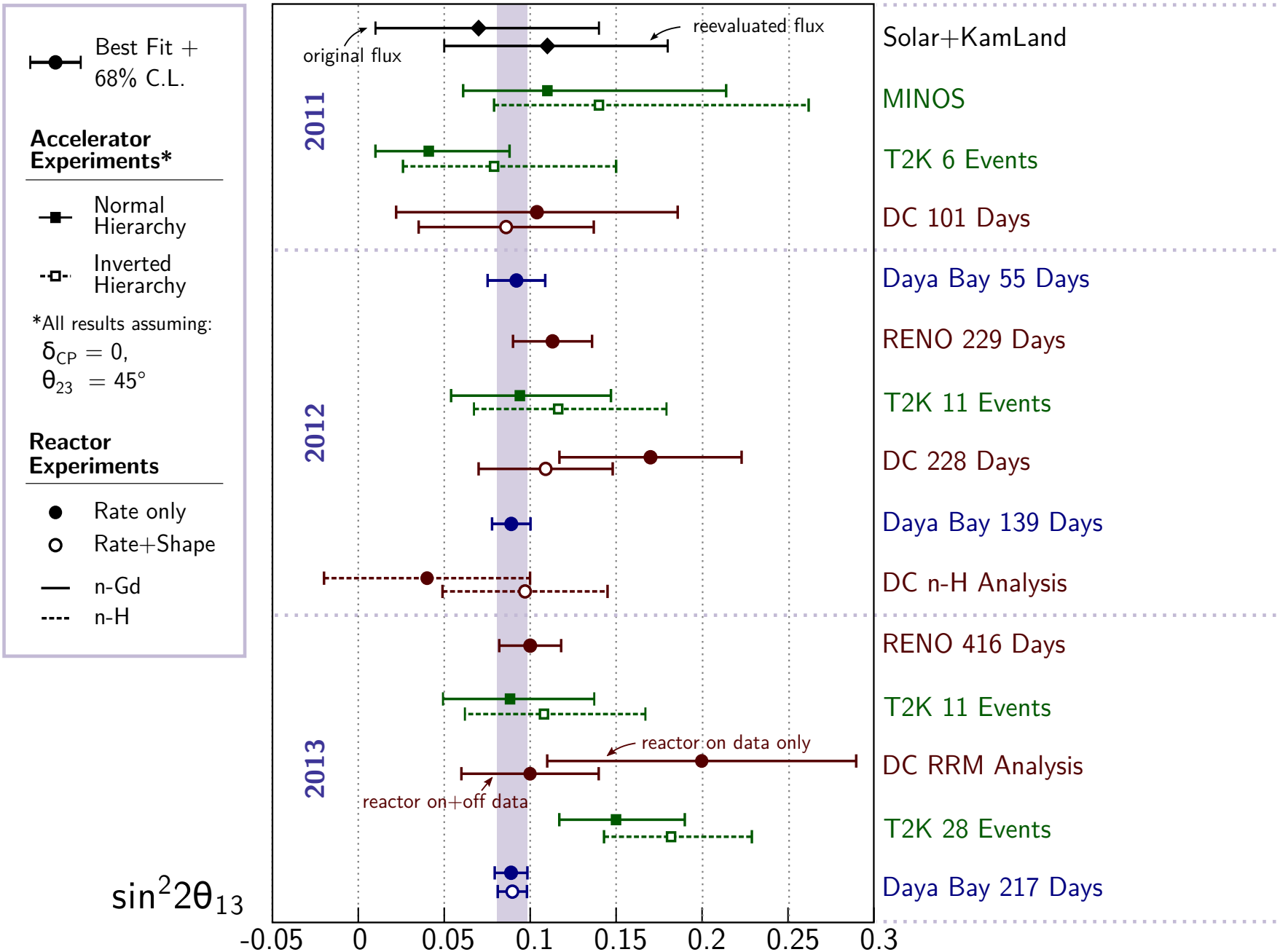

Daya Bay Onsite Progress

Final two detectors installed, operating since Oct. 2012.

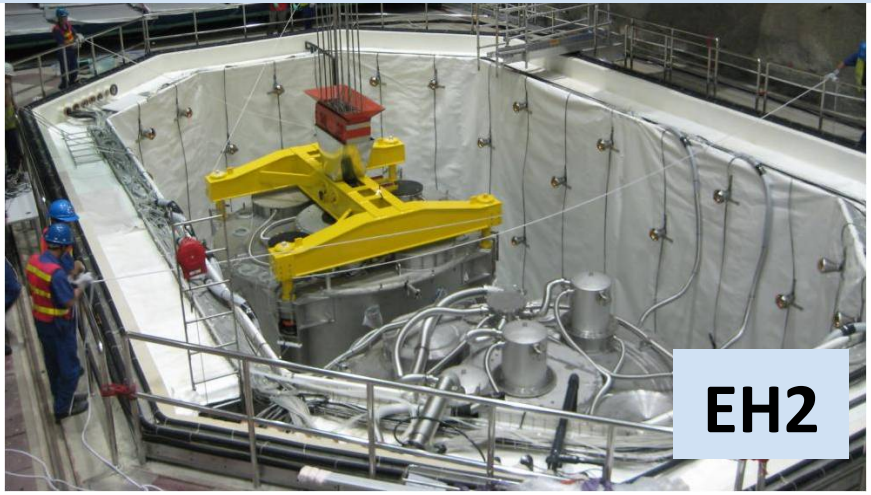

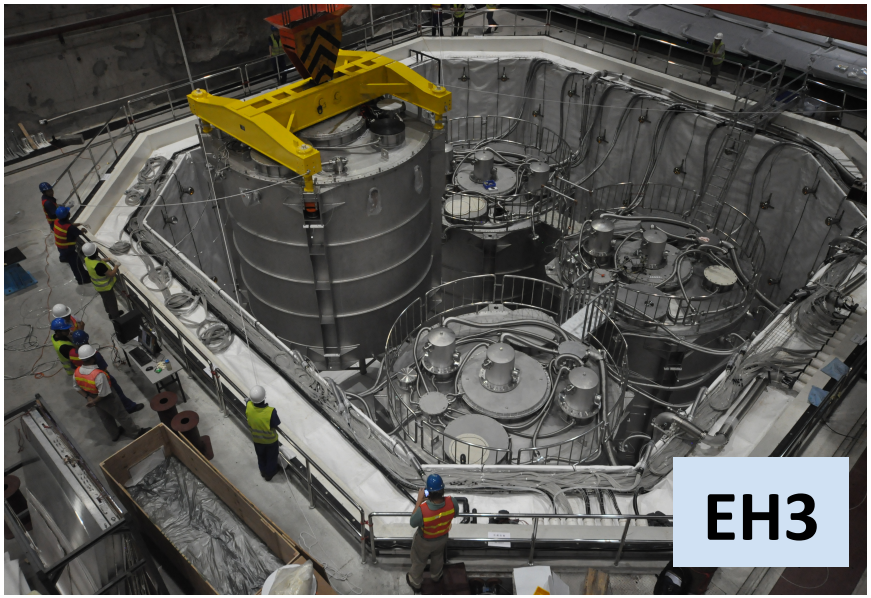

Full 4π detector calibration in Sep. 2012.

Sensitivity Projection

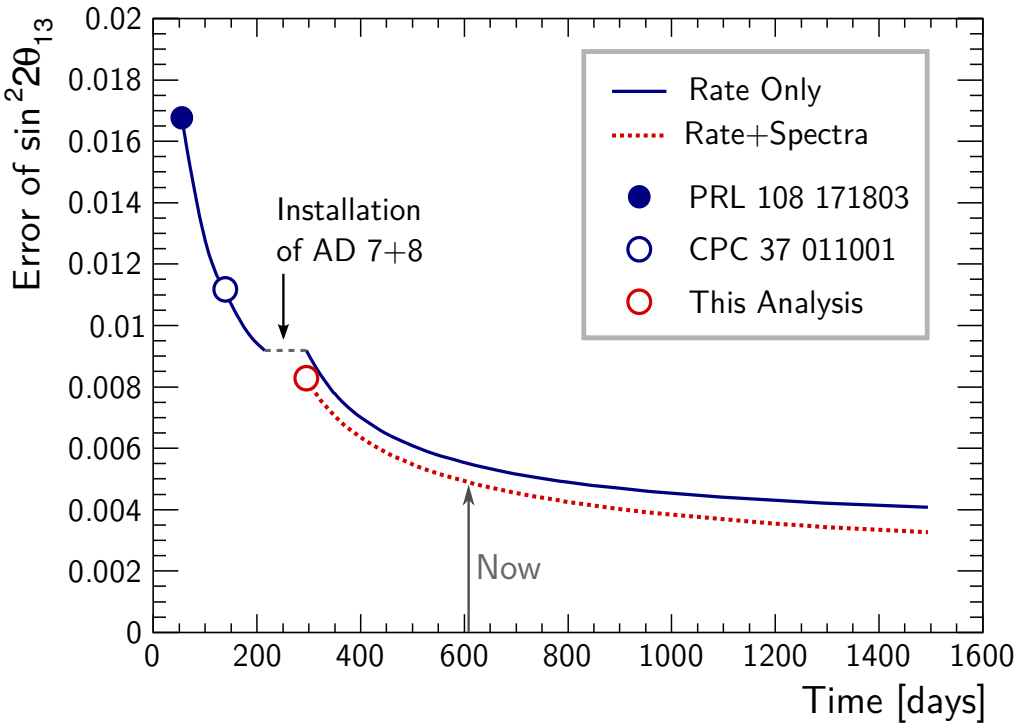

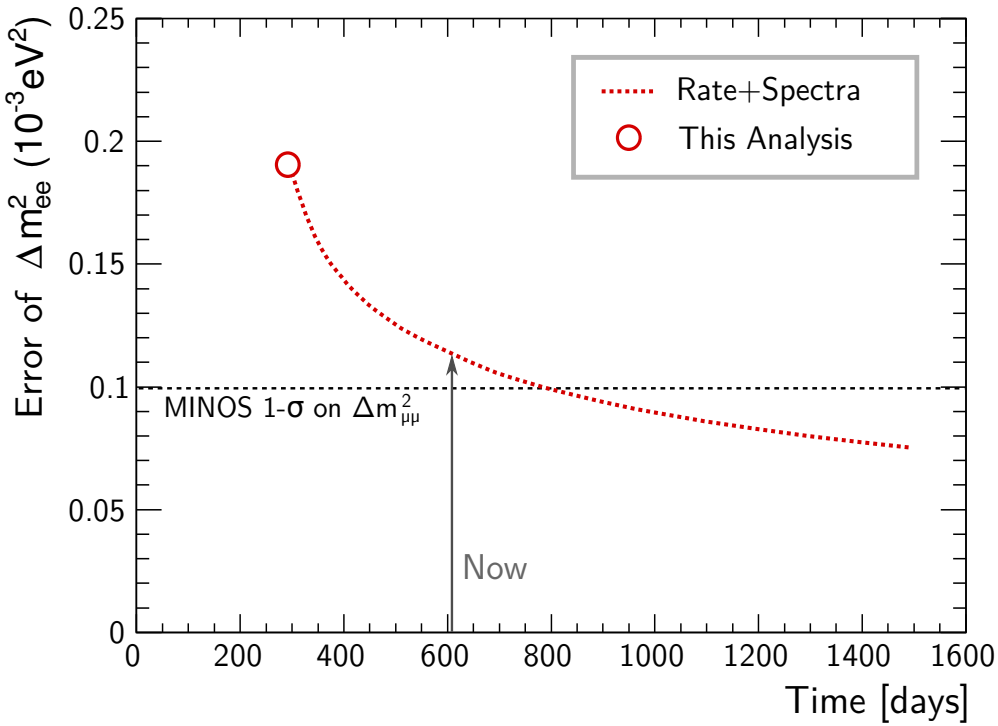

Sensitivity still dominated by statistics

- Statistics contribute 73% (65%) to total uncertainty in $\sin^2 2\theta_{13}$ ($|\Delta m^2_{ee}|$)
- Major systematics:
  - θ_{13}: Reactor model, relative + absolute energy, and relative efficiencies
  - $|\Delta m^2_{ee}|$: Relative energy model, relative efficiencies, and backgrounds
- Precision of mass splitting measurement closing in on results from μ flavor sector

Daya Bay Future

Improved precision on oscillation parameters

- Constrains non-standard oscillation models
- Improves reach of future neutrino experiments

Measure absolute reactor neutrino flux

- Explore the 'reactor antineutrino anomaly'
- Precise spectrum probes reactor models

Cosmogenic Backgrounds

- Measurement of cosmogenic production vs. depth

Supernova Neutrinos

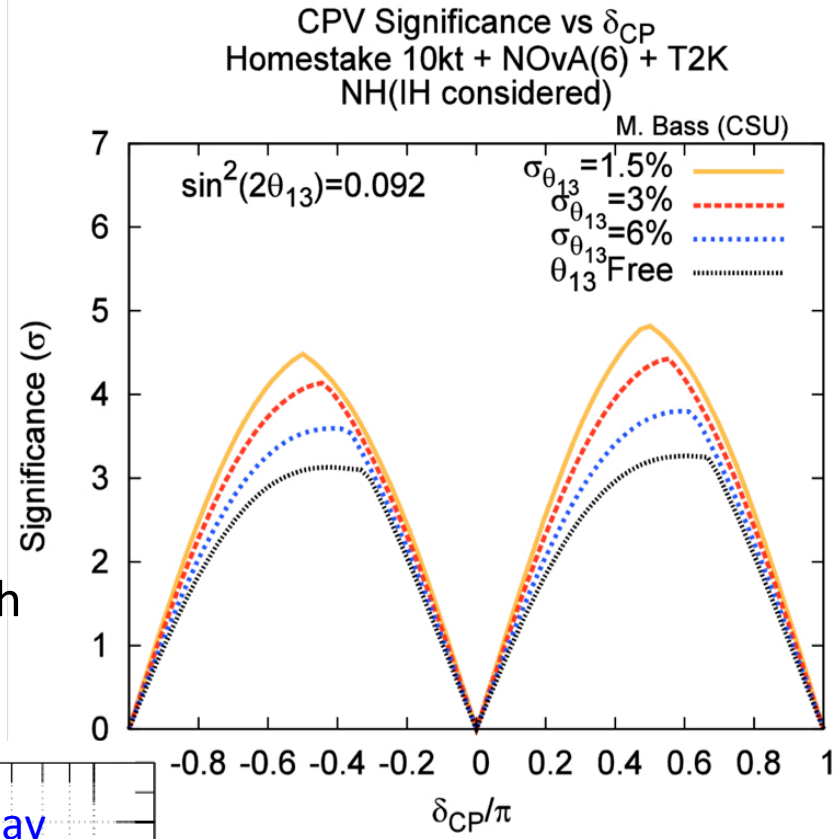

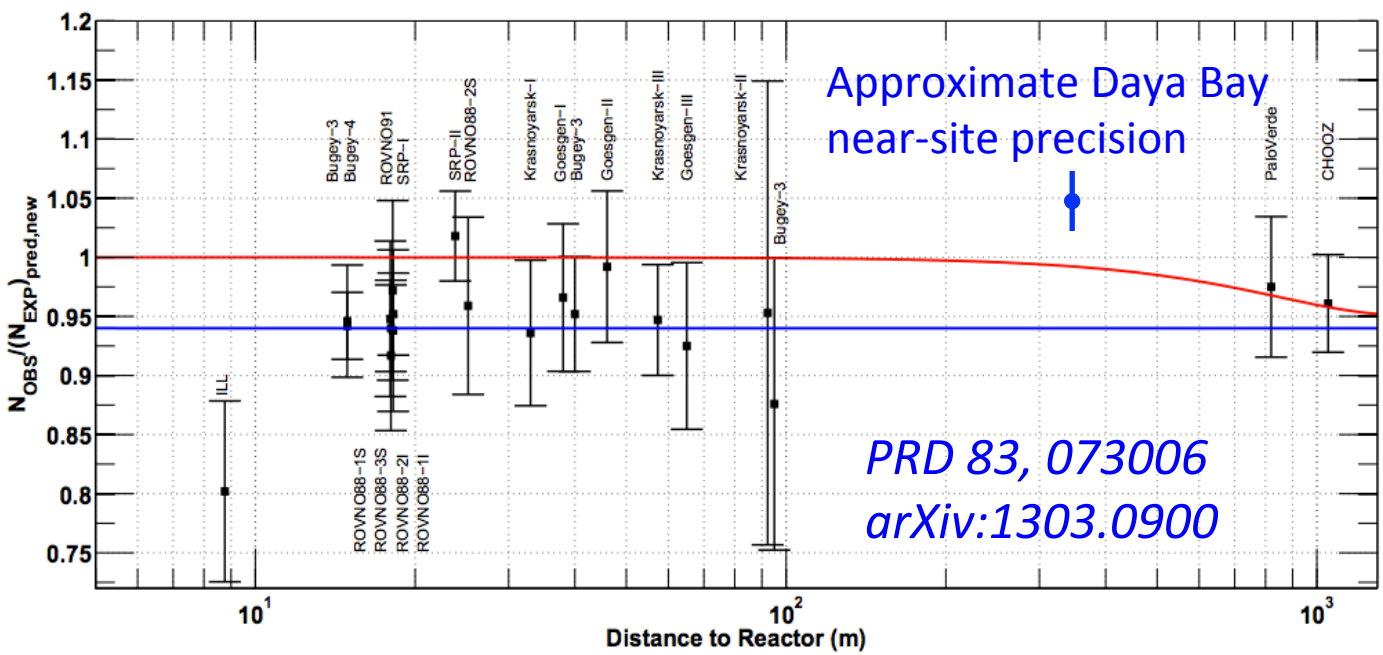

Summary

The Daya Bay Experiment has reported the first direct measurement of the short-distance electron antineutrino oscillation frequency:

$$\left|\Delta m^2_{ee}\right| = 2.59^{+0.19}_{-0.20} \times 10^{-3}\mathrm{eV}^2$$

The measurement has also produced the most precise estimate of the mixing angle:

$$\sin^2(2\theta_{13}) = 0.090^{+0.008}_{-0.009}$$

Expect more from Daya Bay:

- Measurement of the absolute reactor flux, addressing the reactor anomaly
- Constraints on non-standard neutrino models
- Significantly increased precision (all 8 detectors, >2 years of operation)

Backup

Trigger Performance

Trigger Thresholds:

- AD: >45 PMTs (digital trigger)
  >0.4 MeV (analog trigger)
- Inner Water Veto: > 6 PMTs
- Outer Water Veto: >7 PMTs
- RPC: ¾ layers in module

Trigger Efficiency:

- No measureable inefficiency >0.7 MeV
- Minimum energy expected for prompt antineutrino signal is ~0.9 MeV.

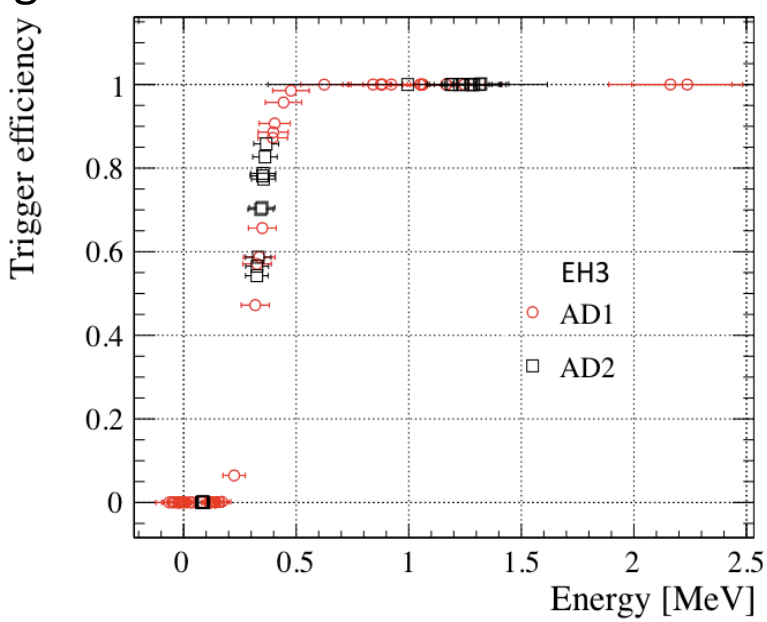

Digital Trigger (Nhit)

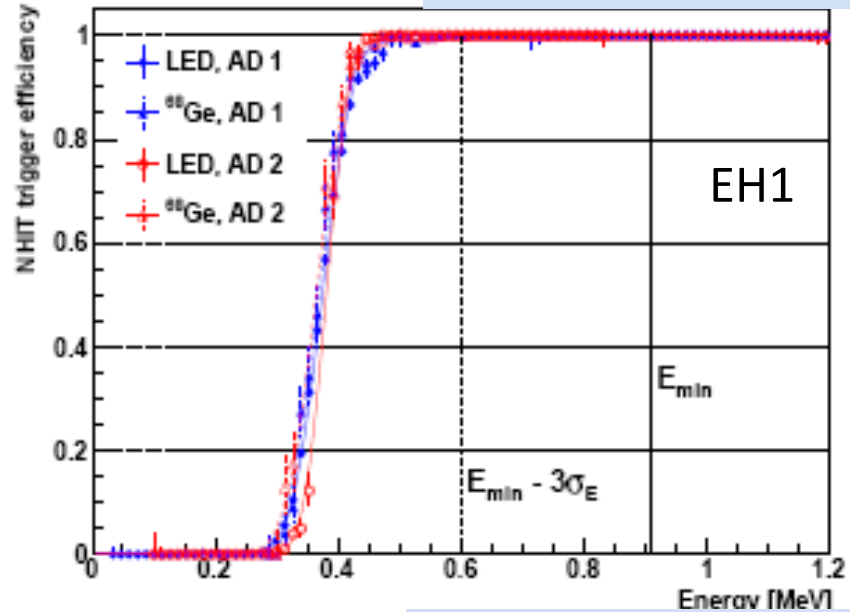

Analog Trigger (Esum)

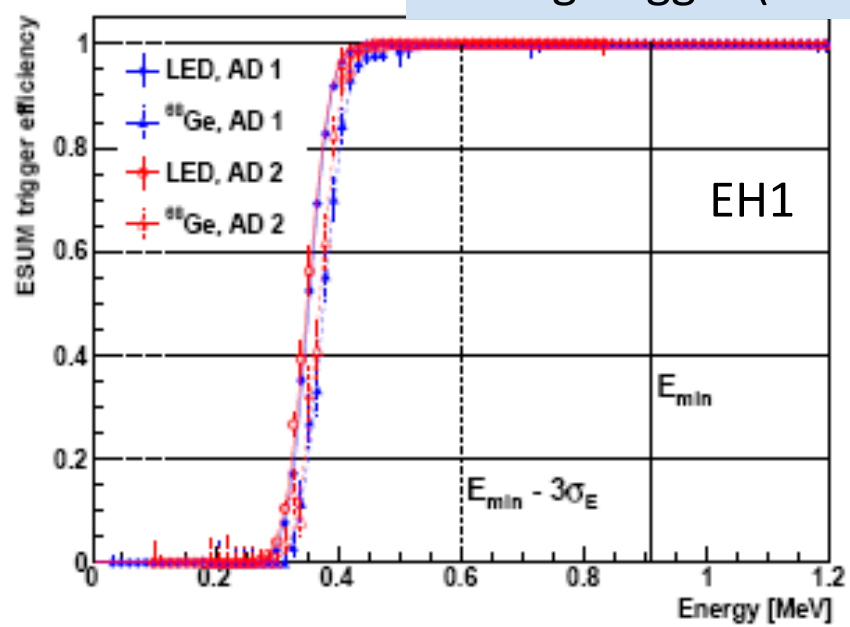

PMT Light Emission (Flashing)

Flashing PMTs:

- Instrumental background from ~5% of PMTS
- 'Shines' light to opposite side of detector
- Easily discriminated from normal signals

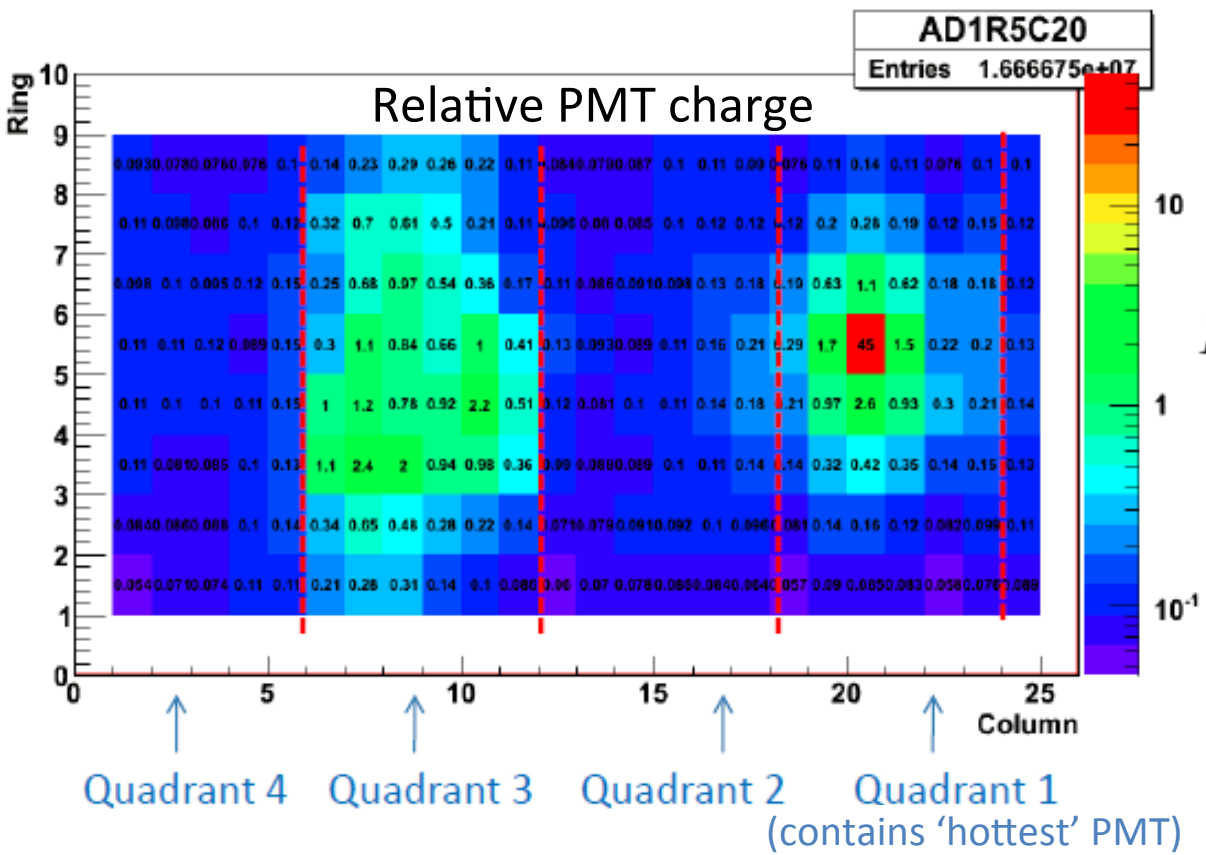

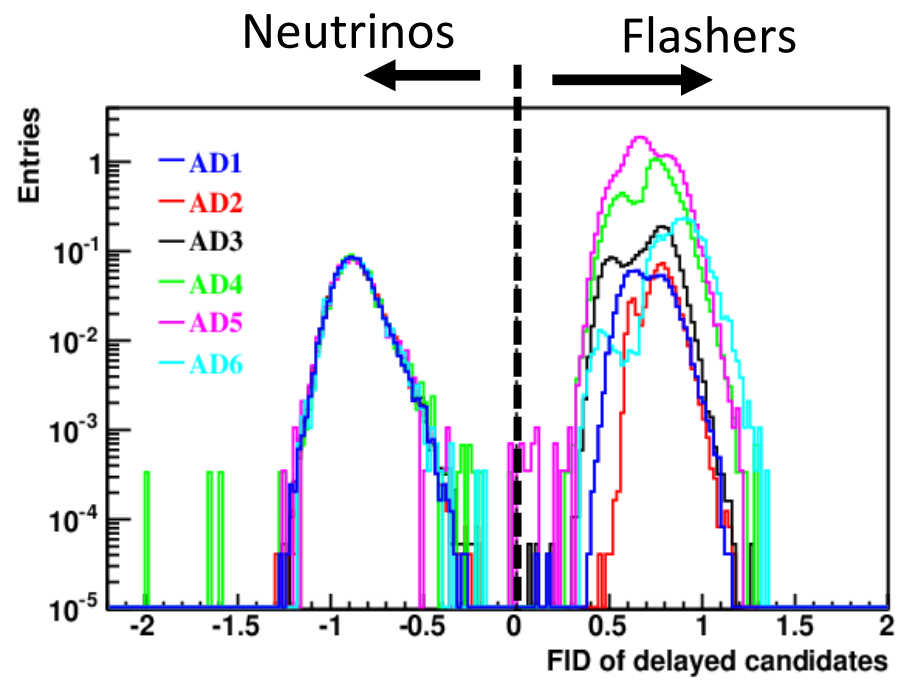

$$FID = \log_{10}((MaxQ)^2/(0.45)^2 + (Quad)^2)$$

Quadrant = Q3/(Q2+Q4)
MaxQ = maxQ/sumQ

Inefficiency to antineutrinos signal:
0.024% ± 0.006%(stat)
Contamination: < 0.01%

Calibration: PMT+Electronics Gain

Measure charge from single photons in-situ with data

Use out-of-time PMT signals hits to calibrate the PMT + electronics response to single photons.

Cross-check with weekly LED deployments.

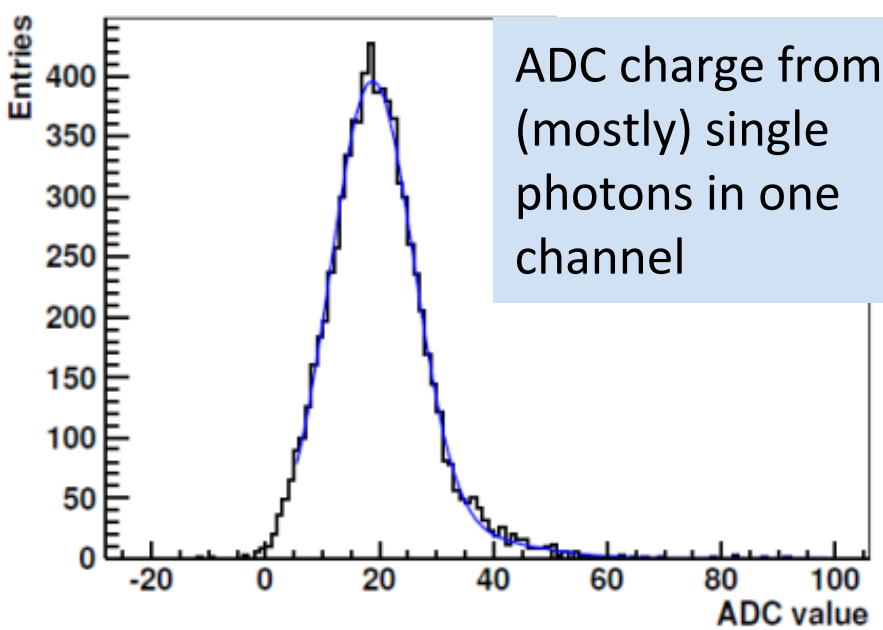

ADC charge from (mostly) single photons in one channel

Gain variation with time

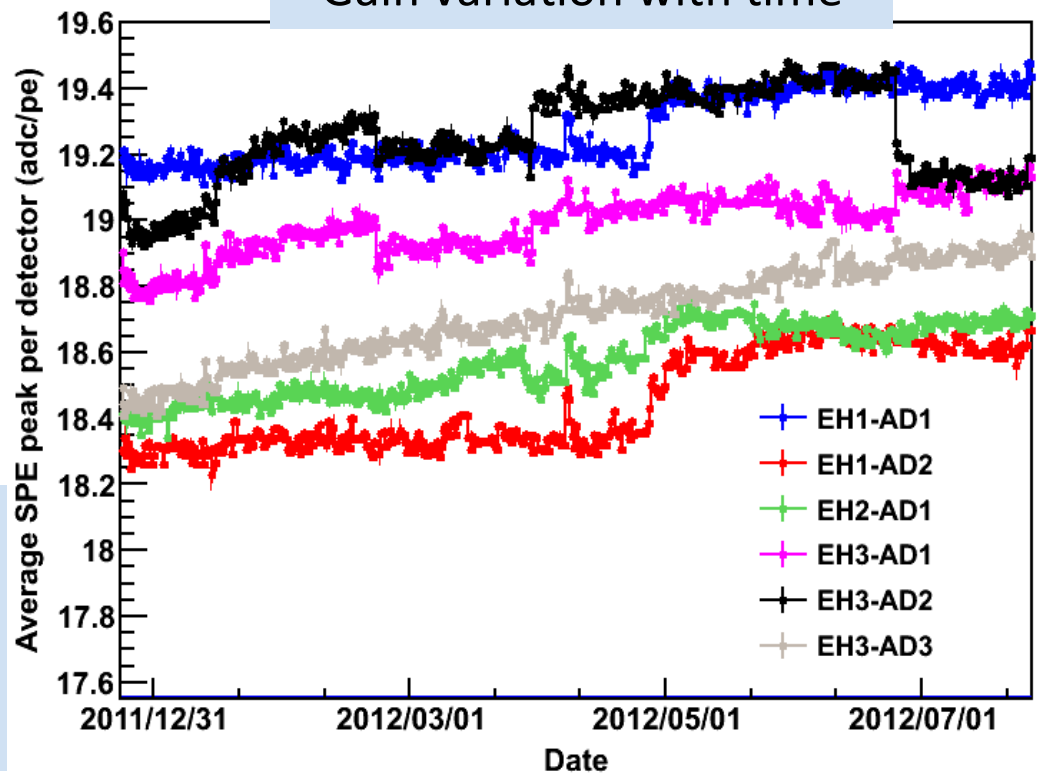

Calibration driven by uncertainty in relative detector efficiency

$$\frac{N_{\mathrm{f}}}{N_{\mathrm{n}}} = \left(\frac{N_{\mathrm{p,f}}}{N_{\mathrm{p,n}}}\right)\left(\frac{L_{\mathrm{n}}}{L_{\mathrm{f}}}\right)^2\left(\frac{\epsilon_{\mathrm{f}}}{\epsilon_{\mathrm{n}}}\right)\left[\frac{P_{\mathrm{sur}}(E,L_{\mathrm{f}})}{P_{\mathrm{sur}}(E,L_{\mathrm{n}})}\right]$$

Calibration: Energy Scale

Measure energy scale in-situ with data

Calibrate charge (photoelectrons) collected per MeV in-situ using spallation nGd capture events. Also use weekly deployments of ^{60}Co source.

Spallation *n*Gd capture (uniform throughout detector)

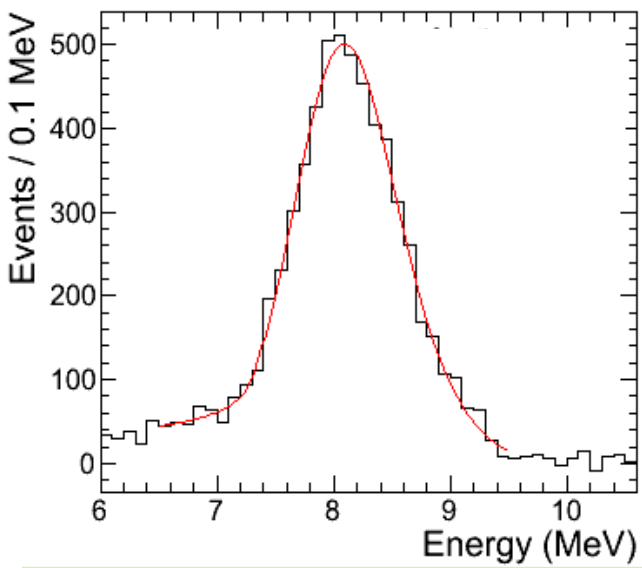

Energy Scale = Q / E

Measured charge of nGd peak

Average energy released in nGd

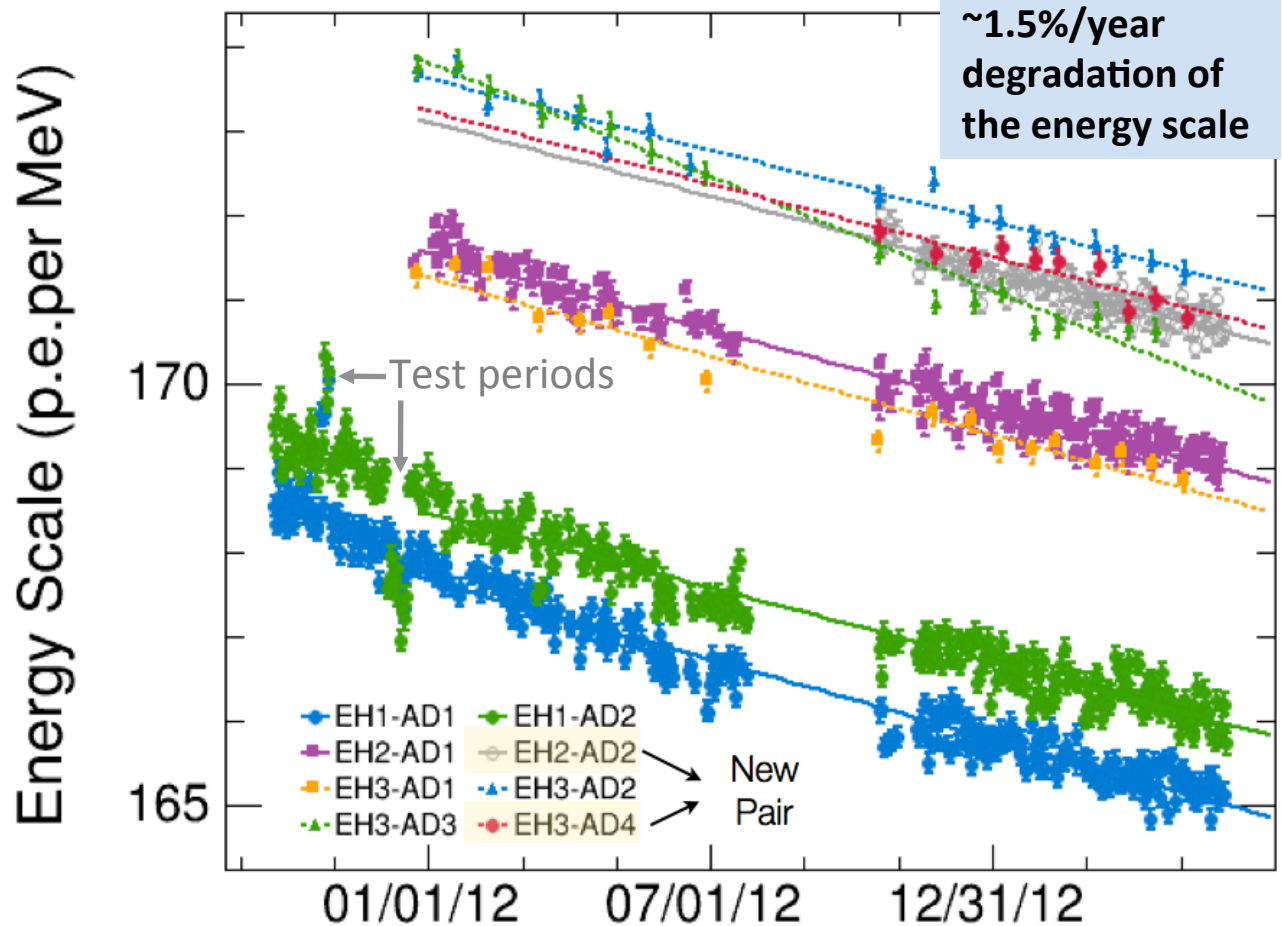

Small degradation of energy scale is seen with nGd, ^{60}Co, and other event types. Its origin is still unknown, but do not anticipate any problems in experiment's lifetime.

Calibration: Detector Uniformity

Measure uniformity with sources placed along three axes and spallation nGd events

Example: ^{60}Co

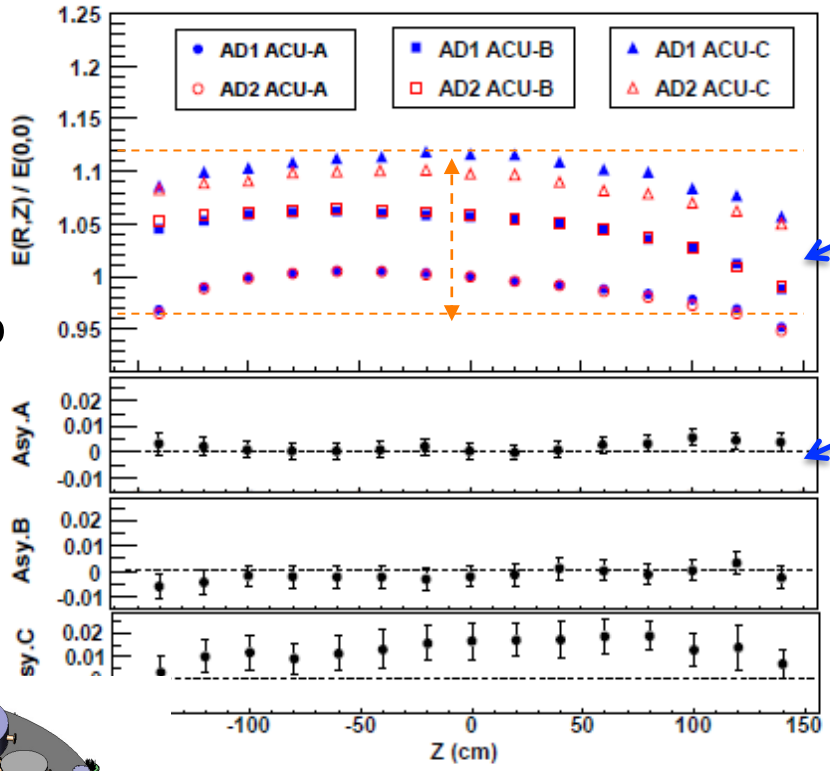

Energy response varies across detector…

…but still consistent between detectors

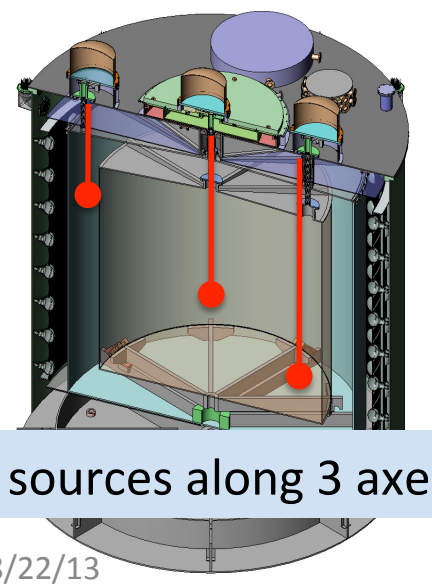

3 sources along 3 axes

After first-order correction, energy is more uniform.

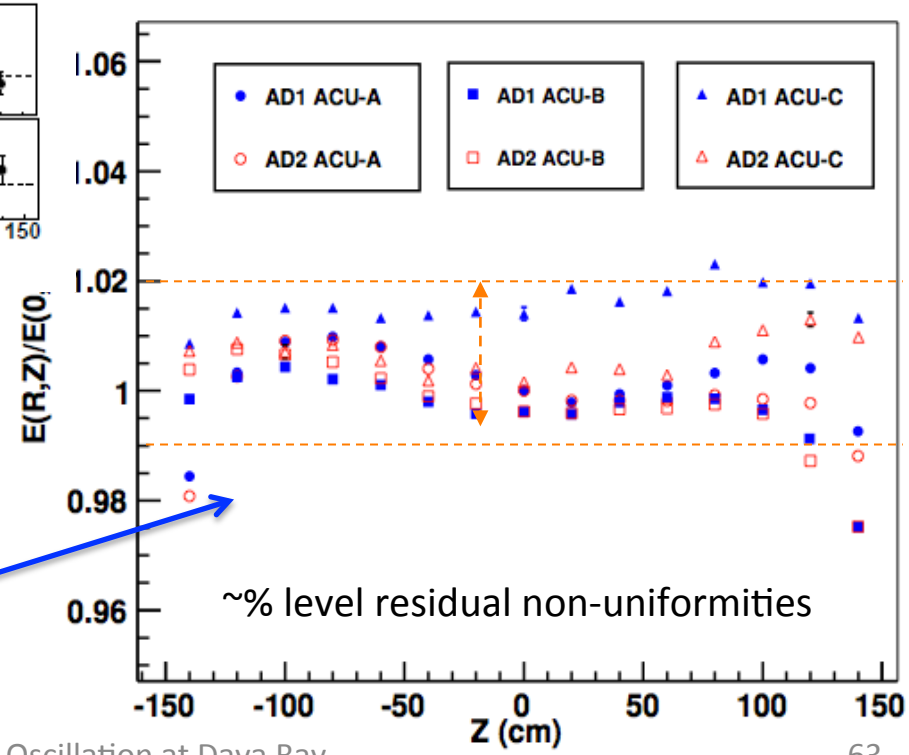

Detector Response: Non-Uniformity

Predicted prompt spectrum assumes totally flat non-

We know percent-level non-uniformities in E_{rec} exist. **Does this matter?**

Will cause percent-level spectral broadening, less than from photon statistics (~7%)

Can complicate distortion from acrylic vessel, which is also position dependent.

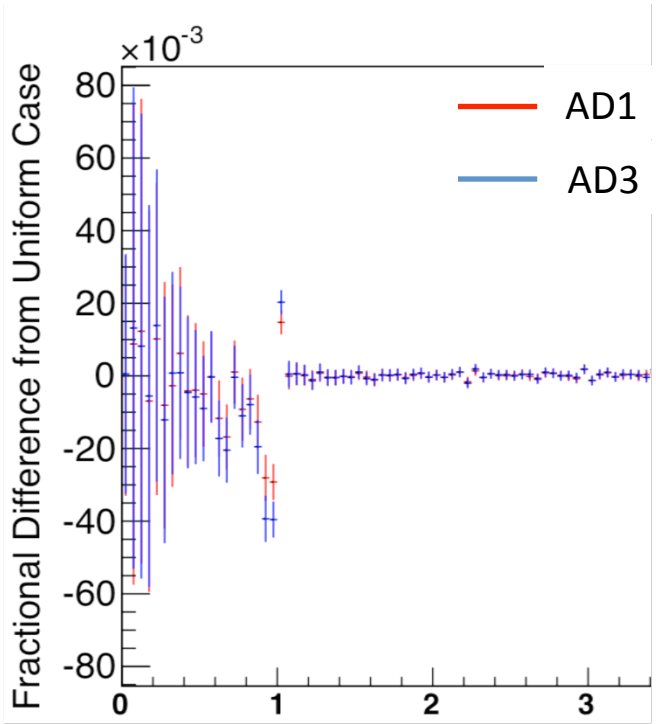

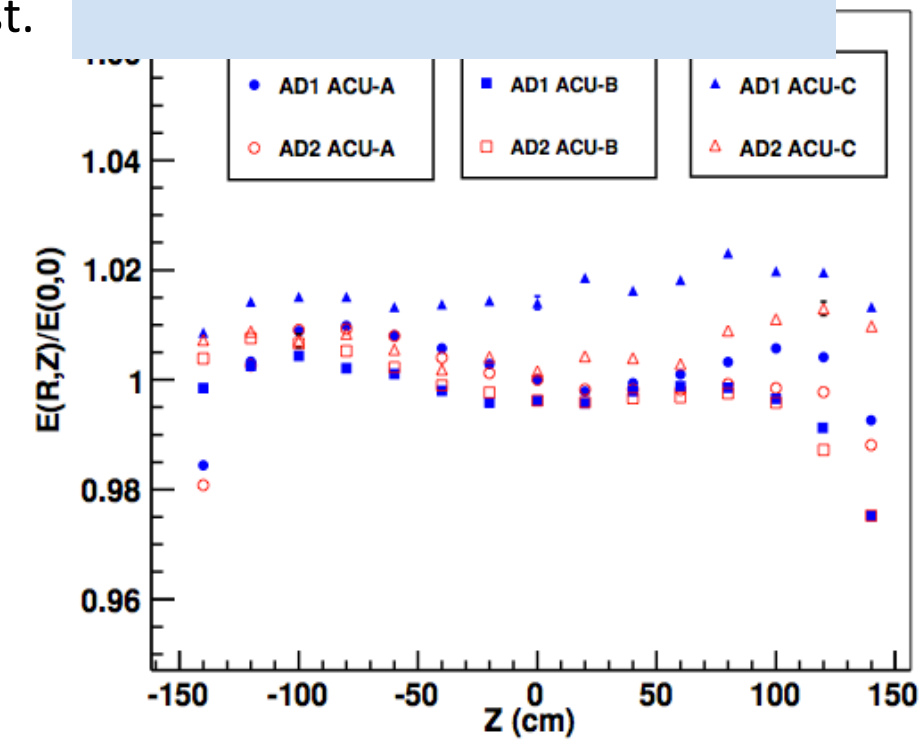

Simulate prompt spectrum for flat, AD1 and AD3 residual non-uniformities

Differences much smaller than spectral uncertainties from other sources.

All energy scale non-uniformities have a negligible effect on Daya Bay prompt spectra

Gamma + Beta Spectra

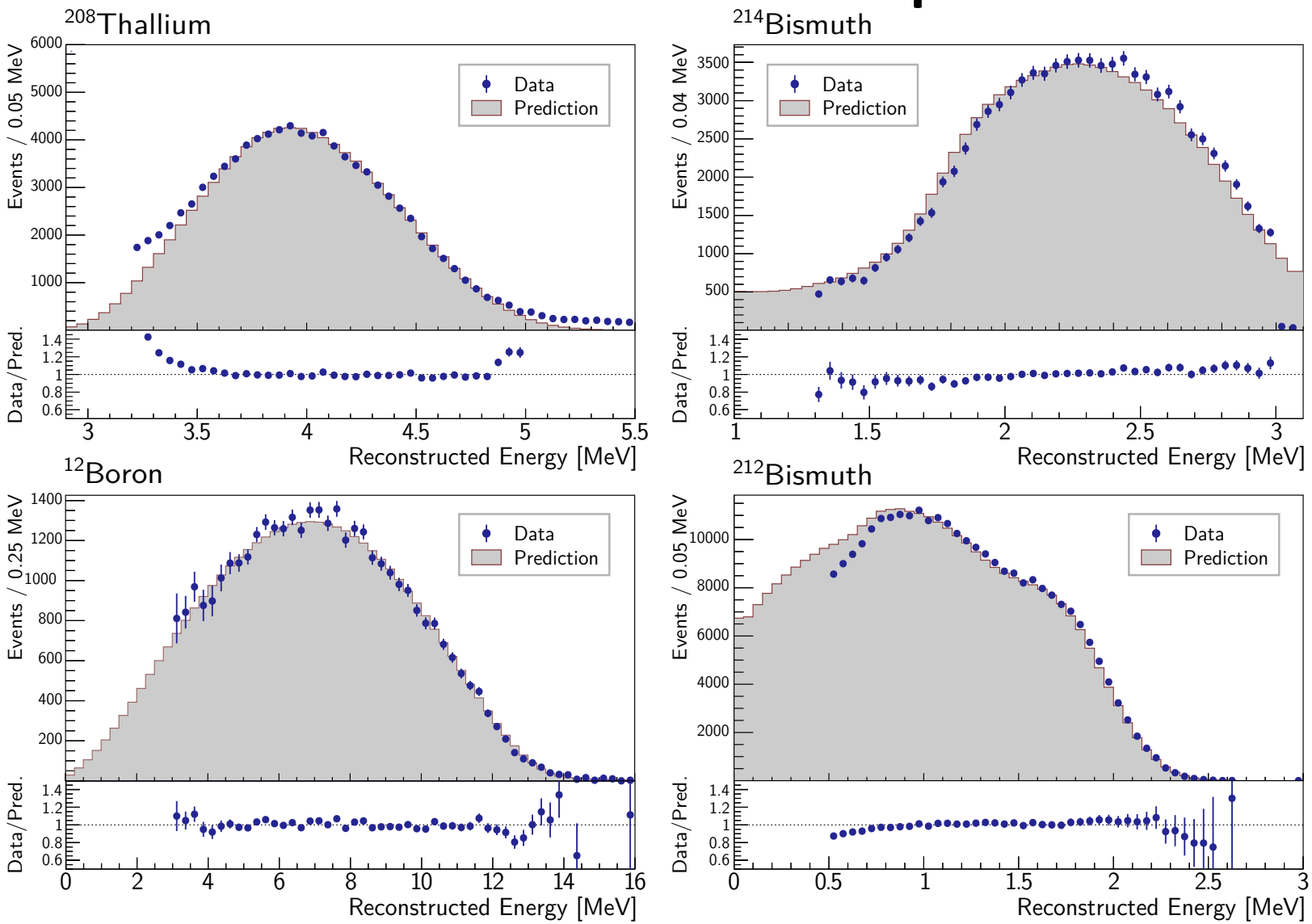

Additional spectra from ^{212}Bi, ^{214}Bi and ^{208}Tl decays

- Sizable theoretical uncertainties from 1st forbidden non-unique beta decays
- ^{212}Bi, ^{214}Bi and ^{208}Tl spectra only utilized to cross-check results

Singles Spectrum

Triggered signals dominated by low-energy radioactivity

Measured Rates: ~65 Hz above 0.7 MeV in each detector

Black:
After muon veto

Red:
Isolated events
(-400μs to 200μs)

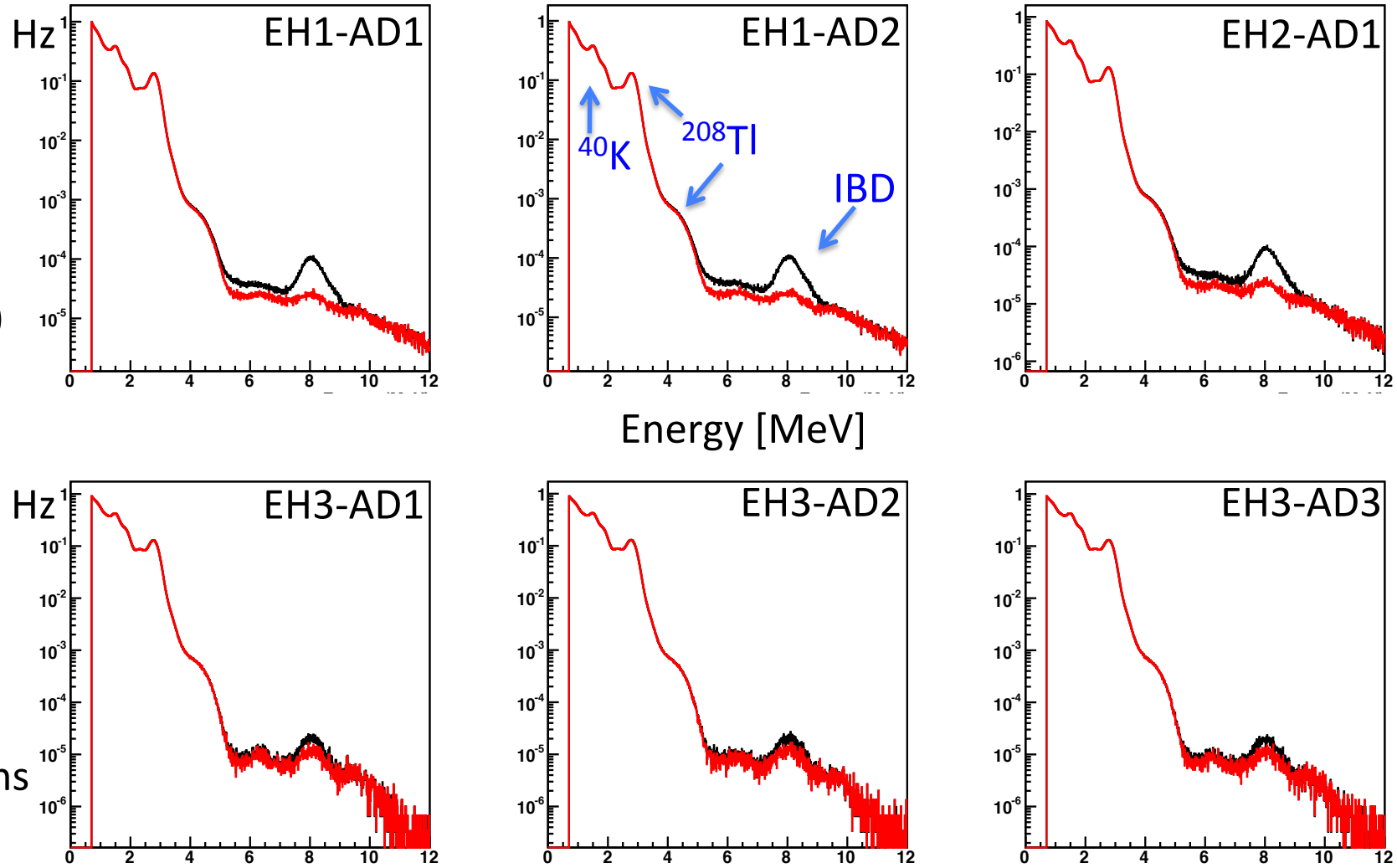

Sources:
Stainless Steel:
U/Th chains
PMTs:
40K, U/Th chains
Scintillator:
Radon/U/Th chains

Delayed Energy Cut

Largest uncertainty between detectors

Some *n*Gd gammas escape scintillator region, visible as tail of *n*Gd energy peak.

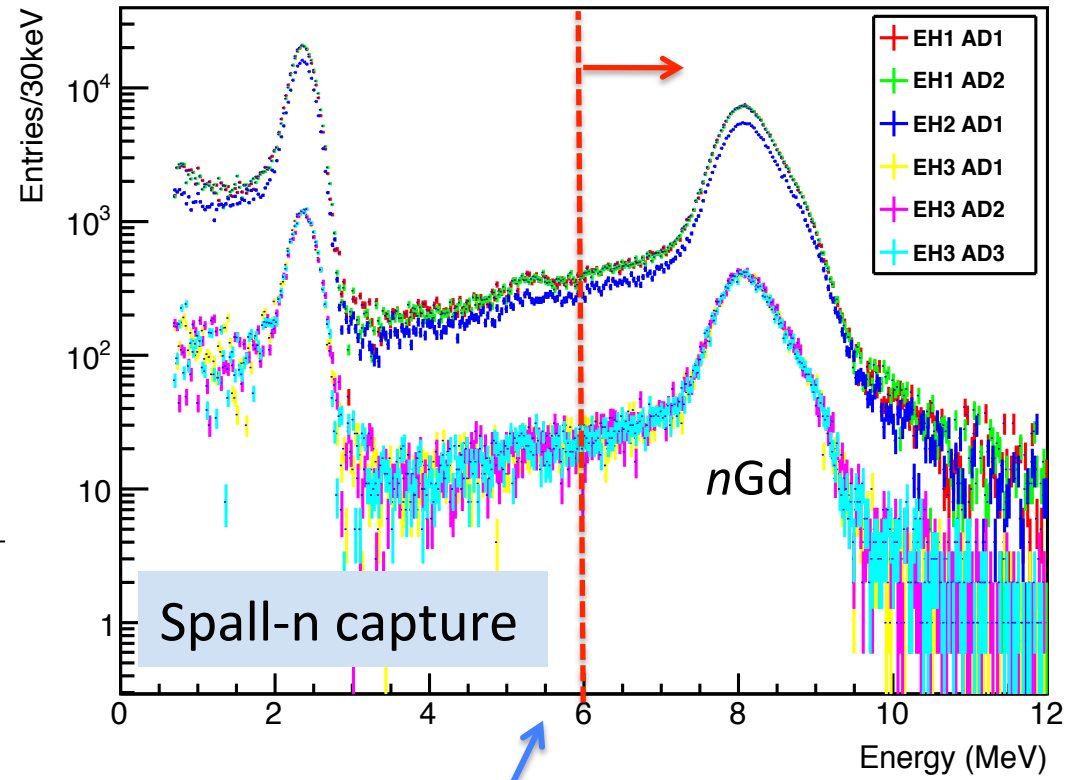

Use variations in energy peaks to constrain relative efficiency.

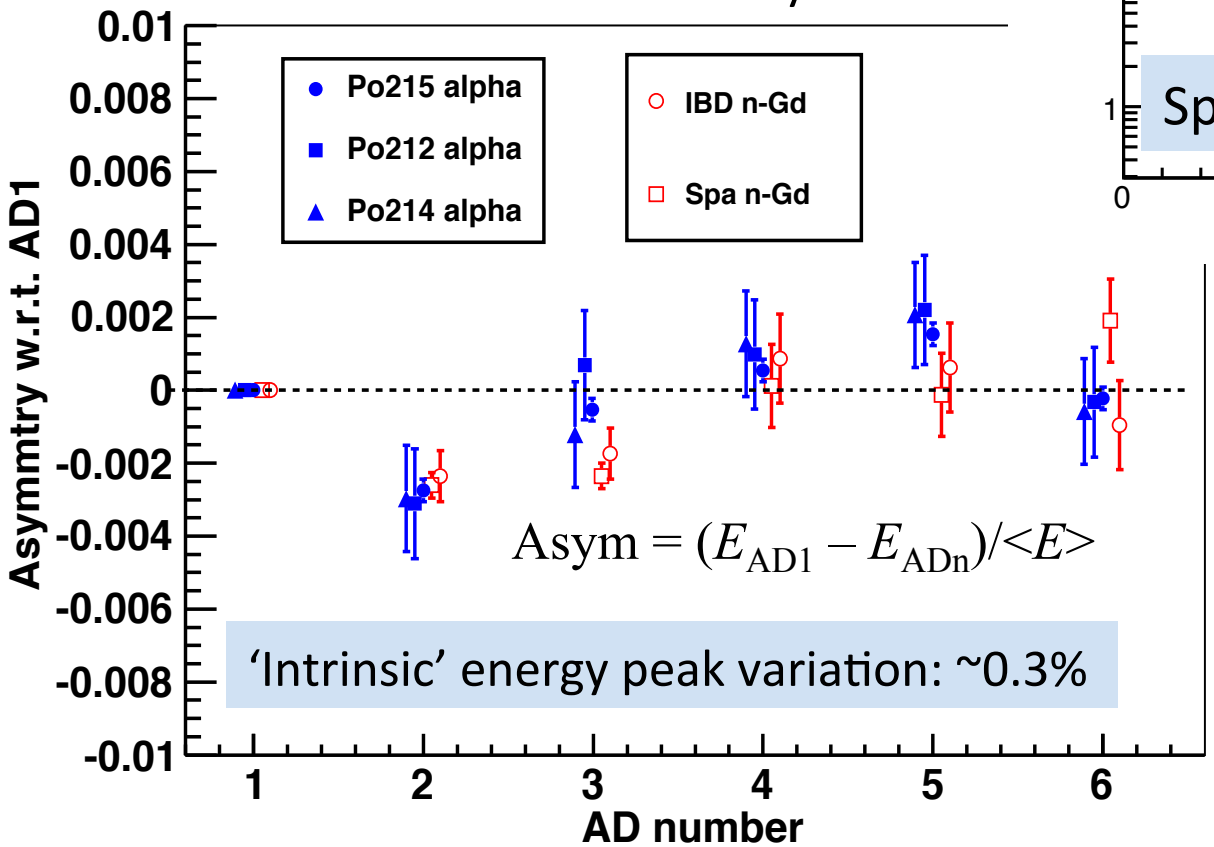

Efficiency variations estimated at 0.12%

Motivation for 3-zone design

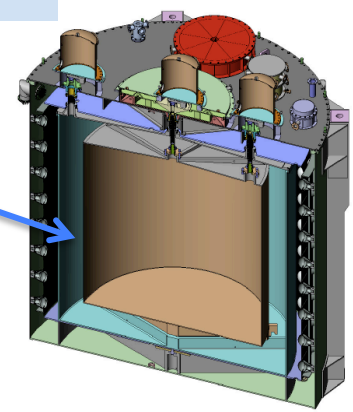

Capture Time

Consistent IBD neutron capture time measured in all detectors

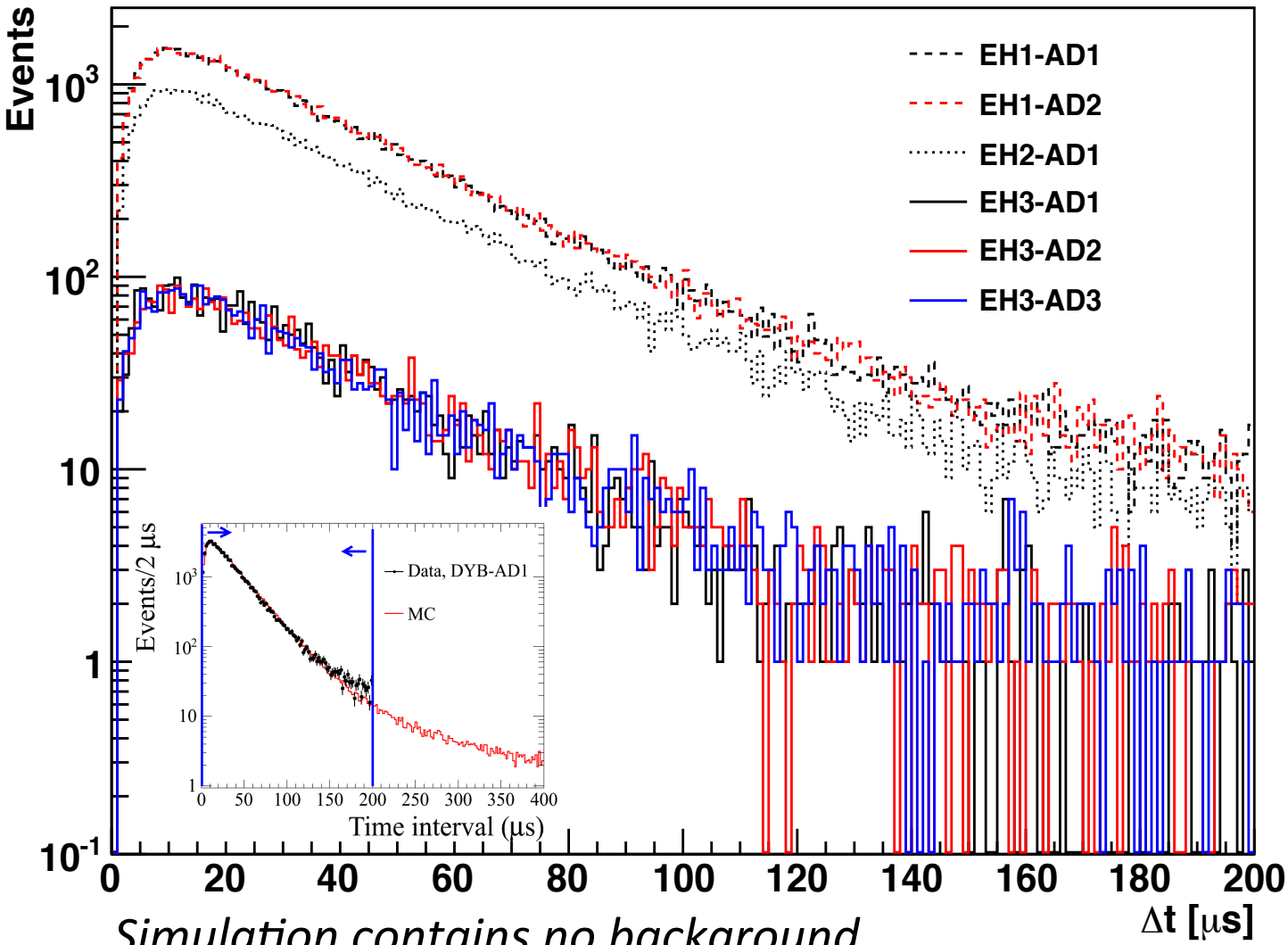

Simulation contains no background (deviates from data at >150 μs)

Capture time cut:
1μs to 200μs

Efficiency uncertainty within 0.01% between detectors.

Background: Fast neutrons

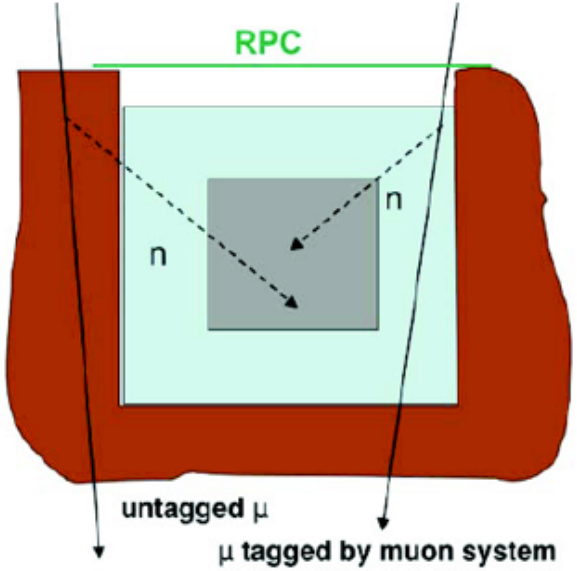

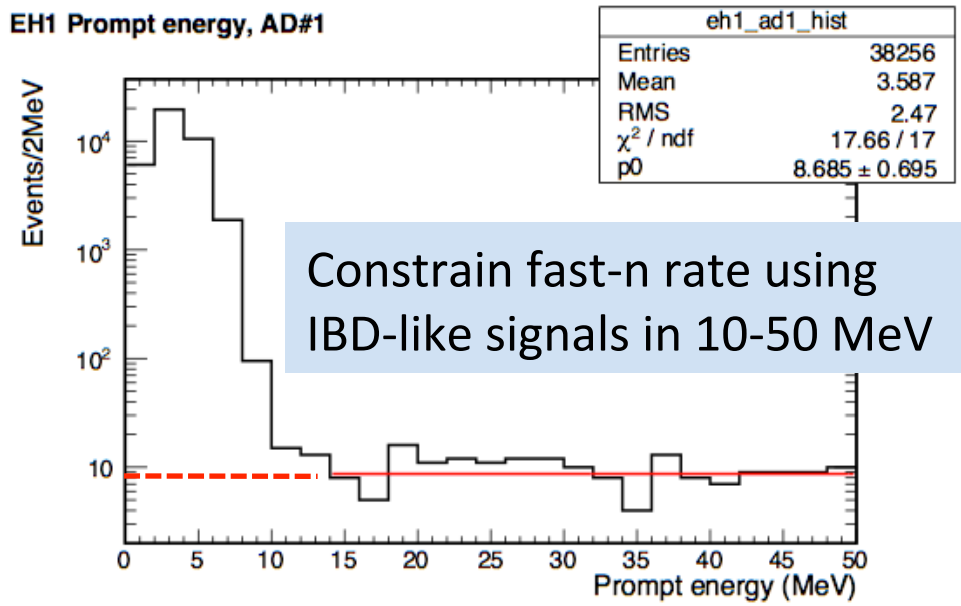

Constrain fast-n rate using IBD-like signals in 10-50 MeV

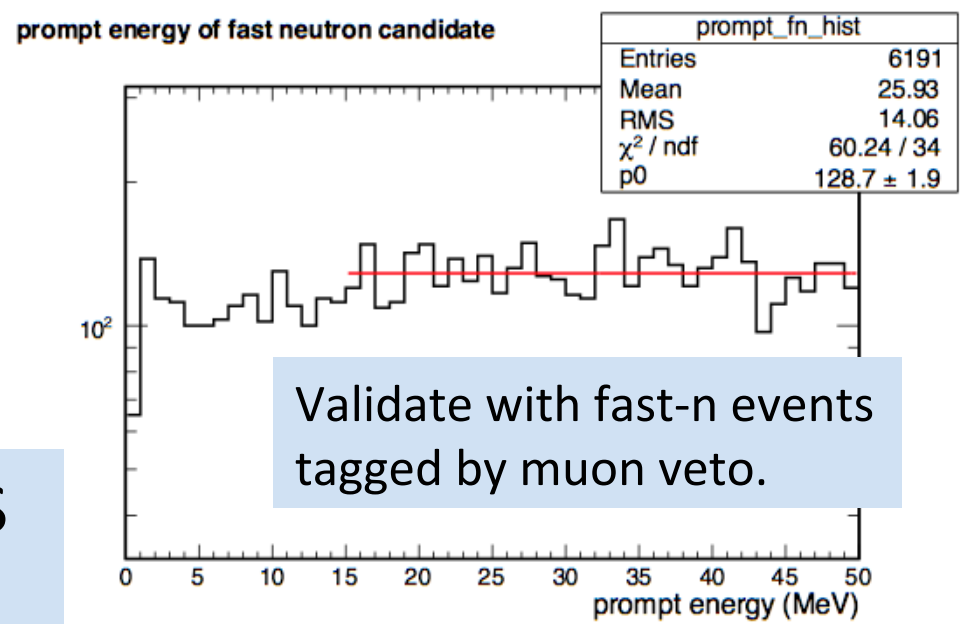

Validate with fast-n events tagged by muon veto.

Fast Neutrons:

Energetic neutrons produced by cosmic rays (inside and outside of muon veto system)

Mimics antineutrino (IBD) signal:

- Prompt: Neutron collides/stops in target
- Delayed: Neutron captures on Gd

Analysis muon veto cuts control B/S to 0.06% (0.1%) of far (near) signal.

Background: $^{13}C(\alpha,n)^{16}O$

Alphas from intrinsic radioactivity (^{238}U, ^{232}Th, ^{235}U, ^{210}Po) measured in-situ.
Background rate and spectra modeled using known $^{13}C(\alpha,n)^{16}O$ cross-section.

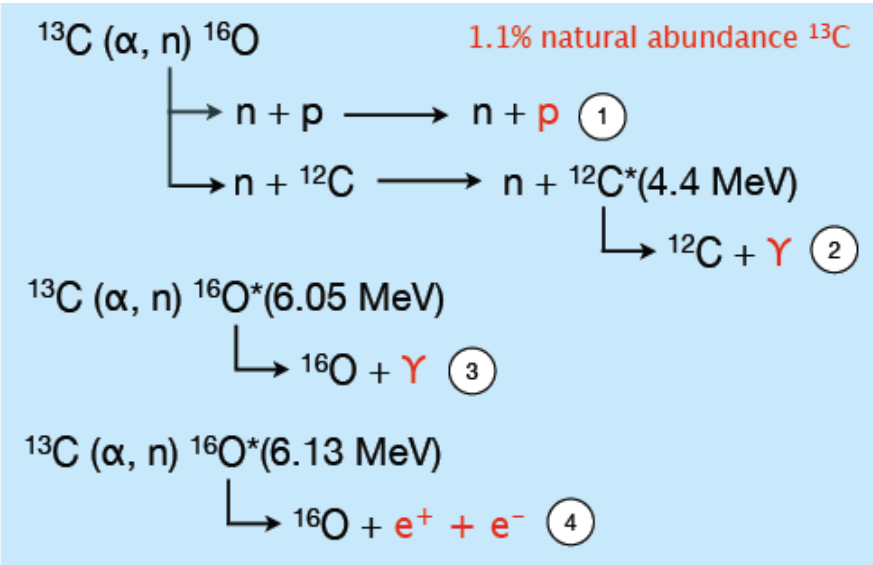

Example alpha rate in AD1	^{238}U	^{232}Th	^{235}U	^{210}Po
Bq	0.05	1.2	1.4	10

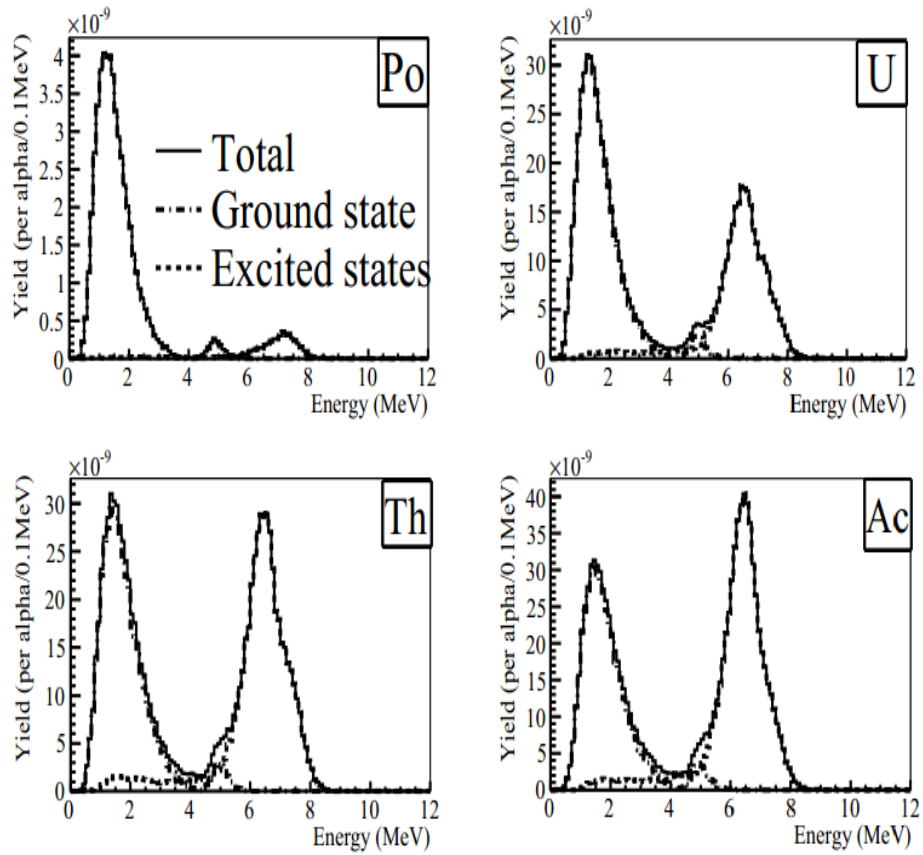

Near Sites: (0.05 to 0.08)±0.04 per day, B/S (0.01±0.006)%

Far Site: 0.04±0.02 per day, B/S (0.05±0.03)%

Reactor Flux Expectation

Antineutrino flux is estimated for each reactor core

Flux estimated using:

$$S(E_\nu) = \frac{W_{th}}{\sum_i (f_i/F) e_i} \sum_i^{istopes} (f_i/F) S_i(E_\nu)$$

Reactor operators provide:
- Thermal power data: W_{th}
- Relative isotope fission fractions: f_i

Energy released per fission: e_i

V. Kopekin et al., Phys. Atom. Nucl. 67, 1892 (2004)

Antineutrino spectra per fission: $S_i(E_\nu)$

K. Schreckenbach et al., Phys. Lett. B160, 325 (1985)
A. A. Hahn et al., Phys. Lett. B218, 365 (1989)
P. Vogel et al., Phys. Rev. C24, 1543 (1981)
T. Mueller et al., Phys. Rev. C83, 054615 (2011)
P. Huber, Phys. Rev. C84, 024617 (2011)

Isotope fission rates vs. reactor burnup

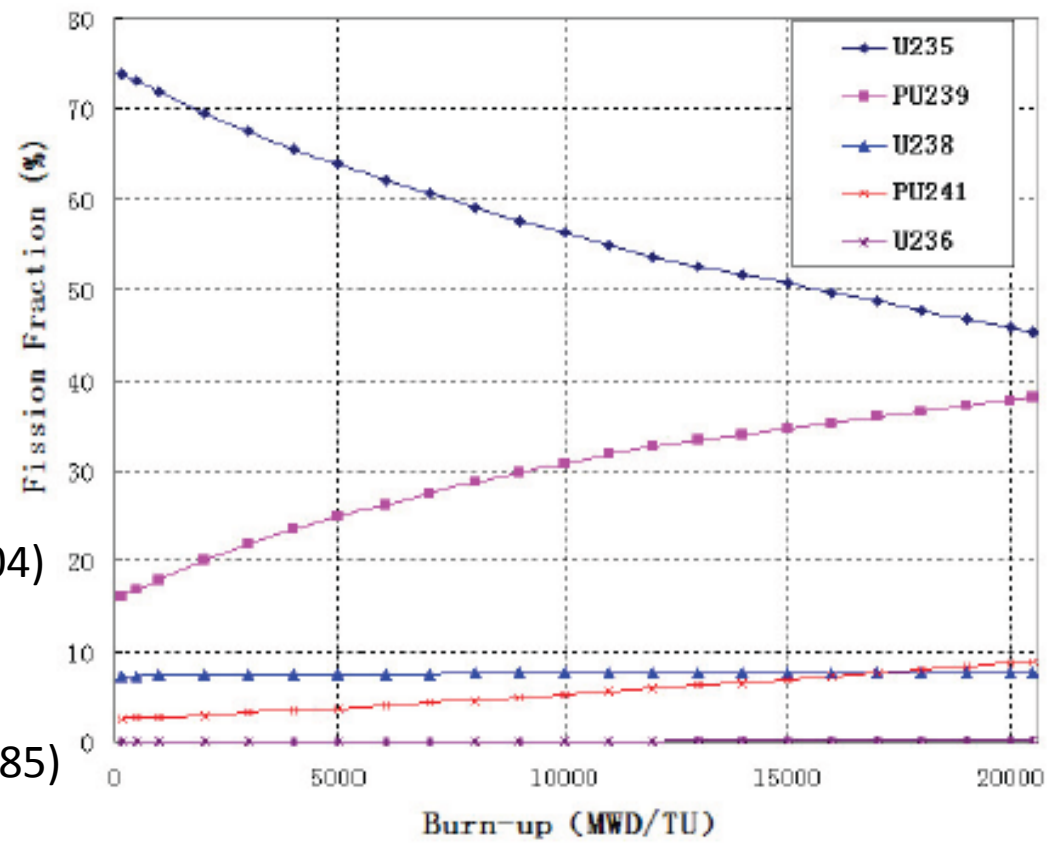

Flux model has negligible impact on far vs. near oscillation measurement

Reactor Flux Models

Antineutrino flux S(E) from each reactor used to predict IBDs at each detector

	^{235}U	^{238}U	^{239}Pu	^{241}Pu
AD 1	63.3	12.2	19.5	4.8
AD 2	63.3	12.2	19.5	4.8
AD 3	61.0	12.5	21.5	4.9
AD 4	61.5	12.4	21.1	4.9
AD 5	61.5	12.4	21.1	4.9
AD 6	61.5	12.4	21.1	4.9

Approximate percentage of IBDs from each fission isotope at each detector

New model:

P. Huber, Phys. Rev. C84, 024617 (2011),
T. Mueller et al., Phys. Rev. C83, 054615 (2011)

Old model:

K. Schreckenbach et al., Phys. Lett. B160, 325 (1985)
A. A. Hahn et al., Phys Rev Lett. B218, 365 (1989)
P. Vogel et al. Phys. Rev. C24, 1543 (1981)

New/Old flux model difference in unoscillated IBD prediction by hall

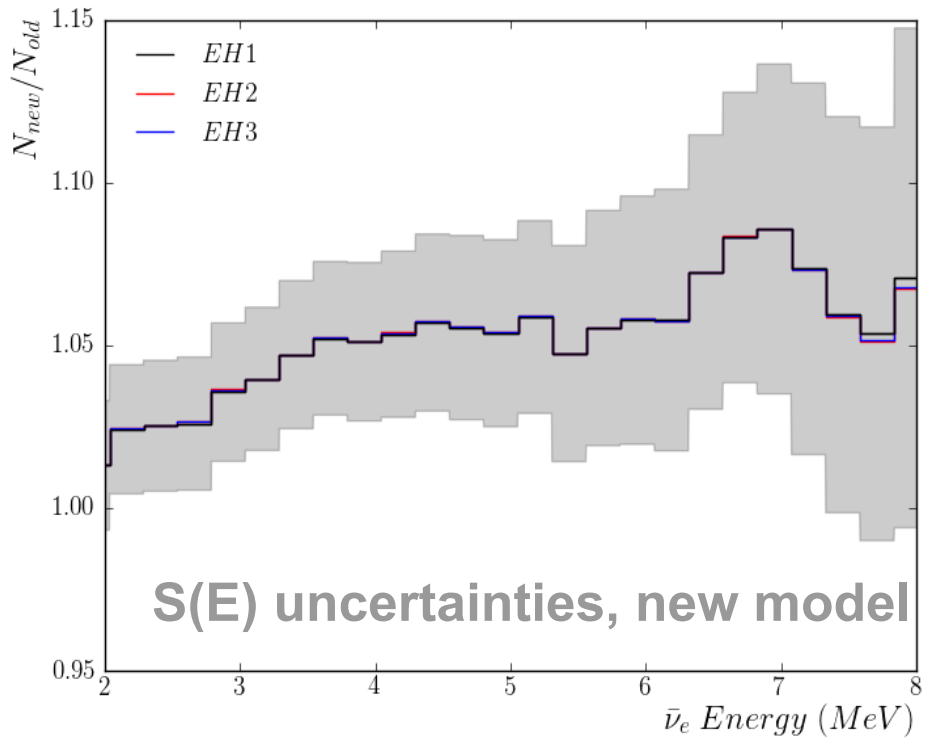

Flux model has negligible impact on far vs. near oscillation measurement

Pure Spectral Analysis

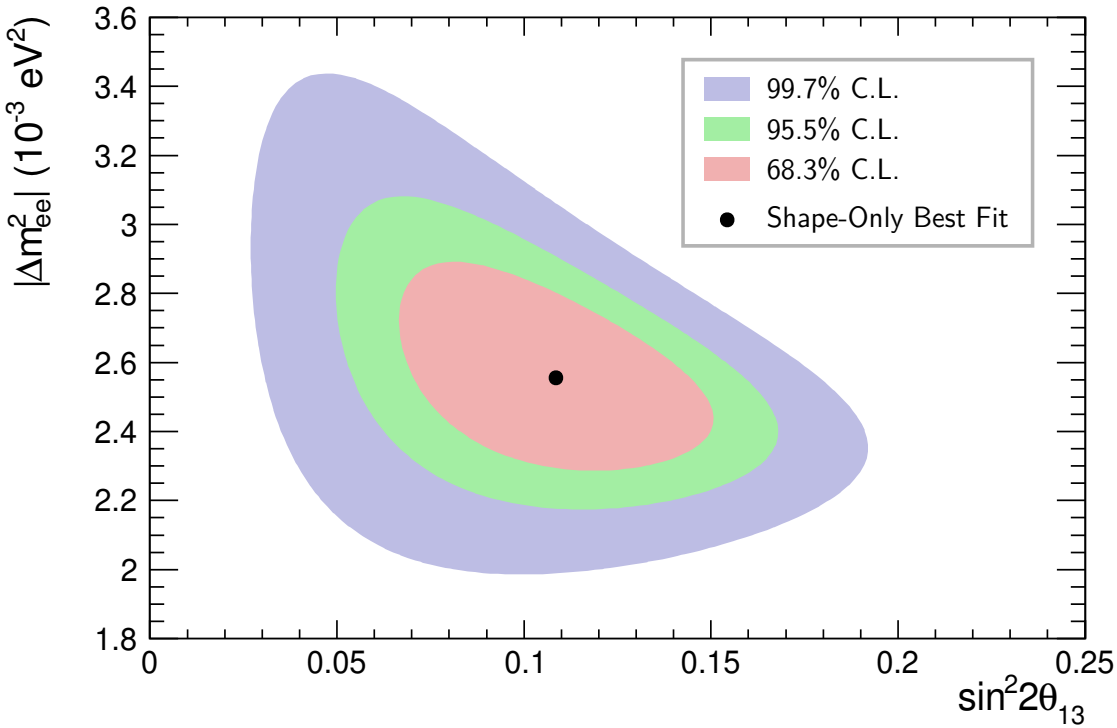

$$\sin^2 2\theta_{13} = 0.108 \pm 0.028$$

$$|\Delta m^2_{ee}| = 2.55^{+0.21}_{-0.18} \cdot 10^{-3}\text{eV}^2$$

$$\chi^2/N_{\text{DoF}} = 161.2/148$$

$\theta_{13} = 0$ can be excluded at > 3σ from spectral information alone

- For each AD, total event prediction fixed to observed data:

  1 θ_{13} free-floating: $\chi^2/N_{\text{DoF}} = 161.2/148$

  2 $\theta_{13} = 0$: $\chi^2/N_{\text{DoF}} = 178.5/146$

$\Rightarrow$ $\Delta\chi^2/N_{\text{DoF}} = 17.3/2$, corresponding to $p = 1.75 \cdot 10^{-4}$

Pure Relative Shape Analysis

Independent oscillation analysis with pure relative shape comparison:

Predict far spectra directly from measured near site spectra
→ Minimizes impact of absolute flux and spectra prediction

Use covariance matrices to account for systematic errors
→ Eliminates all nuisance parameters from the fit

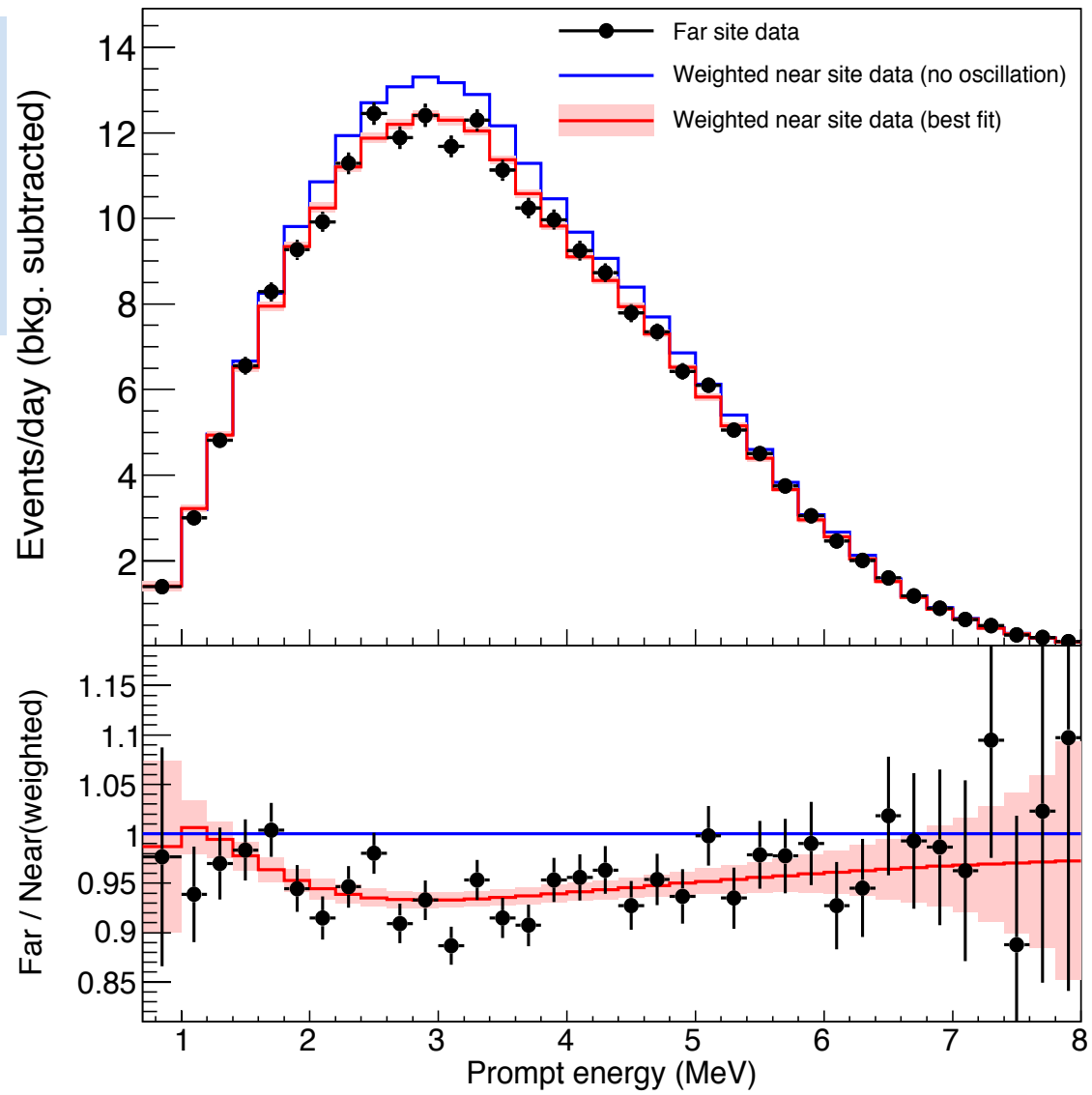

$$\chi^2 = \sum_{i,j}^{E_{rec}\ \text{bins}} (N_i^{far} - N_i^{near(weighted)})(V^{-1})_{ij}(N_j^{far} - N_j^{near(weighted)})$$

Relative Shape Method Results

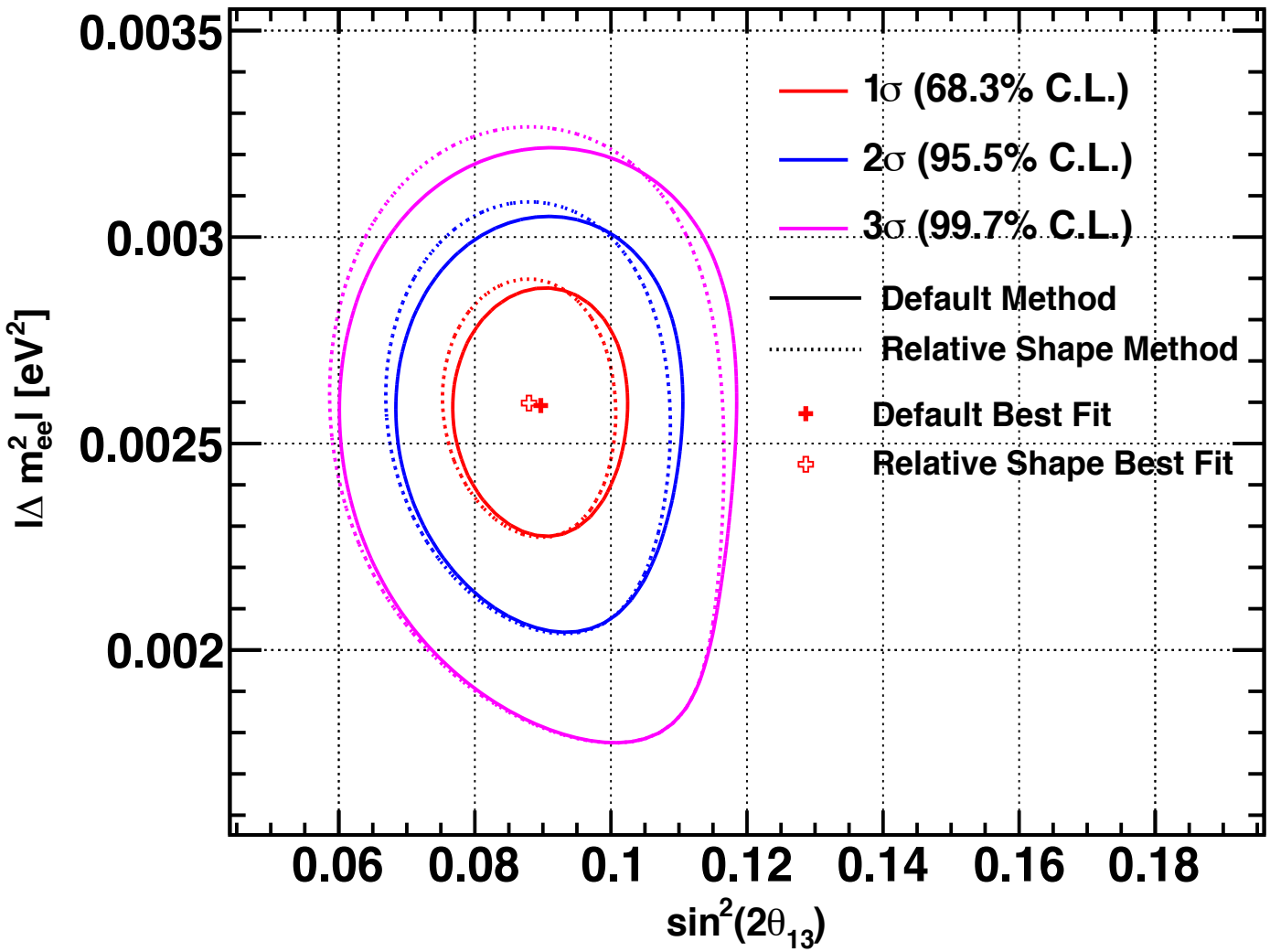

Obtained consistent fit results with the default method

Making a Far Site prediction from the Near Site data

From the

- relative reactor core power info
- experimental layout geometry

it is possible to determine what fraction of events in each near detector at each true energy bin originate from each core.

Each of these components is then individually extrapolated to the far site

All reactor and detector correlated systematics, including the absolute flux and shape uncertainties, **cancel to first order.**

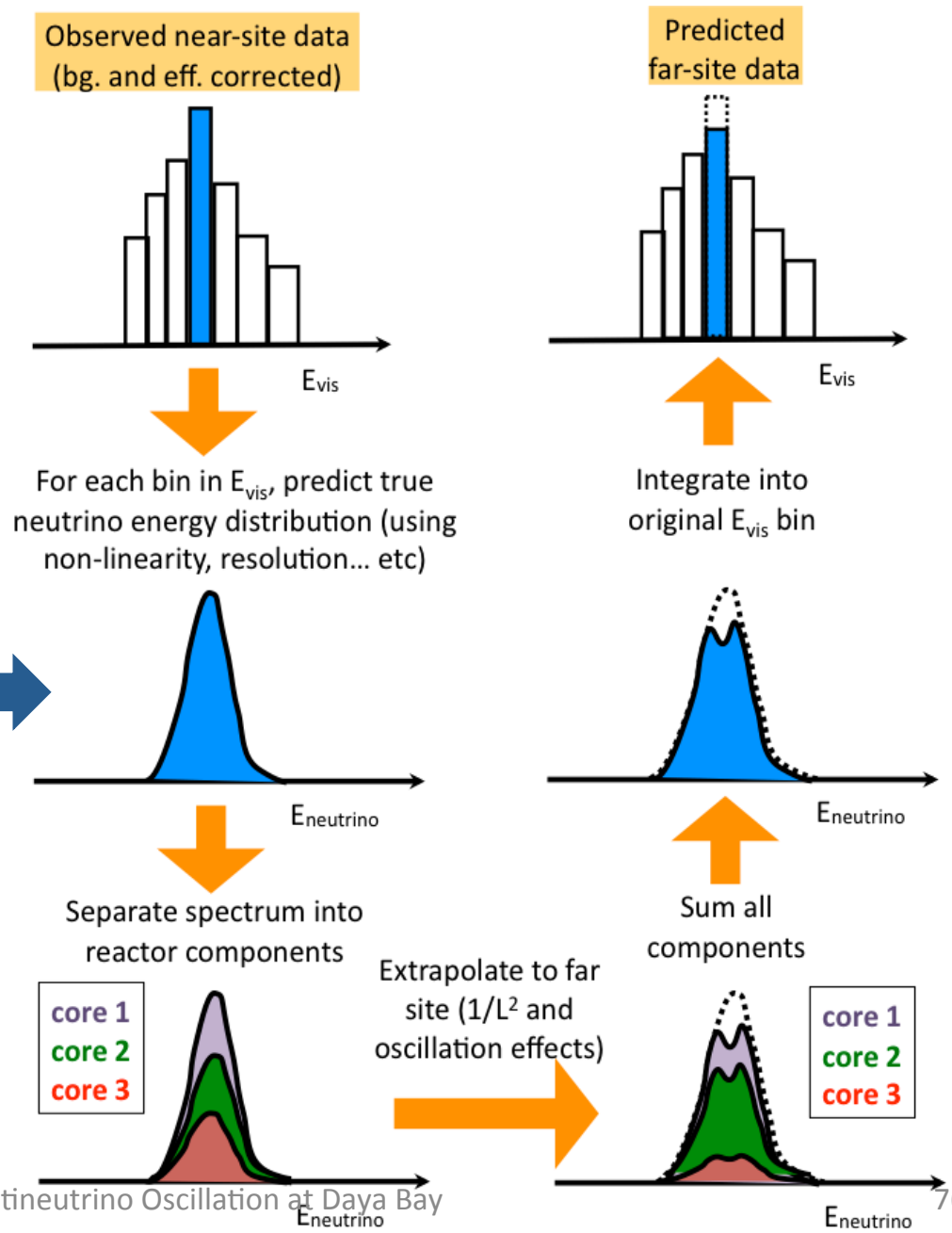

Cross-checking the rate+shape contours with MC statistics

Can verify that Wilk's approximation holds by generating MC samples and checking that a cut at $\Delta\chi^2$=? excludes the expected amount of fake experiments.

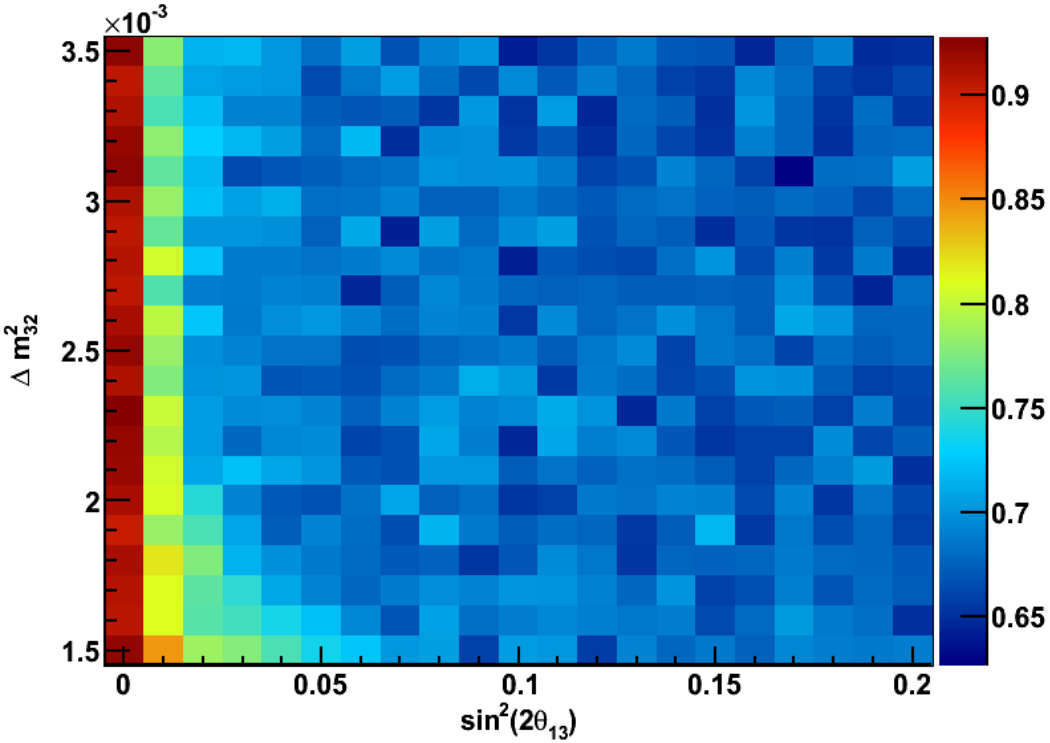

Fraction of events excluded by cutting at $\Delta\chi^2$ = 2.30

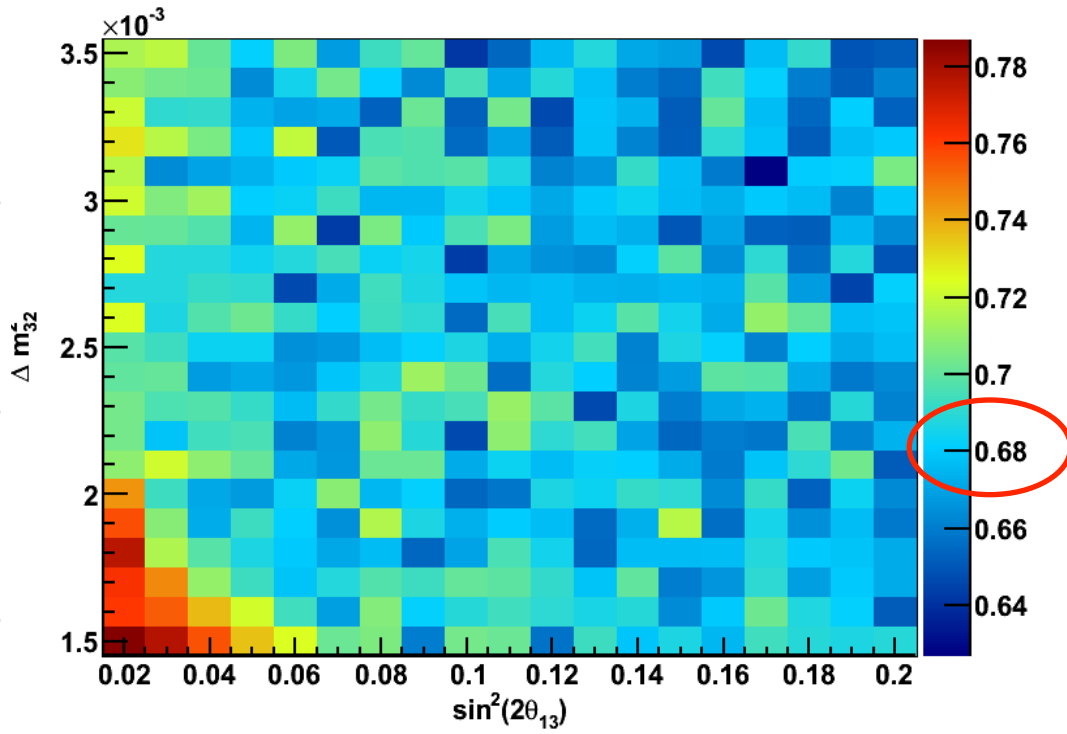

Same as left plot but without first two bins in x-axis

In our area of parameter space, things look

Relative Shape Uncertainties

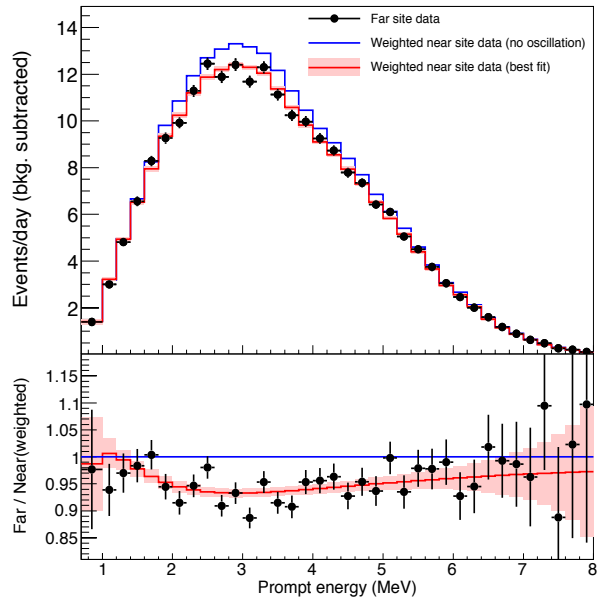

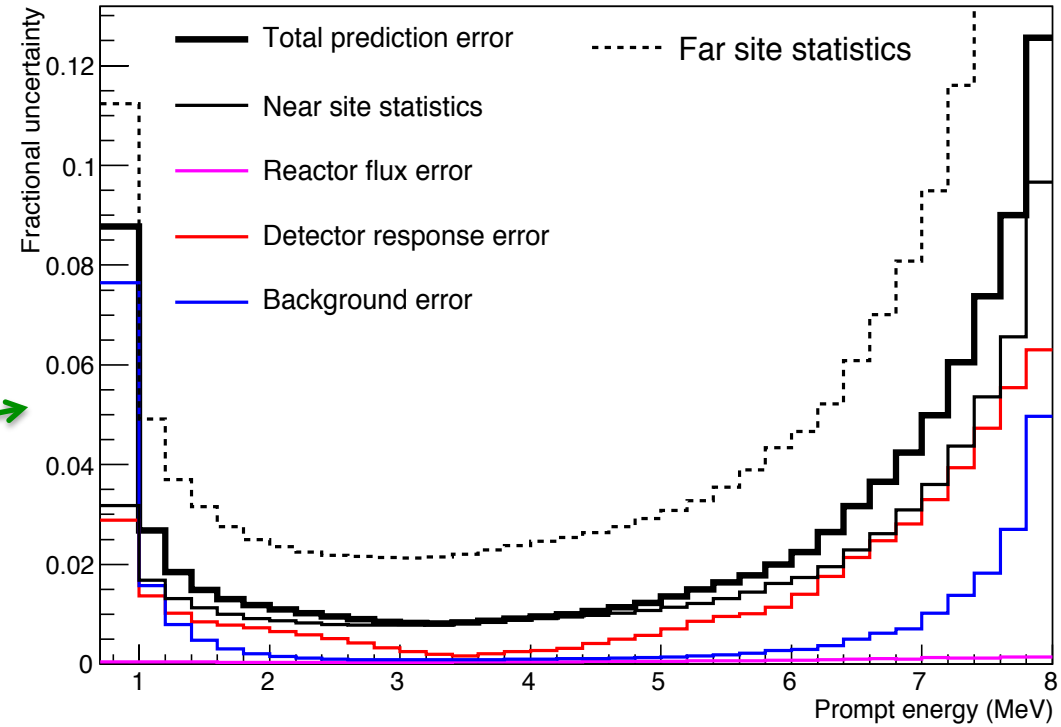

Correlation coefficients for prediction

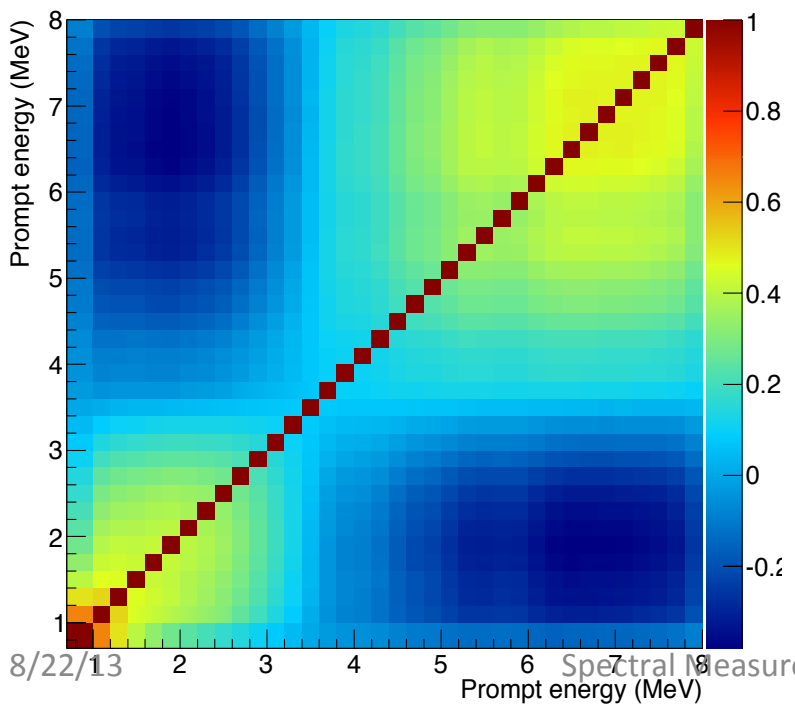

Uncertainty dominated by statistical error

Cross-Check: Pure χ^2 Pulls Approach

Use nuisance parameters to incorporate all systematic uncertainties

Utilize a combination of correlated and uncorrelated nuisance parameters between different energies, reactors, and detectors to take into account uncertainties in:

- Reactor normalization, spectra
- Reconstructed energy scales
- Detector response effects
- Background norm, shape

Tested fitter by observing changes and correlations in fits and nuisance parameters:

- Used 'fake' MC data in place of real data
- Varied input osc parameters, energy scales, etc.
- Fit while removing some nuisance parameters

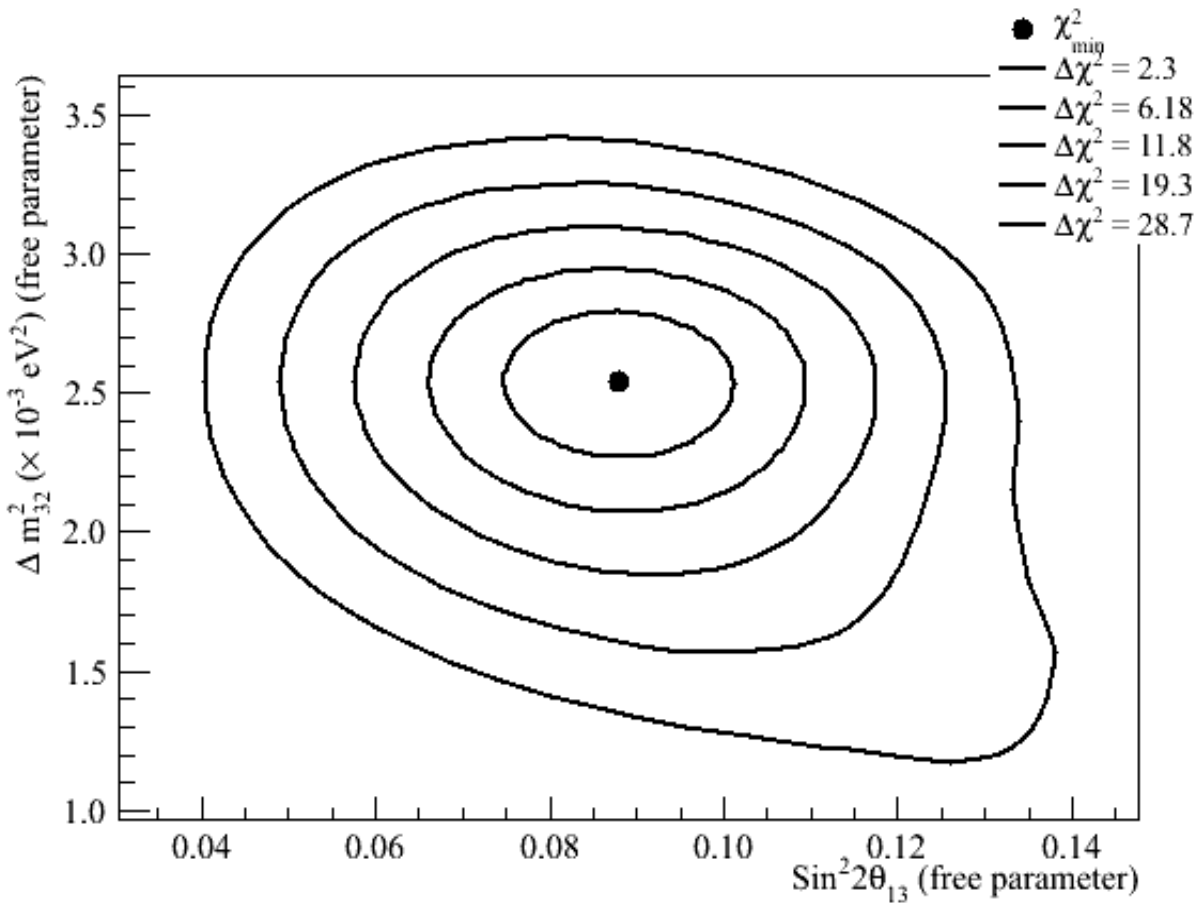

Results are consistent with those from pure covariance or mixed approaches

Oscillation Fits for Different Binning

Best fits should not change drastically with binning

Shape information is slowly 'turned on' as binning is increased

Many reactor and uncorrelated AD fit nuisance parameters, so fit parameters in pure X^2 pulls shape fit exceed total data points below 12 bins

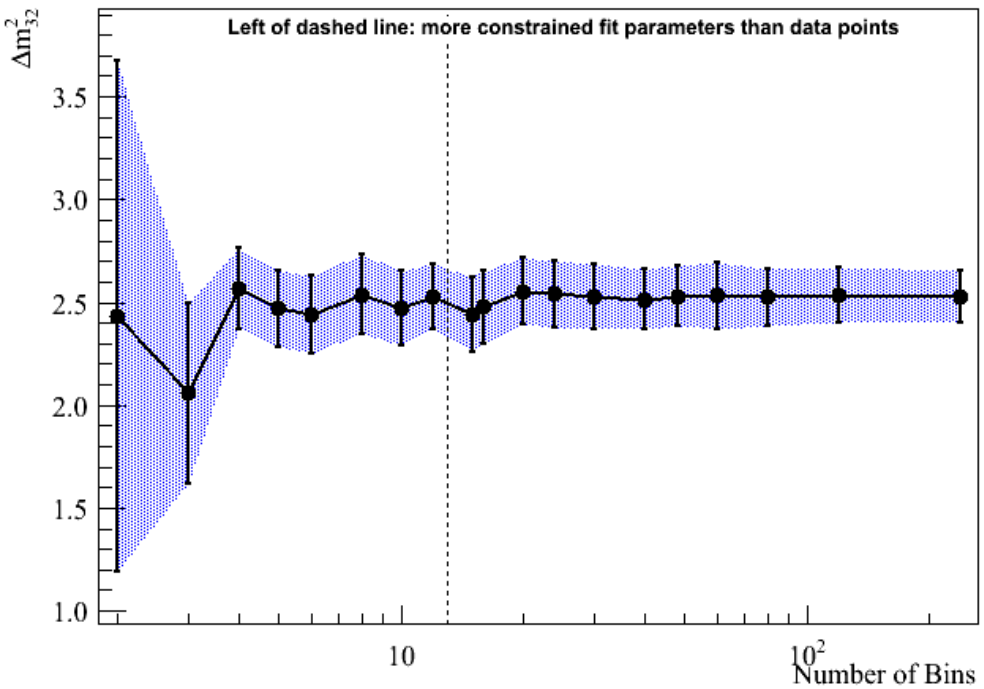

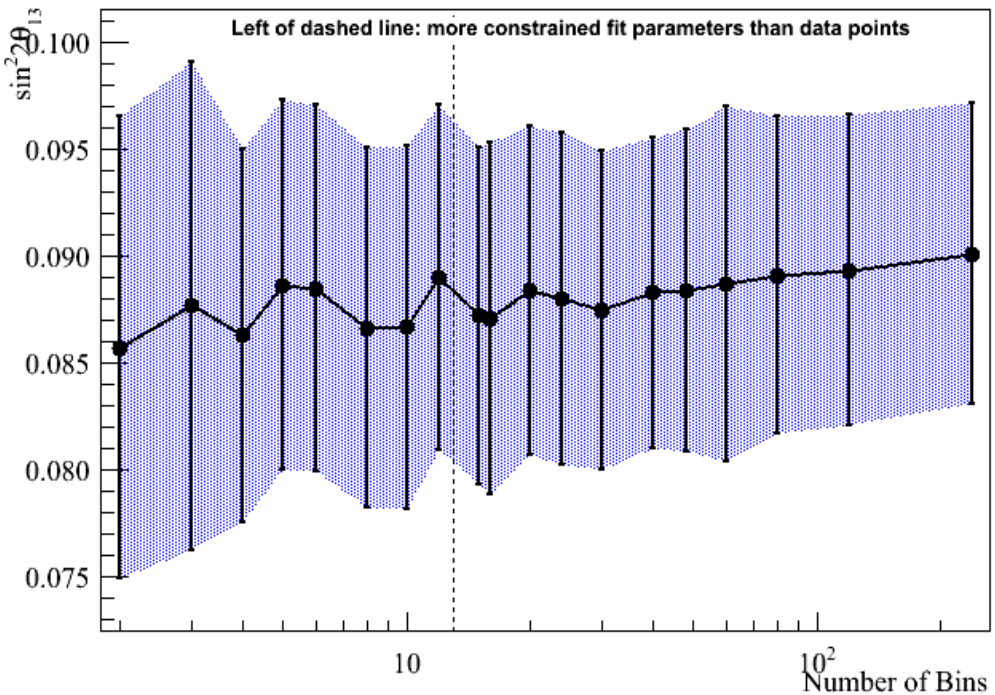

Fits remain stable within uncertainties, especially when data points exceed fit parameters.